THERMAL CONDUCTIVITY AND DIELECTRIC CONSTANT OF SILICATE MATERIALS

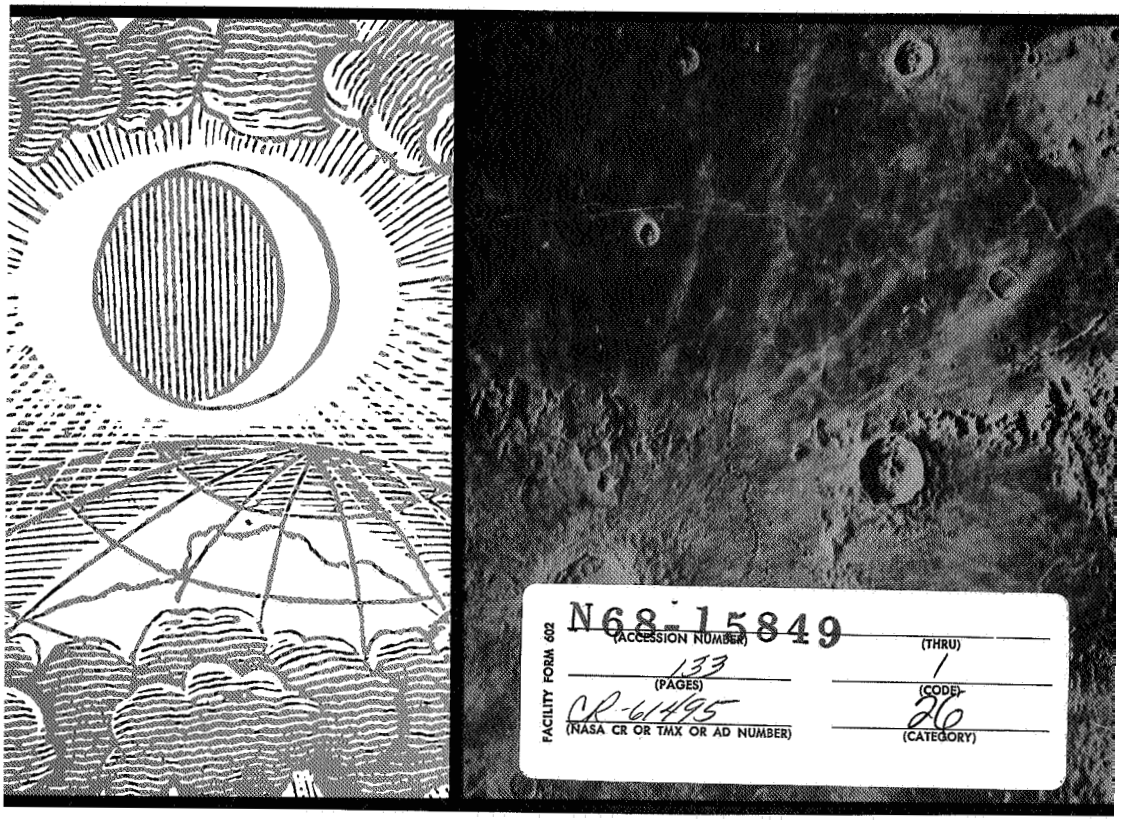

prepared for

NATIONAL AERONAUTICS AND SPACE ADMINISTRATION
GEORGE C. MARSHALL SPACE FLIGHT CENTER

GPO PRICE $ _____

CFSTI PRICE(S) $ _____

Hard copy (HC) 3.00

Microfiche (MF) .65

ff 653 July 65

Arthur D. Little, Inc.

THERMAL CONDUCTIVITY *AND* DIELECTRIC CONSTANT OF SILICATE MATERIALS

Contract No. NAS8-20076

For the Period 1 April 1965 to 31 August 1966

prepared for

National Aeronautics and Space Administration
George C Marshall Space Flight Center
Huntsville, Alabama 35812

prepared by

Arthur D. Little, Inc.
Cambridge, Massachusetts *02140*

Alfred E. Wechsler and Ivan Simon, Authors

December 1966

ABSTRACT

Contract No. NAS8-20076 encompasses an analytical and experimental investigation of the thermal conductivity and dielectric constant of non-metallic materials. Principal emphasis was placed on evaluating the mechanisms of heat transfer in evacuated silicate powders and in establishing the complex dielectric constant of these materials

Experimental measurements of the complex dielectric constant of glass beads, pumice, and basalt powders, and solid glass, pumice, and basalt were made at wavelengths of 3 2 cm and 1 2 cm over the temperature range from 77°K to 400°K The thermal conductivity of these materials and quartz powders were measured using the line heat source method at gas pressures of 10^{-8} to 10^{-9} torr and at temperatures ranging from 150°K to 400°K

The dielectric constants of the silicate powders measured vary from 1.9 to 2 9 The loss tangents of these materials vary from about 0.004 to 0.030 The dielectric constants of the solid silicates from which the powders were prepared range from 5.4 to 8 6

The effective thermal conductivities of the evacuated powders of particle size 5-75μ vary from about 4 x 10^{-6} w/cm°C to near 40 x 10^{-6} w/cm°C over the temperature range from 150°K to 400°K, and can be represented by the sum of a constant term and a term which has a cubic temperature dependence. The ratio of the radiation to solid conduction contributions to effective thermal conductivity varies from less than 0 1 to over 5 depending upon the powder size, composition, and temperature

Experimental measurements and results are discussed in relation to postulated lunar surface materials.

TABLE OF CONTENTS

LIST OF FIGURES

LIST OF TABLES

LIST OF TABLES cont'd

I SUMMARY

A PURPOSE AND SCOPE

Contract No. NAS8-20076 encompasses an analytical and experimental investigation of the thermal conductivity and dielectric constant of non-metallic materials. Principal emphasis has been placed on evaluating the mechanisms of heat transfer in evacuated silicate powders and in establishing the complex dielectric constant of these materials The experimental measurements and results are discussed in relation to postulated lunar surface materials

A brief review of radio astronomical and infrared observations of the lunar surface is given to establish the requirements for dielectric constant and thermal conductivity measurements, Theoretical and empirical relationships among dielectric constant, wavelength, density, and loss tangent are described; and their significance to the interpretation of observational data is reviewed. The mechanisms of heat transfer in particulate and porous silicates are described; theoretical and empirical models for estimation of effective conductivity are proposed; and the significance of available laboratory thermal conductivity data to the interpretation of lunar surface materials data is summarized

Experimental measurements of the complex dielectric constant of glass beads, pumice, and basalt powders, and solid glass, pumice, and basalt were made at wavelengths of 3.2 cm and 1 2 cm over the temperature range from 77°K to 400°K; the terminated waveguide and the slotted waveguide methods were used for the measurements

The thermal conductivity of glass beads, pumice, basalt and quartz powders, and solid glass were measured using the line heat source method, Measurements were made at pressures of 10^{-a} to 10^{-9} torr at temperatures ranging from 150°K to 400°K. The experimental data were examined using empirical models of radiation and conduction in the particulate systems.

B RESULTS AND CONCLUSIONS

1 Dielectric Constant

The dielectric constants of the silicate powders measured vary from 1.9 to 2 9 The loss tangents of these materials vary from about 0.004 to 0.030. The dielectric constants of the solid silicates from which the powders were prepared range from 5.4 to 8.6. There is no significant difference in the dielectric constant of the powders at the two wavelengths investigated. The loss tangents of the powders are larger at the shorter wavelength, The effect of temperature on the real part of the dielectric constant of the powders is negligible over the range from -77°K to 400°K. The imaginary part of the dielectric constant and the loss tangent tend to increase at the upper temperature limit of this range, particularly for basalt powders The dependence of the dielectric constant of the powders on density is adequately represented by theoretical formulas which relate the dielectric constant to the fraction of the solid and the dielectric constant of the solid, There is no well-defined correlation between thermal conductivity and dielectric constant of the silicate powders. The correlation proposed by Troitskiidoes not hold for the powders and solids we studied. If the dielectric properties of the lunar surface are similar to those of the minerals and powders studied in this work, the penetration depth of microwaves is much greater than the thermal penetration depth (approximately 40 times greater for 3 28 cm waves and 10 times greater for 1.18 cm waves) Small amounts of metallic (iron) particles present in the dielectric silicates tend to decrease the penetration depth significantly

2 Thermal Conductivity

The effective thermal conductivities of the evacuated powders of particle size 5-75μ vary from about 4 x 10^{-6} w/cm°C to near 40 x 10^{-6} w/cm°C over the temperature range from 150°K to 400°K, and can be represented by the sum of a constant term and a term which has a cubic temperature dependence, In the temperature range of 150°K to 400°K, the ratio of the radiation to solid conduction contributions to effective

thermal conductivity varies from less than 0.1 to over 5 depending upon the particular powder size and composition

The solid conduction contribution to effective thermal conductivity decreases with increasing particle size, and the radiation contribution increases with increasing particle size The radiation contribution to effective thermal conductivity can be predicted adequately on the basis of available correlations which take into account the refractive index and its variation with wavelength. The solid conduction contribution to thermal conductivity cannot be predicted adequately using correlations which consider only Hertzian contact areas and the thermal conductivity of the solid There is no direct correlation between thermal conductivity of particulate, vesicular, and solid silicates and density The structure of the material influences thermal conductivity more than density

C RECOMMENDATIONS

In analyzing lunar infrared temperature data, the thermal parameter should not be treated as independent of temperature A more desirable procedure is to include the variation of both specific heat and density with temperature,

Additional measurements of dielectric constant at other wavelengths, and of thermal conductivity of other postulated lunar materials at low temperatures should be carried out

In order to develop a better understanding of contact between particles, additional experiments are required under conditions where conduction heat transfer can be measured independently of other mechanisms

II. INTRODUCTION

The flow of heat in heterogeneous materials can be described by thermal conduction and radiation processes acting simultaneously in series and parallel combinations in each phase. In a dispersed system consisting of a gas phase and a non-metallic solid phase confined by boundaries with specified temperatures and properties (typically a powder or fibrous material within a container), heat may flow from one boundary to another by gaseous conduction, solid conduction (i.e., through the solid phase across areas of contact between particles or fibers), and radiation from surface to surface through the gas phase and within the solid phase

In many practical applications the total heat flux through a heterogeneous material is the important quantity to be specified or measured In some simple systems, the heat flux is uniquely determined by the average temperature gradient in the material and the bulk thermal properties of the material In the general case, however, the heat flux depends upon the radiation characteristics of the boundary surfaces (their emittance and reflectance) and the thickness of the material as well as the temperature gradients and thermal properties of heterogeneous material Accordingly, effective thermal conductances are used to characterize the heat flow in heterogeneous systems The effective thermal conductivity can be defined as a conductivity value which, if substituted into a Fourier-type equation, will result in the correct heat flux for a particular system with specified boundaries and dimensions For an isotropic opaque solid material, the effective thermal conductivity equals the true thermal conductivity (i.e., it is independent of boundary properties, system dimensions and temperature gradients, and is a function only of the material and its temperature) In heterogeneous systems, because of the multiplicity of heat transfer mechanisms and their non-linearity, the effective thermal conductivity does not have the intrinsic properties of the true thermal conductivity Extrapolation of thermal test data and use of effective thermal conductivity values for conditions other than those during which the values were obtained can lead to significant errors.

An important application illustrating the ambiguity of thermal conductivity data can be found in the interpretation of lunar thermal data Photometric, polarization, and infrared observations of the moon have led to the general conclusion that the lunar surface is covered with a highly porous material of low thermal conductivity. In analyses of the temperatures of the lunar surface, it is generally assumed that the covering material is opaque in the infrared region and that its conductivity is constant, independent of the thickness, temperature, or temperature gradients. Because of the apparent high porosity and large temperature gradients, radiation transmission in the lunar surface material could be significant and calculations based upon single valued thermal conductivities may yield results which are not representative of the true thermal conditions on the lunar surface

The attempts to characterize the nature of the lunar surface have proceeded along another line of investigation, i.e , microwave observations at different stages of lunations and eclipses to provide detailed signature maps of lunar subsurface temperatures The complex dielectric constant and its dependence on material type and density are parameters of significance in evaluating the properties of the surface and subsurface materials by microwave measurements.

Within the past two years, measurement capabilities in the millimeter and microwave portions of the spectrum have experienced dramatic improvement, and detailed infrared thermal maps for many individual regions of the moon over a full lunation cycle are now available. Insufficient data are available to correlate thermal properties and electrical properties of materials currently under investigation as representative of the lunar surface and to provide signature characteristics of microwave and millimeter radiation for such materials As a result, some controversy exists as to the interpretation of lunar thermal and microwave data

One analytical technique for studying heat transfer in heterogeneous materials is to ascribe the total heat flow to the super position of heat flow due to the mechanisms previously listed, The effective thermal conductivity can be partitioned into contributions for each mechanism, and

each contribution can be analyzed in terms of the physical quantities responsible for the mechanism of heat flow. Although this technique is not rigorous (there is an interaction between the heat flow mechanisms), it is useful in explaining the overall properties of heterogeneous materials and forming a sound basis for engineering use of thermal property data

In our work under Contract NAS8-1567 (Everest, et al , 1962; Wechsler, et al , 1963, and Wechsler and Glaser, 1964), we have measured the effective thermal conductivities of solid, powdered, and vesicular non-metallic materials Although some information has been obtained on the importance of the various heat transfer mechanisms, the program has been directed mainly toward obtaining data on the properties of postulated lunar surface materials, Because of the fundamental importance of the knowledge of the mechanism of heat transfer in heterogeneous materials and the applicability of the knowledge to both lunar surface conditions and other systems where insulating materials are used, our studied of non-metallic materials have been extended

In the work described in this report, we have carried out experimental and theoretical studies of the mechanisms and rates of heat transfer in particulate and sintered materials to permit estimates of the separate contributions of radiation and conduction to be made We have also measured the dielectric properties of the materials used in the thermal studies in an attempt to relate thermal conductivity, density, and dielectric constant data. This information will aid in the understanding of the thermal behavior of lunar surface materials as well as other planetary surface materials

III DIELECTRIC CONSTANT

A REVIEW OF EXISTING DATA

1. Radio-Astronomical Observations

Thermal emission of a celestial body, such as the moon, can be observed over a very wide frequency interval including short radio waves and microwaves From the measured radiant power density, one can determine the brightness temperature of the body, and, if the emittance is known, the black-body temperature of its surface Conversely, if the surface temperature is known from the other measurements (e.g , infrared radiometry), the emittance may be determined and from it the dielectric constant In the case of lunar thermal emission, the situation is somewhat complicated by two circumstances: (a) because the rocks and minerals are fairly "transparent" to the radio waves, the radiant energy emitted by the surface contains components from various depths; and (b) the temperature of the moon varies periodically during lunation, though not in a simple harmonic manner.

The following formulation of the problem was originated by Piddington and Minnett (1949), who were the first to obtain quantitative microwave measurements of the lunar thermal emission at 1 25 cm wavelength over the entire lunation period. The problem was subsequently treated theoretically by Jaeger (1953) If the temperature of the lunar surface varies in time as:

$$T(0,t) = \sum_{n=0}^{\infty} T_n \cos (n \Omega t - \phi_n) \qquad \text{(III-1)}$$

and the observed microwave brightness temperature contains contributions from varying depths according to the expression;

$$T_b = (1 - R) \int_0^{\infty} T(x)\, e^{-\alpha x}\, dx \qquad \text{(111-2)}$$

then the solution of the heat transfer equation yields the following expression for the time dependence of the observed microwave surface brightness temperature:

$$T_b(t) = (1 - R) \sum_{n=0}^{\infty} T_n \left(1 + 2\delta_n + 2\delta_n^2\right)^{-1/2} \cos\left(n\,\Omega\,t - \phi_n - \psi_n\right) \qquad \text{(III-3)}$$

This solution applies for the homogeneous lunar model.

$\Omega = 2\pi/P$ is the lunation frequency (P = 29 53 days)

$(1 - R)$ = the radiofrequency emittance of the moon

R = reflectance

a = attenuation factor for the radiofrequency waves in the lunar material

$\delta_n = L_r/L_t$ is the ratio of the radiofrequency penetration depth (L_r) to the heat wave penetration depth (L_t)

$L = a^{-1}$

$L_t = \left(\frac{n\Omega}{2} \cdot \frac{\rho c}{k}\right)^{-1/2}$

ρ = density

c = specific heat

k = thermal conductivity

$\tan \psi_n = \left(\frac{\delta_n}{1 + \delta_n}\right)$

In practice, the limited accuracy of the radio-astronomical observation permits only the first two terms of equation III-3 to be determined. The first term, $(1 - R)\,T_o$, is the (constant) brightness temperature, and the second term represents the phase-shifted first harmonic component of the periodic brightness temperature It is apparent that by definition the radiofrequency phase lag ψ_n cannot exceed 40°; if it is found to be greater than 45°, as it has been claimed to be by some observers, the homogeneous model of the lunar surface would have to be replaced by a more general one (e.g , a stratified model)

From two observed parameters, such as the amplitude and the phase of the brightness temperature, one can determine, at least in principle, the two components of the complex dielectric constant that characterize the dielectric properties of the lunar surface, since:

$$R = \left(\frac{1 - \sqrt{\varepsilon}}{1 + \sqrt{\varepsilon}}\right)^2 \qquad \text{(III-4)}$$

and

$$\tan \psi = \frac{1}{1 + \alpha L_t} \qquad \text{(III-5)}$$

where

$$\varepsilon = \varepsilon' - i\varepsilon'' \qquad \text{(III-6)}$$

and

$$\alpha = \frac{\pi}{\lambda_o} \frac{\varepsilon''}{\varepsilon'} \sqrt{\varepsilon'} \quad (\text{for } \varepsilon'' \ll \varepsilon') \qquad \text{(III-7)}$$

The magnetic permeability of the lunar surface is here assumed to be equal to 1 The early radio-astronomical observations by Piddington and Minnett (1951), indicated a phase lag of approximately 45° and thus justified the assumption $\alpha \approx 0$, $\varepsilon'' \approx 0$ Accordingly, ε' could be obtained by equation III-4 from the observed value of $(1 - R)$.

In this way, Gibson (1958) estimated the real part of the dielectric constant of the lunar surface material to be between 3 and 5 More recent measurements seem to indicate that this estimate is too high The Russian workers made several studies of lunar thermal emission at wavelengths from 0.4 to 3.2 cm. A summary of this work may be found, e g , in Troitskii (1962) From his own measurements as well as those summarized in the above mentioned papers, Troitskii concluded that the lunar surface has a dielectric constant $\varepsilon' \approx 1\ 6$ This estimate appears to be rather low compared with other data Most recent measurements made by Gary, Stacey and Drake (1965) led the authors to assume a value of $\varepsilon' \approx 2\ 8$ for the lunar surface.

The paucity of results and the wide spread of the values derived from the observations are indicative of the difficulties involved in the data acquisition and their reduction. Moreover, the approximate analysis based on the Piddington and Minnett method has a drawback in requiring a priori knowledge of the surface temperatures (from the infrared measurements) and of the thermal parameters of the surface material This situation makes it desirable to determine in the laboratory both the dielectric properties and the thermal parameters on representative samples of probable lunar materials prior to further evaluation of radio-astronomical data.

2. Radar Observations

The moon and several of the near planets have been studied in numerous investigations by radar at wavelengths ranging from *0.86* cm to *784* cm. Radar studies of the moon have been reviewed in detail by Pettengill and Evans *(1965).* The radar method is capable of providing manifold information about the moon, including its distance, rotation, and topography; we shall discuss here only that part of the radar information which relates to the dielectric properties of its surface.

If the moon were a perfect sphere having a reflectance R determined by the dielectric constant of its surface material according to equation III-4, its radar scattering cross section would be:

$$a = R\pi a^2 \qquad \text{(III-8)}$$

where a is the radius of the moon. Equation III-8 is valid under the following assumptions; (a) the beam of the radar antenna is wide enough to illuminate the whole moon, (b) the pulse is sufficiently long to allow the reflections from the most distant parts of the limb to be received, and (c) the wavelength λ_o is short compared with the radius of the moon Most of the moon's surface is actually found to be gently undulating about the mean spherical shape (Nagfors, 1964) This can be formally described by an amendment of equation *111-8*

$$a = g\, R\pi a^2 \qquad \text{(III-9)}$$

where g is a directivity factor of the form:

$$g = 1 + n\alpha^2; \qquad \text{(III-10)}$$

here n is a constant ($\approx$ 2) and a is a term comparable to the mean square surface slope Some areas of the moon's surface reflect as a rough (Lambertian) scatterer, in that case g has a theoretical value of 8/3 The total radar cross section contains both components. Pettengill and Evans estimated about 82% of the projected surface to be of the "diffuse" kind and 18% to be of the "smooth" kind, when observed with a 68 cm wavelength radar.

The directivity factor g has been calculated theoretically for different kinds of scatterers (Grieg, et al , 1948; Daniels, 1961; Evans and Pettengill, 1963; and Rea, et al , 1964) This makes it possible to determine the reflectance R from the experimentally observed value of σ by using equation III-9 Earlier determinations of the scattering cross section were subject to fairly large errors because of instrumental difficulties, such as calibration of the system, antenna gain, transmitted power variations and atmospheric attenuation, the effect of pulse-length dependence on the radar return, the effect of localized scatterers, and the Doppler shift in the return pulse frequency caused by lunar rotation Consequently, the original estimates of the dielectric constant of the lunar surface were not very reliable,

From a compilation of radar data, Senior, Siegel, and Giraud (1962) estimated the real part of the dielectric constant to have a value of approximately $\varepsilon' \approx 1.08$, which is undoubtedly too low Evans and Pettengill (1963) obtained a value of $\varepsilon' \approx 2.6$ to 2 8 from their measurements; and Rea, Hetherington, and Mifflin (1964) arrived at a value $\varepsilon' \approx 2\ 8$ by a method of analysis different from those previously cited Most recently, Hagfors and his coworkers (1966) concluded from their measurements made with circularly polarized radar at 23 cm wavelength that a two-layer model of the lunar surface provides the best fit with the observation The top layer was estimated to have a dielectric constant

ε' of about 1.7 to 1.8 and a depth of approximately 20 cm, on the average, The base layer would have a value of $\varepsilon' \approx 4.5$ to 5.

3 Laboratory Measurements

Laboratory data on dielectric properties of particulate materials measured at microwave frequencies are very sparse. The early work of Straiton and Tolbert (1947) deals with a few terrestrial materials defined only as "Arizona soil", or "Austin, Texas, soil, very dry"; data were obtained at a wavelength of 3.2 cm. For the two materials referred to above, the dielectric parameters measured by Straiton and Tolbert are, respectively, $\varepsilon' = 3.2$, $\varepsilon'' = 0.19$ and $\varepsilon' = 2.8$, $\varepsilon'' = 0.014$. Similar sets of data on various types of soils are tabulated in the compendium on dielectrics edited by Von Hippel (1954). The value of this particular tabulation is in the wide frequency range it covers (10^2 to 10^{10} cps)

Fensler and coworkers (1962) made an extensive study of electromagnetic parameters, including the dielectric constants, of numerous rocks and meteorites both in solid and powdered form. Their work includes an experimental study of the effect of particle size and packing factor on the effective dielectric constant of some of the selected materials, Because these measurements were made at low frequencies (1000 cps) the comparison with those made at UHF and microwave frequencies (10^7 to 10^{10} cps) is uncertain. Only the solid chondrites and tektites were measured at UHF frequencies (between 420 and 1800 Mc) The dielectric constant ε' of glassy tektites from various localities was found to vary between 3 88 and 8.03 (measured at 500 Mc) Chondrites had values of ε' between 10.4 and 45.9 and high dielectric loss tangent (between 0 028 and 0 199)

Troitskii (1962) refers to (unpublished) measurements made at a wavelength of 3 2 cm (≈ 10^{10} cps) on various terrestrial volcanic rocks of Armenia and Kamchatka (tuff, tufo–lava, volcanic slag, obsidian, pumice, clay, etc.). Without further detail regarding the experimental work, he states that the dielectric constant ε' was in the range from 1.65 to 3.3 for different rocks having density between 0 5 and 1 25 g/cm^3 The loss tangent of these materials was between 6 x 10^{-3} and 23 x 10^{-3}; the specimens were measured in dry air under ordinary conditions

B. THEORETICAL CONSIDERATIONS

1. Reflectance and Emittance of Dielectric Materials

Reflectance of a semi-infinite dielectric body bounded by a plane surface is given, for normal incidence, by formula III-4 cited earlier At angles of incidence other than zero (normal incidence), reflectance is given by the well-known Fresnel formulas.

These formulas (including equation III-4) are valid under the following assumptions: (a) the curvature of the surface is large compared with the wavelength, (b) the surface roughness is small compared with the wavelength, (c) the dielectric body is homogeneous on a scale small compared with the wavelength; and (d) the dielectric body is thick compared with the penetration depth ("semi-infinite"). These conditions can be readily met under laboratory conditions with carefully prepared powdered samples It is obvious, however, that when applied to celestial bodies, such as the moon, the formulas may not strictly apply Assumption (a) is usually justified by the observation that the radar reflection obtained with a narrow-beam antenna and a short-pulse resolution comes predominantly from the central area of the disc, the reflected power falling off very rapidly toward the limb Assumption (b) may be somewhat in doubt in view of the surface profile information gathered from the Surveyor experiment If the surface is rough on a scale comparable to the wavelength, diffuse reflection will occur in addition to the specular reflection. Smooth undulation of the surface on a scale greater than the wavelength can be accounted for by the method of Hagfors (1964) Homogeneity of the dielectric material constituting the surface of the moon or the planet is likely to be good on the scale of short-wavelength microwaves However, numerous observations indicate that the dielectric properties of the lunar surface vary considerably over areas of distinctly different geology (e.g., maria vs crater rims) (Pettengill and Evans, 1965) Finally, the assumption of "semi-infinite" thickness is certainly valid, inasmuch as the penetration depth is only of the order of a few wavelengths

The analysis of radar data in terms of the dielectric properties of the spherical celestial bodies based on Fresnel formulas has been

criticized by Rea and coworkers (1964) These authors claim that the quantity R in equations III-8 and III-9 cannot be interpreted as the Fresnel reflection coefficient at normal incidence (equation III-4), but rather has the meaning of the albedo averaged over the hemisphere. Their approach is based on treatment of the scattering of light by rough dielectric surfaces where the surface elements are large in comparison with the wavelength. The results of analysis of existing radar reflection data by their method do not differ appreciably in numerical values from other results as far as the dielectric constants are concerned; some differences appear in the values of average slope data.

Emittance E of a dielectric body can be obtained from the reflectance by means of the relation:

$$R + E + T^* = 1 \qquad \text{(III-11)}$$

where T^* is the transmittance In this relation we made implicit use of Kirchhoff's law by substituting emittance for absorptance. In a "semi-infinite" body $T^* = 0$ and, consequently,

$$E = R - 1 \qquad \text{(III-12)}$$

The assumption $T^* = 0$ is justified for a celestial body of a large size, such as the moon. Under laboratory conditions this may not be the case and transmittance resulting from the finite thickness must be taken into account

If the reflectance R in formula III-12 is taken to be the Fresnel reflectance as given by equation III-4, E has the meaning of the directional, normal emittance. However, it can be shown (Gardon, 1950) that the thermal radiation emerging from the plane boundary of a semi-infinite dielectric body is not directional but diffuse, obeying very nearly a cosine directional law. Consequently, E should be interpreted as a hemispherical emittance, in a way analogous to the argument given by Rea, Hetherington, and Mifflin *(1964)* for the diffuse reflectance

2 Complex Dielectric Constant and the Penetration Depth

Electromagnetic waves traveling through a lossy medium are characterized by the two complex parameters:

$$\varepsilon = \varepsilon' - i\varepsilon'' \text{ (dielectric constant)} \qquad \text{(III-13)}$$

$$\mu = \mu' - i\mu'' \text{ (permeability)}$$

The amplitude varies exponentially as:

$$e^{iwt - ax}$$

where ω is the angular frequency and

$$\gamma = \alpha + i\beta \qquad \text{(III-14)}$$

is the propagation constant. As a is assumed always positive, the waves are attenuated as they proceed forward:

$$e^{-ax}\, e^{i(\omega t - \beta x)} \qquad \text{(III-15)}$$

a is the absorption coefficient and $\beta = \omega/v$ is the phase constant From Maxwell's equations, one obtains for the phase velocity v in the medium:

$$v = c\,(\varepsilon\mu)^{-1/2} \qquad \text{(III-16)}$$

and for the propagation constant;

$$\gamma = \frac{i\omega}{c}\sqrt{\varepsilon\mu} \qquad \text{(III-17)}$$

Inserting in III-17 from III-13 and equating the real parts of III-17 and III-14, one obtains for the attenuation factor:

$$a = \frac{\omega^2}{4nc^2}\,(\varepsilon'\mu'' + \varepsilon''\mu') \qquad \text{(III-18)}$$

Planetary rocks and soils may reasonably be assumed to be non-magnetic, hence $\mu' = 1$ and $\mu'' = 0$ In this case, equation III-18 simplified to:

$$\alpha = \frac{\lambda\omega}{4nc}^2 \varepsilon'' = \frac{n}{\lambda_o} \frac{v}{e} \varepsilon'' \qquad \text{(III-19)}$$

If, furthermore, $\varepsilon'' << \varepsilon'$ and $\mu = 1$, we obtain from 111-16:

$$\alpha = \frac{\pi\sqrt{\varepsilon'}}{\lambda_o} \frac{\varepsilon''}{\varepsilon'} \qquad \text{(III-20)}$$

and for the penetration depth $L_r = a^{-1}$

$$L_r = \frac{\lambda_o}{\pi\sqrt{\varepsilon'}} \frac{\varepsilon'}{\varepsilon''} \qquad \text{(III-21)}$$

This may be expressed in terms of other parameters often used in the radio engineering practice, the loss tangent defined as:

$$\tan\delta = \frac{\varepsilon''}{\varepsilon'} \qquad \text{(III-22)}$$

or the dielectric conductivity, defined as:

$$a = \omega\varepsilon'' \qquad \text{(III-23)}$$

Then we obtain:

$$L_r = \frac{\lambda_o}{\pi\sqrt{\varepsilon'}\tan\delta} = \frac{\lambda_o \omega\sqrt{\varepsilon'}}{\pi\sigma} \qquad \text{(III-24)}$$

However, a does not necessarily represent the conductivity in the conventional sense. It may include the motion of free charge carriers (electrons) if conducting material is present in the medium, and may also result from other dissipative processes on the molecular scale, even in the absence of free carriers.

From the definition of a (equation III-15), the penetration depth is seen to represent that depth at which the amplitude of the electromagnetic

wave decreased to e^{-1} or to about 37% of its value at the surface. According to the exponential law, the amplitude would drop to 13 5% at a depth of $2L_r$, to 4.98% at $3L_r$, and so forth.

Equation 111–24 shows that the penetration depth decreases with free-space wavelength λ Taking as typical values ε' = 2 3 and tan δ = 0 01, we can estimate the penetration depth for 3 cm wavelength radiation L_r = 63 cm; for 3 mm wavelength, the penetration depth would be only 5.3 cm.

It is also seen that penetration depth increases with decreasing value of tan 6 In materials of low dielectric loss ($\varepsilon'' << \varepsilon'$), tan 6 is the dominant factor determining the penetration depth; at the same time, the real part of the dielectric constant (ε') becomes the factor determining the reflectance.

3 Dielectric Properties of Solids and the Nature of the Loss Mechanism

Both ε' and ε'' are frequency–dependent and interrelated in such a manner that if one is given as a function of frequency over the entire frequency range from zero to infinity, the value of the other is uniquely determined This mutual dependence of ε' and ε'' may be mathematically described, for instance, by the Kramers–Kronig relations, which are a general form of dispersion relations.

The physical reason for the existence of dispersion relations in dielectric materials is the presence of permanent or induced molecular and atomic dipoles in the structure of material, capable of resonant interaction with the electromagnetic waves The resonances are sharp and clearly observable only in gases and liquids possessing simple molecular structure, which, because of dispersion relations, also permit quantitative calculations to be made with a fair degree of accuracy

In solids, the situation is complicated by the simultaneous action of several dispersive mechanisms. At low frequencies, dielectric after-effects of the Maxwell type cause dissipation of energy in the medium, particularly if it is heterogeneous. Another mechanism effective in heterogeneous media is the migration of ions adsorbed on internal surfaces At higher frequencies the molecular dipole orientation effects of the

Debye type are the principal source of dissipation. According to the Debye theory, molecules or parts of molecules carrying an electrical dipole moment tend to orient themselves along the alternating electric field of the electromagnetic wave This tendency to rotate is opposed by "frictional" or "viscous" forces assumed to be proportional to the angular velocity Consequently, the orientation lags behind the electric field by an angle 6. At very low frequencies $6 = 0$; as the frequency increases, a resonance is approached and passed. At resonance, $|\tan 6|$ attains a maximum and then decreases to low values at very high frequencies as the dipoles cease to follow the rapid vibrations of the wave field. Since natural solid materials involve a great variety of molecular groupings, the resonance frequencies are spread over a wide frequency spectrum from about 10^5 to 10^{10} cps Beyond about 10^{10} cps, electronic polarization in the individual atoms is responsible for the dielectric properties of solids

As a result of this spread of dispersion frequencies, the dielectric parameters of silicate minerals and rocks are found to vary with frequency only to a slight degree; in fact, both ε' and ε'' are found in practice nearly constant between about 10^7 to 10^{10} cps (von Hippel, 1954)

The real part of the dielectric constant ε' is determined largely by the chemical structure of the solid and is relatively insensitive to the presence of impurities The reverse is true of the loss tangent (tan 6) which is strongly influenced by the presence or absence of impurities This may be illustrated on the example of the simplest silicate, i.e , silica (SiO_2) Pure silica in the vitreous form ("fused quartz") has the lowest loss tangent of all silicates As shown in Table III-1, when additional ions are introduced, the loss increases

Addition of ions other than sodium produces similar effects Unfortunately, no simple rules correlating tan δ with the concentration of any particular ion in a given silicate matrix seem to be evident, and the body of empirical facts is very limited. Consequently, it appears impossible to draw any conclusions regarding the presence of minor constitution elements in naturally occurring silicates from the experimentally determined values of tan 6

TABLE III-1

DIELECTRIC LOSS IN SILICA AND SODIUM SILICATE GLASSES AT A FREQUENCY OF 10^{10} c/s AND 25°C

100% SiO_2	0.0001
96% SiO_2, 4% B_2O_3 and Na_2O	0.0009
91% SiO_2, 9% Na_2O	0.013
80% SiO_2, 20% Na_2O	0.020
70% SiO_2, 30% Na_2O	0.024

Source: von Hippel (1954)

4. Dielectric Constants of Particulate Media and Mixtures

One of the objectives of the present investigation was to study the dielectric properties of particulate media For this reason we shall briefly review the theoretical basis of determining the effective dielectric parameters of such media from the properties of the solid We shall assume from the outset that the medium consists of particles uniformly smaller than the wavelength, and that the volume fraction occupied by particles of i-th kind is f_i and the volume fraction of the voids f_o is vacuum, the volume fraction: being normalized, $\sum_{o}^{n} f_i = 1$

The problem of the effective dielectric constant of a dilute medium containing small particles has been solved by many researchers, starting with Maxwell in 1873 Some of the often used formulae are valid only for special cases (e.g , spherical particles) or over a small concentration range. Troitskii (1962) uses a formula of the following type:

$$\bar{\varepsilon}' = \varepsilon' \left[1 - 3f_o \left(\frac{2\varepsilon' + 1}{\varepsilon' - 1} + f_o\right)^{-1}\right] \qquad \text{(III-25)}$$

This formula, which Troitskii attributes to Odelevskii and Levin, gives the effective dielectric constant $\bar{\varepsilon}'$ of a porous medium containing only one kind of particle of dielectric constant ε'; it refers to the real parts of ε only Pettengill and Evans make use of an equivalent formula adapted for the volume fraction f of the particles rather than that of the voids:

$$\bar{\varepsilon}' = 1 + \frac{3y}{1 - y} \qquad \text{(111-26)}$$

where

$$y = f\,\frac{\varepsilon' - 1}{\varepsilon' + 2}$$

All of these formulas can be deduced from a general expression derived by Emslie (1966) of the form:

$$\frac{(\bar{n} - i\bar{k})^2 - 1}{(\bar{n} + i\bar{k})^2 + 2} = \sum_i f_i \frac{(n_i - ik_i)^2 - 1}{(n_i - ik_i)^2 + 2} \qquad \text{(III-27)}$$

Here, n and k designate the real and imaginary parts of the refractive index, defined by the following relation:

$$(n - ik)^2 = \varepsilon' - i\varepsilon'' \qquad \text{(III-28)}$$

The "barred" quantities represent the effective parameters of the particulate medium The quantities with indices refer to the parameters of the i-th (solid) component, i = 0 refers to vacuum (voids). Furthermore, from equation III-28 we obtain;

$$\varepsilon' = n^2 - k^2,$$

$$\varepsilon'' = 2nk, \text{ and} \qquad \text{(III-29)}$$

$$k = (1/2)\, n \tan \delta.$$

Formula III-26 is obtained from 111-27 simply by substituting the following values. $\varepsilon' = n^2$, k = 0 (hence tan δ = 0), and $f_i = f$ These formulas have been used in radio-astronomical and radar investigations of the moon to infer the degree of porosity of the surface material We shall make use of them in the interpretation of the experimental results

The real part of the dielectric constant ε' of solid terrestrial rocks of the types likely to occur on the moon ranges from about 5 (quartz sandstone) to 17 (olivine basalt); at the same time, the observations of the lunar properties result in estimates of ε' between 1 6 and 2 8 (Section 111, A, 1 and 2) The difference can be explained by the assumption that the lunar surface is porous or vesicular, in which case its effective void fraction is then calculated from equation 111-25 or III-26.

In this way Troitskii (1962) estimated the effective density of the lunar surface to be between 0,5 and 1 25 gm/cm^3; similarly, Pettengill and

Evans (1965) concluded the effective density of the lunar surface to be approximately 40% of the solid.

5. Relations Between the Dielectric Thermal Properties of Particulate Materials

In radio-astronomical studies of the lunar surface the thermal and dielectric properties are related by virtue of equations 111-2 and 111-3 It seems reasonable, therefore, to inquire whether there is any fundamental relation between the electrical and thermal parameters of particulate materials pertinent to the present investigation.

In a general sense, we may assert that there is no fundamental connection between the dielectric constant and thermal conductivity or specific heat The well-known Wiedemann-Franz law which expresses the proportionality between thermal and electrical conductivities applies only to a very special class of solids, namely metals It results from the fact that free electrons are responsible both for the current flow and most of the heat flow.

In dielectric solids there are normally no free electrons and the electric polarization and heat conduction are caused by entirely independent mechanisms. The dielectric constant is a measure of the deformability of the electron orbitals responsible for chemical bonding of the solid (polarizability) by the electric field. The thermal properties of solids are determined in principle by their elastic properties Specific heat is related to the distribution of energy of thermally excited quantized lattice vibrations (phonons), while heat conductivity is determined by scattering of phonons by lattice imperfections. Consequently, any relations between dielectric and thermal properties are indirect and are certainly not established at present on a consistent theoretical basis.

However, when density is considered a variable, as is the case in particulate materials, electrical and thermal properties become implicitly dependent. Semi-empirical investigations of this dependence have been discussed by Troitskii (1962), who noted that the ratio δ_n of the electrical penetration depth to the thermal penetration depth is very nearly proportional to the wavelength λ_o of the radio waves in the range from 0.4 to

3.2 cm and has a numerical value of about 2 cm^{-1}, i e ,

$$\delta_n = \frac{L_r}{L_t} = 2\,\lambda_o \qquad \text{(III-30)}$$

From this relation and from equation 111–24, Troitskii concluded that the loss tangent of lunar surface material is independent of wavelength He considered his findings to be consistent with the behavior of typical silicate minerals *(see* also preceding section), and he observed that such behavior would not be the case if there were any appreciable fraction (greater than 2–3%) of metallic particles of meteoritic origin present in the surface material By inserting for L_t from equation 111–3 and for L from equation 111–24, he deduced from equation 111–30 an equation of the form:

$$\sqrt{\varepsilon'}\,\frac{\tan\delta}{\rho} = C_1 c\gamma \qquad \text{(III-31)}$$

Where c is the specific heat of the surface material, $\gamma = (k\rho c)^{-1/2}$ and C_1 is a constant independent of the constitution of the material and its density Troitskii used this equation to derive $\sqrt{\varepsilon'}$ of the lunar surface from electrically measured values of tan δ/ρ of terrestrial materials and radiometric values of γ of the lunar surface In doing so, Troitskii arrived at a value of effective dielectric constant $\bar{\varepsilon}'$ near unity; by adjusting both ε' and density, he estimated $\bar{\varepsilon}'$ to be near 1.6 and effective density $\bar{\rho}$ to be 0.5, The value of ε' obtained in this manner is too low in comparison with more recent data. This is not surprising because equation 111–31 is at best an empirical correlation and has no basis in fundamental relations.

C. DIELECTRIC CONSTANT MEASUREMENTS AT WAVELENGTHS OF 3.2 CM AND 1.2 CM

1. Methods

We used two methods to measure the complex dielectric constants of particulate materials at microwave frequencies For measurements in vacuum and over a temperature range from 77°K to 400°K, we used the terminated waveguide method (Roberts and von Hippel, 1954) For dielectric

powders in air and at ambient temperatures, we supplemented the data by measurements of attenuated standing waves in a slotted waveguide filled with the sample (Redbeffer, 1947)

The principle of the terminated waveguide method is shown schematically in Figure III-1. The sample of thickness D fills the end section of a waveguide terminated by a short circuit. A slotted section of the waveguide interposed between the sample and the generator makes it possible to determine the position of the first minimum (x_o) and the relative amplitude $r = E_{min}/E_{max}$ of the maxima and minima by means of a traveling detector probe Because there is a length of waveguide intervening between the slotted section and the sample, and the scale on the probe reads from an arbitrary origin, the position of the first minimum must be found by taking a reference reading of the minimum in the absence of sample If the position of the minimum in the absence of sample is read on the scale of the slotted section at x_1, and in the presence of the sample is read at x_2, then:

$$x = x_1 - x_2 + n_1 \frac{\lambda_1}{2} - n_2 \frac{\lambda_1}{2} - D \qquad \text{(III-32)}$$

where n_1 and n_2 are two integers.

If the sample is thin ($D < 1/4\ \lambda_1$), the number of half-wavelengths in the waveguide is the same with or without sample ($n_1 = n_2 = n$), and we may write:

$$x = x_1 - x_2 + n \frac{\lambda_1}{2} - D, \qquad \text{(III-33)}$$

It can be shown from transmission line theory that upon reflection at a short-circuit termination overlaid by a thickness D of sample having a complex propagation constant $\gamma = a + i\beta$ (*see* equations III-14 to III-19), the following relation holds:

$$\tanh \gamma D = -i \frac{\lambda_1}{2\pi D} \frac{r - i \tan (2\pi x_o/\lambda_1)}{1 - i\, r \tan (2\pi x_o/\lambda_1)} \qquad \text{(III-34)}$$

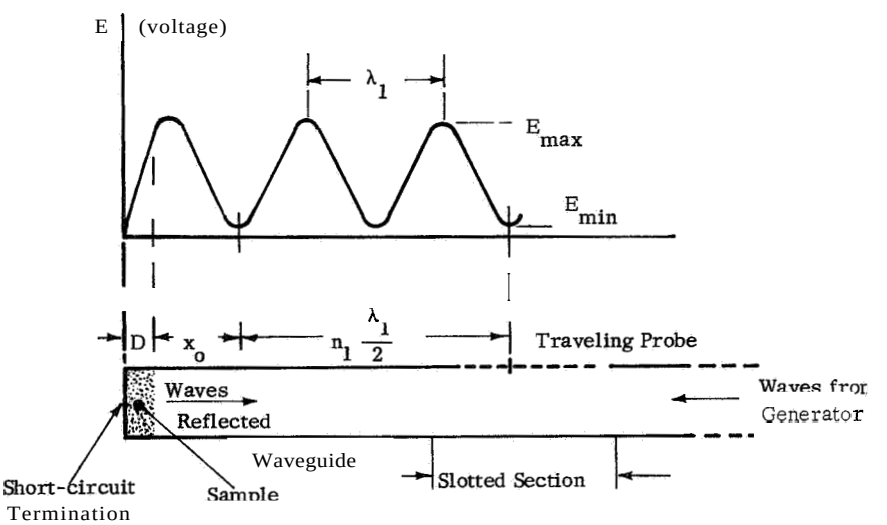

Source. Roberts and von Hippel

FIGURE III-1 PRINCIPLE OF THE TERMINATED WAVEGUIDE METHOD

Here λ_1 is the wavelength in the empty waveguide, which for the TE mode is given by the formula:

$$\lambda_1 = \lambda_o \left[1 - (\lambda_o/\lambda_c)^2\right]^{-1/2} \qquad \text{(111–35)}$$

where $\lambda_c = 2a$ is the cutoff wavelength corresponding to the dominant mode in the rectangular guide of width a

If the sample has a low dielectric loss, the ratio $r = (E_{min}/E_{max})$ tends to zero and equation III-34 simplifies to:

$$\frac{\tan \beta D}{\beta D} = - \frac{\lambda_1}{2\pi D} \tan (2\pi x_o/\lambda_1) \qquad \text{(III-36)}$$

This equation is solved numerically for $\beta D = y$ by using some of the existing tables of the function tan y/y Having found y, we obtain the wavelength in the sample:

$$\lambda = 2\pi D/y$$

Finally, the real part of the dielectric constant ε' is obtained from the relation:

$$A = \lambda_o \left[\varepsilon' - (\lambda_o/\lambda_c)^2\right]^{-1/2} \qquad \text{(III-37)}$$

which represents the wavelength of the waves propagating the waveguide filled with the sample (assuming $\varepsilon'' << \varepsilon'$)

The imaginary part of the dielectric constant or, rather, the tan $\delta = \varepsilon''/\varepsilon'$ is obtained by equating the imaginary parts of equation III-34, assuming $\alpha D << 1$, which is equivalent to $\varepsilon'' << \varepsilon'$ After considerable manipulation we obtain:

$$\tan \delta = \frac{\lambda_o}{\pi} \frac{(\beta/\beta_1)\tan(2\pi x_o/\lambda_1)[1 + \cos 2\beta D + \sin 2\beta D]}{(1/r\beta_1)(1 + \cos 2\beta D) - 2 D \tan (2\pi x_o/\lambda_1)} \left[\frac{1}{\varepsilon'} - \frac{1}{\varepsilon'^2} \left(\frac{A_o}{\lambda_c}\right)^2 1\right]^{1/2}$$

(III-38)

where $\beta_1 = 2\pi/\lambda_1$ is the imaginary part of the propagation constant in the empty waveguide.

The measured parameter in equation 111–38 is the ratio $r = E_{min}/E_{max}$, which we chose to measure directly, by means of a calibrated precision attenuator We found this method to be more accurate than the often used indirect method, based on the measurement of the width of the standing wave curve near the minimum

The values of tan 6 obtained by this method must be corrected for the resistive loss in the waveguide, which is not negligible in spite of the gold plating of the inner walls. This correction is determined by measuring the ratio r in the absence of sample. An "effective" loss tangent ($\tan \delta_o$) is then calculated from equation 111–38 by putting $D = 0$, $\beta = \beta_1$:

$$\tan \delta_o = \frac{2\lambda_o}{\lambda_-} r \tan (2\pi x_o/\lambda_1) \left[\frac{1}{\varepsilon'} - \frac{1}{.2} \left(\frac{\lambda_o}{\lambda}\right)^2\right] \qquad (111–39)$$

and the corrected tan 6 of the sample is obtained as:

$$\tan \delta_{corr} = \tan 6 - \tan 6 \qquad (111–40)$$

The second method used for measuring the dielectric constants makes use of the direct measurement of wavelength and attenuation in a waveguide filled with the sample The method is particularly suited for powders which can be easily filled into the slotted waveguide The probe in the slotted section is inserted only far enough to "plough" gently through the powder In this case, ε' is obtained directly from the measured value of A by means of equation 111–37. The loss tangent in the sample is calculated from the formula:

$$\tan \delta = \frac{\lambda\, r}{\pi\, \ell \sqrt{\varepsilon'}} \qquad (III-41)$$

where ℓ is the length of the waveguide from the short circuit termination to the probe.

2 Description of Apparatus

The microwave apparatus for measurement of dielectric constants of powders and other materials in vacuum is shown schematically in Figure III-2. This apparatus functioned according to the terminated waveguide method described in the preceding section. The waveguide was mounted in the vertical position so that the sample rested at the bottom of the waveguide by its own weight.

Starting from the bottom, we note the individual components of the microwave system. All waveguides are of the standard type (RG 52/U, 0 900 x 0 400 in., inside dimensions) appropriate for the X-band (3 2 cm wavelength). The sample waveguide is 20 inches long, with a solid short-circuit plate silver-soldered to the bottom and an O-ring gasketed flange (choke flange) at the top The inside of the waveguide is gold plated to minimize losses and to prevent oxidation of the surface. A small slot milled through the wall of the waveguide provides connection to a high-vacuum system consisting of an 8 liter/sec VacIon pump backed by a sorption-type forepump

The lower end of the waveguide containing the sample may be maintained at any desired temperature Measurements were made at 77°K by immersing the waveguide in a dewar with liquid nitrogen and at temperatures up to 400°K by heating it in a small oven. A thermocouple attached to the wall measured the temperature, which was assumed to be equal to that of the sample

The sample waveguide is closed off against the atmosphere by a special glass-metal window soldered into the flange mating with the upper end The window (Type MA-1338, Microwave Associates, Inc.) was especially selected to have a minimum reflection at the operating frequency Its standing-wave ratio was less than 1 0 2 at 9 150 Gc/s

Immediately above the connecting piece containing the vacuum window is the slotted waveguide section with the traveling probe. This precision slotted section (Type 809B, Hewlett-Packard Co.) carries a scale permitting the determination of the position of the standing-wave minima and maxima (and thus of λ for equations 111-38 and III-39) with a

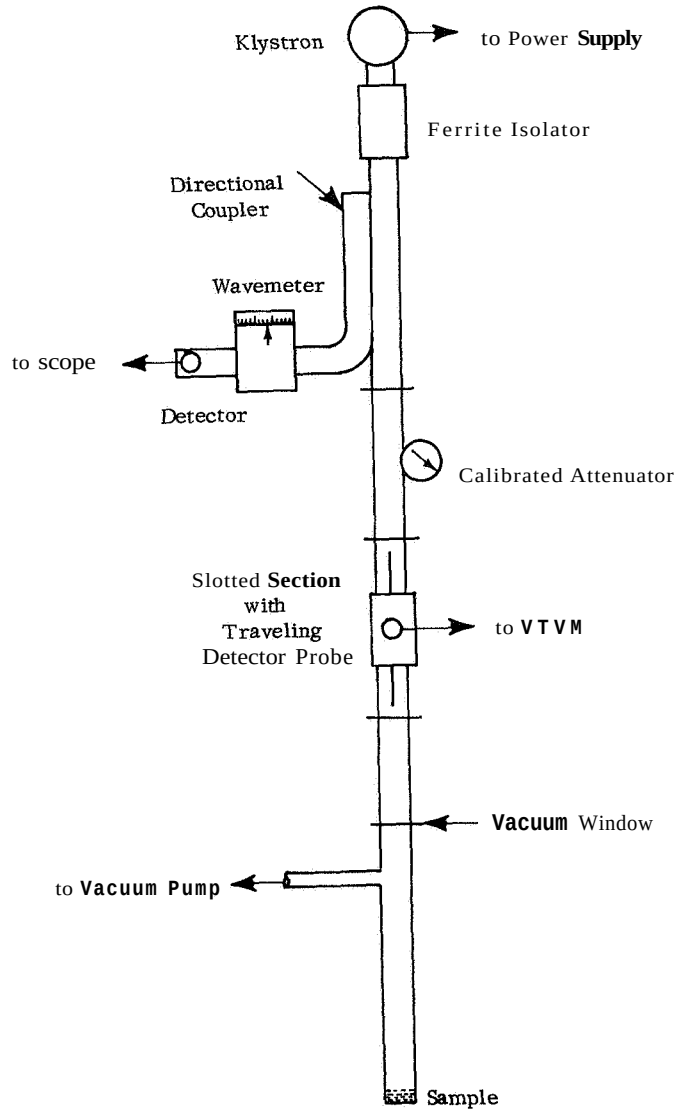

FIGURE III-2 DIAGRAM OF THE APPARATUS FOR MEASURING THE DIELECTRIC CONSTANTS

repeatability of better than 0.01 cm. The probe itself is an adjustable extension of a coaxial line protruding only a few tenths of a millimeter into the waveguide It is integrally connected to a silicon diode detector which is matched by a tunable stub. Its output is measured by a cathode-ray oscilloscope or a standing-wave detector (Model B812A, FXR Co.)

The slotted section is preceded by a precision calibrated attenuator (Model 195B, PRD Co) which is used in measuring the ratio $r = E_{min}/E_{max}$, required for the determination of tan δ For this purpose the traveling probe is set to a minimum voltage and the indication of the standing-wave detector noted, the probe is then set to the maximum and the attenuation increased until the same voltage is indicated by the standing-wave detector. The difference of the two attenuator readings (in db) gives the ratio r, independent of the linearity and calibration of the standing-wave detector.

The frequency of the microwaves is measured by a direct-reading cavity wavemeter (Model 410A, FXR Co.) fed from the main waveguide by a directional coupler (Model X 610A, FXR Co.). The microwave power is supplied by a klystron (Type VA-58, Varian Assoc) connected to the main line through a ferrite isolator (Model 1203, PRD Co), which prevents any reflections that might occur in the measurement system from influencing the frequency of the klystron, The klystron is supplied from a stabilized power supply (Model 716A, H-P Co), which also provides a square-wave modulation at 1000 cps The components just described refer to the X-band (3.2 cm wavelength) system

The K-band (1.2 cm wavelength) system was essentially identical to the one described above; only the components were different.

Waveguides: RG 53/U (0.420 x 0.170 in , inside dimensions)
Slotted section: Model K 102A (FXR Co)
Precision attenuator: Model K 164F (FXR Co)
Wavemeter: Model K 410F (FXR Co)
Directional coupler: Model K 611C (FXR Co.)
Ferrite isolator: Model K 131 (Cascade Res. Co)
Klystron: VA 254 (Varian)
Power supply: Mod. 716A (H-P Co.)

For measurements by the sample–filled waveguide method the same apparatus were used, only the long sample section was omitted and a short-circuit termination was bolted directly at the flange of the slotted section. This termination was made of a flat, heavy brass plate which was gold plated for low loss and good electrical contact. The entire set–up was placed horizontally on the bench so that the measuring section could be filled with powder up to the slot, The powder was prevented from pouring out into the attenuator and the waveguide by a tightly fitting plug of Styrofoam which was tapered at the front end to prevent reflections

3 Sample Materials

The materials used in the microwave measurements of dielectric constants and those used in the thermal conductivity measurements described in Section IV, C were the same: natural pumice, basalt, and commercial soda–lime glass The powders were prepared from natural minerals and graded to sizes listed in Table IV-5 (where two size powders are listed in the table, the larger was used in the dielectric constant measurements) The natural minerals from which the powders were prepared were also measured in their solid form. The pumicite was measured not only in its vesicular form but also as a solid glass, melted down from the mineral Glass beads were also melted to solid glass for measurement of the dielectric constants,

The density of solid samples was determined from the volume of rectangular blocks and their weight The bulk density of powdered samples, as measured in the waveguide, was determined from the height to which a known weight of powder settled under its own weight. This was done in a transparent (Plexiglas) container of exactly the same cross section as the waveguide. Since it was desirable to vary the bulk density over a fairly large range and mostly toward values lower than the "naturally packed" density, we diluted the mineral powders with polyethylene powder. Having determined the dielectric constant ε' of polyethylene powder and knowing the amount added to the sample, we could derive the dielectric constant of the mineral sample at any desired bulk

density by using the mixing formula 111–27. The dielectric constant of solid polyethylene was found to be $\varepsilon' = 2.25$, and the loss factor tan 6 was smaller than the limit of sensitivity of our method (approximately 0.0005) .

Prior to dielectric measurements, powders were stored in closed jars in dry atmosphere, but no particular effort was made to remove traces of adsorbed atmospheric water We found, however, that a sample of powdered pumice, which had a moisture content of approximately 0.5%, gave the same values of ε' and tan 6 (within limit of our experimental error) as the sample that was thoroughly outgassed in the evacuated waveguide (16 hours at 200°C at 10^{-6} torr pressure)

4. Results of Measurements

The principal objective of the microwave measurements of dielectric constants was to obtain a consistent set of data on the same powders which were the subject of thermal measurements The results of these measurements, performed at two wavelengths (3.28 cm and 1 18 cm), are summarized in Tables III-2, and 111-3. The average experimental error of the values of ε' and ε'' is estimated to be approximately $\pm$ 5% Powders referred to in Tables III-2 and III-3 were lightly packed by their own weight. The bulk densities indicated are typical average values from many individual determinations Particle size and composition of the powders were given in the preceding section

In order to test the applicability of equation III-27 to the powders being tested, we determined the dielectric constant ε' and loss tangent of the solid materials and then calculated the values appropriate to the volume fractions $f = \rho_{powder}/\rho_{solid}$. Results of the measurements are shown in Table 111-4, and results of calculations are shown in Table III-5. The calculated values of ε' were computed from equation 111–27 under assumption of $k = 0$, which is justifiable since $\varepsilon'' << \varepsilon'$ Under this assumption and for a single component, equation III-27 simplified to:

$$\frac{\varepsilon' - 1}{\varepsilon' + 2} = f \frac{\varepsilon'_s - 1}{\varepsilon'_s + 2} \qquad \text{(III-42)}$$

TABLE 111–2

DIELECTRIC CONSTANTS OF POWDERS AT 9.150 Gc/s (λ_o = 3.28 cm)

Sample	Temperature (°C)	ε'	tan δ	ε''
Glass Beads ($\rho \approx 1.60$ gm/cm^3)	-196	2.9	0.0077	0.022
	+ 24	2.9	0.0077	0.022
	+ 98	2.9	0.0082	0.024
Pumice Powder ($\rho \approx 0.90$ gm/cm^3)	-196	2.1	0.0042	0.0088
	+ 24	2.1	0.0045	0.0095
	+124	2.0	0.0051	0.0102
Basalt Powder ($\rho \approx 1.20$ gm/cm^3)	-196	2.9	0.0060	0.0172
	+ 24	2.9	0.0067	0.0194
	+ 98	2.8	0.0136	0.0380

TABLE 111-3

DIELECTRIC CONSTANTS OF POWDERS AT 25.35 Gc/s (λ_o = 1.18 cm)

Sample	Temperature (°C)	ε'	tan δ	ε''
Glass Beads ($\rho \approx 1.60$ gm/cm^3)	−196	2 9	0.0075	0 022
	+ 25	2.9	0.0077	0 023
	+110	2.8	0.010	0 029
Pumice Powder ($\rho \approx 0$ 90 gm/cm^3)	−196	1 9	0.0060	0.011
	+ 25	1.9	0 0070	0.013
	+124	2.0	0.015	0.030
Basalt Powder ($\rho \approx 1.20$ gm/cm^3)	−196	2.8	0.010	0 028
	+ 25	2.8	0.012	0 033
	+125	2.7	0 030	0,080

TABLE III-4

DIELECTRIC CONSTANTS OF SOLID MATERIALS AT 9.150 Gc/s (λ_o = 3.28 cm) **AND** 25°C

Sample	ε'	tan δ	ε''
Glass (melted beads) ($\rho \approx 2.50$ gm/cm^3)	6.5	0.013	0.085
pumice (melted pumicite) ($\rho \approx 2.50$ gm/cm^3)	5.4	0.0072	0.039
Basalt (solid mineral) ($\rho \approx 2.78$ gm/cm^3)	8.6	0.014	0.12

TABLE III-5

DIELECTRIC CONSTANTS OF POWDERS CALCULATED AND MEASURED AT 9.150 Gc/s AND 25°C

Sample	E'		tan δ	
	Calculated	Observed	Calculated	Observed
Glass Beads (f = 0.57)	2.7	2.9	0.0072	0.0077
Pumice Powder (f = 0.36)	1.8	2.1	0.0025	0.0045
Basalt Powder (f = 0.43)	2.7	2.9	0.0062	0.0067

where ε' denotes the dielectric constant of the solid

Similarly, a simplified formula was used for calculation of the loss tangent:

$$\tan 6 = f \tan \delta \qquad \text{(111-43)}$$

where δ_s refers to the solid.

With the exception of pumice powder, the calculated values were found to be in agreement with the measured values within the limits of our experimental accuracy Encouraged by this agreement, we made additional measurements of ε' with a two–component system in which basalt powder was diluted with polyethylene powder. These tests were made at 25 35 Gc/s (λ_o = 1.18 cm) and 25°C The dielectric constant of polyethylene was found to be 1.6. The powders were mixed volumetrically at predetermined volume fractions f The results are shown in Table 111-6. The agreement between calculated and measured values is again good, with the exception of one observation (at f = 0.10) which is in error for unknown reasons

We also determined the dielectric constants of pumice in its natural vesicular form. The test samples cut from the natural rock had a bulk density of approximately 0.42 gm/cm^3 At 3 28 cm wavelength, pumice was found to have values of ε' = 1.56 and tan δ ≈ 0.002; at 1.18 cm wavelength, the values were ε' = 1.59 and tan 6 = 0,008

At the suggestion of Dr Klaus Schocken, we made a few experiments with mineral powders to which a small amount of metallic particles was added In a measurement with pumice powder at 1 18 cm wavelength and 25°C the dielectric parameters of the pure powder were ε' = 1.9 and tan 6 = 0.0070 With a small amount (0 7 wt %) of iron particles added (average size 0.1 to 0.5 micron), the dielectric constant decreased slightly to ε' = 180, and the loss tangent increased appreciably to tan δ = 0,067

TABLE 111–6

DIELECTRIC CONSTANT ε' OF BASALT–POLYETHYLENE POWDER MIXTURES AT 25.35 Gc/s (λ_o = 1.18 cm) AND 25°C

Volume Fraction f of Basalt	ε' Calculated	ε' Observed
1.0	--	2.80
0 5	2 10	2 16
0.33	1 93	1 89
0.20	1 79	1 7 2
0.10	1 70	1.54
0	--	1 60

5. Discussion and Interpretation of Results

Based on the results of the measurements presented in the preceding section we can make the following observations

The three types of silicate materials are characterized by dielectric constants ε' ranging from 5 4 to 8.6 in the solid state and from 1 9 to 2.9 in the powdered state The imaginary parts ε'' of the dielectric constant are quite low (a few per cent of ε')

Dielectric constant ε' is almost independent of temperature from 77°K to 400°K, possibly dropping slightly at the upper temperature limit Also, it is almost invariant with wavelength from 1 18 cm to 3 28 cm. The imaginary parts ε'' of one dielectric constant increase slightly with temperature, particularly from 25 to 125°C This increase is the largest in basalt ε'' and tan δ tend to increase as wavelength decreases but far less than proportionately.

Both ε' and ε'' increase with density of the powder, and their changes with the volume fraction of the solid appear to be expressed with suffi cient accuracy by the theoretical formulas

Penetration depths of microwaves calculated by equation 111–24 from data presented in Tables 111–2, -3, and -4 are summarized in Table III-7 Penetration depths are seen to increase with increasing wavelength The increase is far more than proportional to the increase in wavelength The penetration depth is markedly decreased when a small amount of iron particles is added to the pumice powder.

TABLE 111-7

PENETRATION DEPTH IN MINERALS AND POWDERS AT 25°C

Material	Penetration Depth L_r (cm) at λ_o = 3.28	Penetration Depth L_r (cm) at λ_o = 1.18 cm
Basalt, solid mineral (ρ = 2.78 gm/cm^3)	26	--
Basalt, powder (ρ = 1.20 gm/cm^3)	92	19
Pumice, melted solid (ρ = 2.50 gm/cm^3)	62	--
Pumice, powder (ρ = 0.90 gm/cm^3)	159	39
Pumice, powder (with 0.7 wt % iron particles)	--	4.1

IV THERMAL PROPERTIES

A REVIEW OF EXISTING DATA

In this section we will review briefly pertinent studies of the thermal conductivity of non-metallic materials and the interpretation of lunar infrared measurements which have been reported since our last report (Wechsler and Glaser, 1964) We will not examine these references in great detail but will point out areas which will be discussed in subsequent sections of this report and have significance to our experimental and analytical work,

1 Observational Data and Their Implications

During the past several years, there has been a continuation of observational measurements of infrared and microwave temperatures of the moon during eclipses and lunations Most of these studies have been directed at investigating thermal anomalies which characterize predominant surface features (ray craters, highlands, maria, etc), e.g , Saari and Shorthill (1963) These studies have substantially increased our understanding of the nature of these surface features In addition, several other investigations were carried out by both Russian and American workers

The principal theme of the Russian work is summarized in several papers In a report to the International Space Science Symposium held in Washington in 1962, Troitskii (1962a) presents some results about the nature, thermal conditions, and structure of the lunar surface, obtained from analysis of lunar radio emission data Troitskii makes several interesting conclusions based on measurements of the ratio of the constant part of the lunar radio emission to the amplitude of the first harmonic of this emission The dependence of this ratio on wavelength points out the absence of any visible non-uniformities of the surface up to a depth of several meters Measurements of the lunar radio emission carried out during 1961 resulted in the following temperatures obtained for the constant component; for wavelengths of 1 6 cm, a mean temperature of 208 ± 6°K was obtained; at a wavelength of 3 2 cm, 211 3°K was

obtained; at a wavelength of 9 6 cm, 218 ± 4°K was obtained, On the basis of calculations of the thermal conditions at the lunar surface and measurements of the radio emission at the largest wavelength (9 3 cm), Troitskii concludes that the mean spherical emittance of the moon lies between 0 93 and 0 97 Additional calculations of temperature at the lunar surface and comparison of these temperatures with the radio emission temperatures and the ratio of the constant component to the amplitude of the first harmonic show that the thermal parameter γ has a value of 350 ± 75 Using a specific heat of 0 2 cal/gm°C and a density of 0 5 gm/cm^3 obtained from measurements of dielectric constant, Troitskii concludes that the thermal conductivity of the lunar surface materials is $(1 \pm 0\ 9) \times 10^{-4}$ cal/cm°C sec Thus, Troitskii concludes that the lunar surface material must be porous rather than an unconsolidated dust

Krotikov and Troitskii (1963a) presented a review of data giving the emittance of the moon at centimeter wavelengths From data on the microwave temperatures of the moon, these authors conclude that the reflectivity of the lunar surface at a wavelength of 3 2 cm is between 0 and 0.07 and hence the emittance is greater than 0 93 Further analysis of the radio temperature measurements leads these authors to conclude that the dielectric constant of the surface material lies in the range of 1 1 to 1 7 and that the density of the surface material must be in the range 0 2 to 0.89 gm/cm^3 These values are similar to those reported in the 1962 papers by Troitskii

In a second paper, Krotikov and Troitskii (1963b) report on the thermal conductivity of lunar materials from measurements of lunar radio emission This paper and a companion paper by Krotikov and Shchuko (1963) were discussed in our previous report (Wechsler and Glaser, 1964) The heat balance on the lunar surface during lunation was calculated for homogeneous models of the **lunar** surface as a function of the thermal parameter γ The corrections to the original work by Jaeger were pointed out in our previous report The conclusions drawn from the Krotikov and Troitskii and Krotikov and Shchuko papers are that the best value of the thermal parameter y is 350 ± 75 This, combined with the value of 0 5 gm/cm^3

for the density of lunar material, gives a thermal conductivity, 1×10^{-4} cal/cm°C sec, indicative of a porous material

Three methods are used to obtain this "best" value of thermal parameter The first method relies on the dependence of the time averaged temperature of the lunar surface on the thermal parameter γ Krotikov and Troitskii show that there is a relation between the time averaged temperature and the thermal parameter which decreases from a value of about 280°K at very low values of the thermal parameter to about 220°K at values of gamma of about 1000 Using the microwave measurements of the lunar temperature, the authors conclude that the range of thermal parameters corresponding to a temperature of about 230 to 236°K is between 250 and 450 The authors also show that the ratio of the constant component to the first harmonic term has a much greater dependence on the thermal parameter γ The value of this ratio ranges from about 2 8 at γ = 20 to a value of 1 3 at γ = 1200 From the measurements of this ratio of approximately 1.5 ± 0.1 the range of thermal parameters resulting is between 250 and 550 The third relation that is used to determine γ is the relation between the lunar midnight surface temperature and the thermal parameter Here the dependence of the midnight temperature on γ is about the same as the dependence of the constant component on γ From measured values of approximately 125 ± 5°K, the corresponding values of γ lie in the range 300 to 440, More recent information on the lunar midnight temperature of perhaps 90°K would indicate much higher values of γ, on the order of 1000

Of the three methods used, the dependence of a constant temperature component and a lunar midnight temperature on γ are absolute techniques, i e , lunar surface temperatures are never measured, rather energy emitted from the moon is measured The third technique, using the ratio of the constant component to the fluctuating first harmonic component, does not depend on absolute measurements. From these three techniques the authors conclude that the value of the thermal parameter to within 20% is 350

Estimates of the density of lunar surface materials have been made by Troitskii (1962b), using the following method Troitskii assumes that

the thermal conductivity of rocks in the form of either foams or particulate materials can be expressed as a function of the density of the material and the conductivity of the general group of solid materials of which the foam or particulate material is constituted For both porous foamy materials and friable or particulate materials, Troitskii gives the following relationships:

$$k_1 = k_1 (k_0/\rho_0, \rho), \; k_2 = k_2 (k_0/\rho_0, \rho) \qquad \text{(IV-1)}$$

where subscripts 1 and 7 refer to porous or particulate materials; k_0 and ρ_0 refer to the conductivity and density of the material in the nonporous state; and ρ refers to the density of the material in the porous state Troitskii concludes that for almost all rocks the ratio k_0/ρ_0 varies within the limits of $\pm$ 30% from the value of 0 *8* for material like granite, marble, or basalt; 1 for quartzite; 0 8 for sandstone; and o 6 for limestone. (The units in this equation are conductivity in Kcals-m^{-1} $degree^{-1}$- $hour^{-1}$ and ρ is in $tons\text{-}m^{-3}$) Although Troitskii indicates that the variation of conductivity for various materials under high vacuum has not been studied experimentally to a sufficient extent, there are some data available upon which tentative conclusions of the dependence of thermal conductivity on density may be based For low porosities (up to 20 to 30%), Troitskii indicates that the Maxwell formula for thermal conductivity can be used, i.e., k_1 is approximately equal to k_0/ρ_0 times p For large porosities (greater than *0.4* or 0.5), this formula is incorrect On the basis of experimental data by Woodside and Messmer (1961), Troitskii derives the following formulas:

$$k_1 = a_1 \rho \; k_2 = \alpha_2 \; p, \quad 0 < p < 1.5 \qquad \text{(IV-2)}$$

where α_1 and α_2 are much less than k_0/ρ_0. This expression should be valid in the density interval from 0 to 1.5 g/cm^3 From experimental data on frothy materials in air and data which indicate that the conductivity decreases by a factor of three from air to vacuum, Troitskii concludes that the conductivity of foamy materials is given by the equation:

$$k_1 = 2 \times 10^{-4} \rho \quad (0.2 < \rho < 1.5) \qquad \text{IIV-3)}$$

where thermal conductivity is in the units of cal cm^{-1} sec^{-1} $degree^{-1}$ and ρ is in g/cm^3 For particulate materials, the thermal conductivity has the form given by the following equation:

$$k_2 = 5 \times 10^{-5} \rho \quad (0.2 < \rho < 1.5) \qquad \text{(IV-4)}$$

Using these relationships between conductivity and density, one can then determine the density of lunar materials from measured (or deduced) values of the thermal parameter γ ($\gamma = (k\rho c)^{-1/2}$) The density is given by the formula

$$\rho_1 = \frac{1}{\gamma \times \sqrt{a, c}} \quad (0.2 < \rho < 1.5) \qquad \text{(IV-5)}$$

Substituting the values for *a* derived from the measurements of Woodside and Messmer, Troitskii concludes that $\rho = 160/\gamma$ for a porous frothy material and $\rho = 320/\gamma$ for a friable or particulate material (in these equations γ has cgs units)

Based upon measurements of the thermal parameter γ by Krotikov and Troitskii (1963b), the density of the lunar material is 0.4 ± 0.1 g/cm^3 for porous material or 0.9 ± 0.2 g/cm^3 for particulate material Troitskii concludes that the lower density values correspond better to those obtained from electrical parameters and, therefore, the lunar surface is more probably a porous foamy material Troitskii admits that this method for determination of density is dependent on a rather inaccurate knowledge of the thermal conductivity of material in vacuum and suggests additional studies of the relationship of conductivity and density under vacuum conditions The behavior of conductivity as a function of density and material type has been the subject of a number of investigators. however, little information is available for studies conducted under high vacuum. Later in this report we will examine our experimental data to determine if the relationships between thermal conductivity on density used by

Troitskii are substantiated by our experimental measurements.

The thermal emission in the infrared region of the spectrum for various regions of the lunar surface were examined by Markov and Khokhlova, who measured the radiation emission from the lunar surface in two atmospheric "windows" at 8 to 13 microns and 3 6 microns during the lunar eclipse of August 7, 1963, and during the month of July, 1963 The resolving power of the instrument was about 100 km on the surface of the moon and was thus sufficiently high for reliable separation of the maria and continental lunar areas The authors conclude that the variation in emittance $\varepsilon_{3\ 6\ \text{microns}}$ is from 0.83 (maria) to 0 62 (continent) Although the moon can be considered to be approximately a gray body radiator (i e , no variation in emittance with wavelength), individual sections on the moon show some small variation in infrared emittance It should be noted that these values of emittance are generally lower than those assumed for a lunar surface material in the infrared region From measurements of the unilluminated part of the moon, Markov and Khokhlova conclude that the measured differences in radiative flux from the continental and maria regions of the moon can be ascribed to both variations in emittance of the moon and variation in the thermal parameter $(k\rho c)^{-1/2}$ Based on an average value of γ of 600 (cgs units), the observed difference in radiative flux from the maria and continental areas corresponds to a 20% variation in γ Thus, γ might vary from 480 to 720, with a corresponding 40% variation in thermal conductivity and density

The principal efforts of American and western investigators in the interpretation of lunar observational data involve the examination of lunar surface models in which (1) the thermal properties vary with temperature, (2) thermal properties vary with depth, and (3) the surface material is not homogeneous

The effects of variation of thermal properties with temperature were first considered by Muncey (1962), who assumed that both thermal conductivity and specific heat were proportional to the absolute temperature These assumptions were based upon the data of Scott (1957), which indicated

that the thermal conductivity of evacuated perlite was directly proportional to temperature, and evidence that the specific heat of materials such as Fe_3O_4, $CaCO_3$, and Al_2SiO_5 was directly proportional to temperature Muncey concludes that the observed behavior of lunar temperatures during a lunation and an eclipse can be reproduced very closely by models which consist of a dust layer with a thermal parameter of 1500 at 350°K overlying rock or gravel He also concludes that if the lower substratum were rock with a thermal parameter of 20 at 350°K, up to 80% of the surface might be covered with deep dust

More extensive studies of the effects of variation in thermal properties with temperature have been carried out by Watson (1964), Chiang (1965), and Linsky (1966) Watson examines the eclipse data of Pettit and Nicholson (1930) and Murray and Wildey (1963) using models in which the thermal conductivity and specific heat are either constant or vary with temperature The variation of specific heat with temperature was obtained by least squares quadratic fit to data on quartz and quartz glass (Birch, 1942) The variation of conductivity with temperature had the form:

$$k = B + AT^3 \qquad \text{(IV-6)}$$

with the constants evaluated by experimental measurements with glass beads Watson concludes that: (1) the eclipse data of Pettit and Nicholson may be explained on the basis of models with thermal properties independent of temperature, depth, and lateral variation; (2) the eclipse data of Murray and Wildey cannot be explained using a constant property model or a model in which the material is homogeneous but with thermal properties which vary as indicated above. and (3) no simple model can explain all the eclipse data

Chiang has considered several homogeneous and non-homogeneous models and compared the resultant calculations with the data of Pettit The homogeneous models include:

(1) Constant thermal inertia $(k\rho c)^{1/2}$,
(2) Thermal inertia, $(k\rho c)^{1/2}$, linear dependent on temperature

(i e , k and c are linear dependent on temperature)

(3) Thermal inertia proportional to the square of temperature (i.e., k is proportional to T^3 and c is proportional to temperature)

(4) A combination of models 1 and 2,

(5) A combination of models 1, 2, and 3

Each of these models fails to meet the emphasis in the umbral phase of the eclipse of reaching the observed cooling rate Chiang then considers non–homogeneous models, similar to Fremlin (1959), in which materials of two types, a porous material and base rock, are distributed over the lunar surface Chiang assumes that either the thermal inertia of the porous material is proportional to $T^{1.5}$ (i.e , that ρ and c are independent of temperature and that k is proportional to T^3 >or that the thermal inertia is proportional to T^2 (i.e., c is proportional to T and k is proportional to T^3) Excellent agreement between observational data and calculations is obtained with approximately 3% base rock distributed over the surface Chiang further concludes that the porosity of the surface material is between 69 and 93%, the maximum particle size is in the range from 0 4 to 2 mm, and that the thickness of the porous surface is between 1 and 5 cm. The effective conductivity of the surface material (not the base rock) is in the range from $2\ 25 \times 10^{-13}\ T^3$ (cal/sec cm°C) for a density of 0 89 gm/cm^3 to $1.0 \times 10^{-12}\ T^3$ (cal/sec cm°C) for a density of 0.20 gm/cm^3 Chiang also concludes that the porous material is more likely particulate in nature than a solid with interconnecting pores These conclusions are in substantial agreement with recent Surveyor data

Linsky (1966) considers three different models for lunar surface materials:

(1) Temperature independent thermal properties,

(2) Radiative thermal conductivity ($k = k_c + 4\varepsilon\sigma T^3 S$) specific heat a function of temperature ($C = C_o T^b$), and

(3) Power law approximation to thermal properties (i e,, $k = k_o T^a$ and $C = C_o T^b$).

Linsky also has difficulty in interpreting the eclipse data of Murray and Wildey (1964) and uses the minimum temperature reached during the lunar night for comparison of the different models Because only the minimum temperature is used, each model satisfies the minimum temperature but yields different values of kpc and R (the ratio of radiative to conductive flux) As may be expected from the work of Chiang, the eclipse data of Pettit (1940) is not exactly reproduced by any of the models considered Linsky analyzes the assumptions and conclusions made by Krotikov and Troitskii (1963b) and concludes that the value of 350 ± 20% given for the thermal parameter is based upon dubious infrared measurements, an absolute radio brightness temperature for which small errors greatly affect the conclusions, and an extrapolation procedure that gives ambiguous results In comparing microwave observational data with the temperatures calculated using the various lunar models, Linsky concludes that all of the eight models used are in agreement with the radio data at high angular resolution but that the models including significant radiative energy transfer during lunar daytime are the most plausible The thermal parameters used and corresponding conductivities are given in Table IV-1

Some of the values of conductivity will be compared to our data and other data later These values represent the range of conductivity/density ratios which are in agreement with observational data We note that if the thermal properties are temperature dependent, the most likely values of the thermal parameter are in the range of 625-885 rather than in the range of 280 to 420 given by the Russian investigators

Other calculations of lunar surface temperatures based upon temperature dependent thermal properties have been made by Halajian and Richman (1965) and Winter (1965) Halajian places principal emphasis upon correlating mechanical and thermal properties and relating these to lunar surface materials. Radiative and combined radiative and conductive heat transfer in particulate and vesicular materials are being considered Winter emphasizes examination of the cooling behavior of solids containing periodically spaced deep cavities The results show that there is considerable difference in cooling characteristics of homogeneous solids

Table IV-1

THERMAL PARAMETERS AND CORRESPONDING CONDUCTIVITIES FOR VARIOUS LUNAR MODELS

Model	S (mm)	γ_{350} R_{350}, a, b * (cgs units)	Ratio of Conductivity/Density (k_c/ρ or k_o/ρ) (cal $cm^2/°C$ sec gm)
1		1075	4.33×10^{-6}
2		1075, 250 for x > 30 cm	$4.33 \times 10^{-6}/3.46 \times 10^{-5}$
3	0.16	885, R = 1, b = 0	3.20×10^{-6}
4	0.25	810, R = 2, b = 0	2.55×10^{-6}
5	0.32	750, R = 3, b = 0	2.22×10^{-6}
6	0.27	670, R = 1, b = 1	5.54×10^{-6}
7		850, a = 1, b = 0	1.99×10^{-8}
8		625, a = 1, b = 1	3.63×10^{-8}

* R is the ratio of radiative to conductive heat flux at 350°K, and S is the particle spacing in the radiative model

and materials with parallel wall cavities These differences could explain some of the anomalies in lunar temperature data

2 Analytical Studies

A review of the mechanisms of heat transfer in porous and particulate materials and the analyses which form the basis for our present knowledge of radiation and conduction in non-metallic materials was given in our previous report (Wechsler, et al , 1963) In the interval since this report, few basic analytical investigations of the mechanisms of heat transfer in particulate or porous materials have been reported in the literature We will briefly review those which are pertinent

A critical review of the theoretical equations for predicting the thermal conductivity of mixtures, with particular reference to powders, is given by Godbee and Ziegler (1966) These authors derive a new expression for the effective conductivity of powders in which the effective conductivity is equal to the sum of the contributions of solid conduction only, gas conduction and solid conduction in series and parallel, and radiation. The solid conduction contribution is assumed to be negligible for the authors' investigation (the study of magnesia, alumina, and zirconia powders at elevated temperatures) The radiative contribution is given as:

$$k = 4 n^2 \sigma E (1/V_d - 1) D_s T^3 \qquad \text{(IV-7)}$$

where n is the index of refraction. σ is the Stefan-Boltzman constant. E is the emittance: V_d is the volume fraction of the dispersed phase: D is the particle diameter: and T is the absolute temperature This radiative contribution is similar to that used by many investigators The equations derived for the gas-solid series and parallel conduction were derived using kinetic theory and a simplified model of a well mixed heterogeneous powder in which the isotherms are planes perpendicular to heat flow. The results of the experimental studies confirm the equations derived over a wide range of temperatures However, measurements were not made in vacuum or at low temperatures

Butt (1965) in a study of thermal conductivity of porous catalysts was concerned with the apparent thermal conductivity of the solid phase material. He proposes the use of the following equation originally developed by Wilhelm, et al (1948):

$$\log_{10} (k_s' \quad 10^5) = 0.859 + 3\ 12\ \frac{k_s}{p'} \qquad \text{(IV-8)}$$

where k' is the contribution to conductivity through the solid phase, k_s is the thermal conductivity of the bulk solid, and p' is the porosity of the microporous particles considered (Note that equation (IV-8) is dimensional, i.e., k' is in units of cal/sec cm°C.) The equation is based upon measurements in packed beds with porosities of 0.18 to 0 52 The equation is not suitable for direct correlation with the silver catalyst for which the variation of conductivity with gas pressure was available, With some modifications Butt could correlate conductivity versus pressure data for alumina and silver catalyst pellets

In an examination of heat transfer in non-evacuated cryogenic insulations, Johnson and Hollweger (1965) indicate that a large portion of the heat transferred in gas filled powders occurs in the adsorbed gas film on the particle surfaces as well as across particle contacts These authors also indicate that in many powdered materials extensive relaxation occurs during sample fabrication so that equations in which powder packing loads are used may not be valid

In his study of thermal conductivity of silicate powders in vacuum, Watson (1964) considers the model in which the effective thermal conductivity is represented as:

$$k_{eff} = AT^3 + B \qquad \text{(IV-9)}$$

where A and B are numerical constants dependent upon the particular powder and may be evaluated by experiment The first term represents a "radiative conduction" and is derived in the usual manner, assuming the sample opacity is independent of wavelength and the optical depth of a sample is large. The effects of scattering are neglected but can be considered

as equivalent to an absorption process if the scattering is isotropic The use of equation IV–9 indicates that the solid conduction term is temperature independent Watson indicates that this may not necessarily be the case, but that the other uncertainties in contact conduction make rigorous analyses of the effects of temperature on solid conductivity unwarranted

Watson also analyzes the contact conduction in a bed of uniform size spheres For glass spheres with a Poisson's and Young's modulus of 0.18 and 7 x 10^{11} dynes/cm^2, respectively, the ratio of the solid conduction in a powder bed to the bulk phase solid conduction is given by the formula:

$$\frac{k_{bed}}{k_{bulk}} = \frac{10^{7/3}\, L\, b^{-2/3}}{2 \sum_{i=1}^{L/2b} i^{-1/3}} \qquad \text{(IV-10)}$$

where L is the depth of the bed, and b is the particle radius The sumation takes into account the variation in loading between the spheres at different heights in the bed Table IV-2 presents Watson's numerical results for the solid conduction in the bed

The results given above (for perfect welded contact between the grains across the contact area) indicate that the solid conduction contribution is insensitive to grain size The experimental results, discussed later, indicate that the contact conduction for glass spheres decreases as the particle size increases, and Watson concludes that the thermal contact may be unrelated to the elastic contact The microscopic roughness of the contact surfaces and presence of thin surface films may cause departures from the "welded contact" model

3 Laboratory Measurements

There have been few measurements of evacuated powders or porous materials reported in the literature which are pertinent to the present program. In addition to those discussed in our last report (Wechsler and Glaser, 1964), measurements using ceramic powders and porous catalysts have been carried out but not at significantly low pressures

TABLE IV-2

SOLID CONTRIBUTION TO POWDER CONDUCTIVITY (watt/cm°C)

Particle Size (microns)	L = 0.2 cm	L = 0.5 cm	L = 1.0 cm
1000	8.9×10^{-6}	10.7×10^{-6}	12.8×10^{-6}
200	7.5×10^{-6}	9.7×10^{-6}	11.9×10^{-6}
100	7.2×10^{-6}	9.4×10^{-6}	11.7×10^{-6}
50	7.0×10^{-6}	9.3×10^{-6}	11.6×10^{-6}

Source: Watson (1964)

For example, the work of Mischke and Smith (1962) on alumina catalyst pellets was carried out at 10 to 25 microns; values of conductivity were almost an order of magnitude greater than those reported for evacuated powders in our studies Similarly the conductivity of the catalyst pellets studied by Masamune and Smith (1963a) were on the order of 10^{-3} watt/cm°C at 10^{-2} torr The pellets were quite large and the conductivity value is not representative of a powder material but a pressed or sintered agglomeration of particles

The conductivity values given by Masamune and Smith (1963b) for glass beads were discussed in our previous report The conductivity values obtained at low pressures are on the order of 5×10^{-4} watt/cm°C, an order of magnitude higher than those obtained both in our work and in that of Watson

The most useful and extensive data are those obtained by Watson on silica glass microbeads, quartz, olivine and hornblende powders The particle size, density range, and contributions to thermal conductivity (given by A and B in equation IV-9) are shown in Table IV-3

Several interesting observations may be made from these data. For glass beads, the radiative term is inversely proportional to the particle size down to about 50μ. This suggests two possible causes: (1) an increased opacity with decreasing grain size due to radiative transport between grains and (2) for small grain sizes, thecombined effects of radiation between and through the grains There is no apparent effect of composition on solid conduction or radiative contributions In Watson's experimental method, the density value was obtained from weight and sample height measurements, the latter being difficult to make, Watson did not attempt to correlate the relative contributions with density because of the uncertainties in measurements For most of the materials studied, there appears to be an increasing radiative contribution with increasing density and a decreasing conduction contribution with increasing density This variation is not easily explained. From Table IV-3 it can be seen that the relative magnitude of the radiative to conductive contributions at 300°K varies from about 3 for small glass beads to over 30 for 300 micron beads For other materials the radiative to conductive

TABLE IV-3

THERMAL CONDUCTIVITY OF EVACUATED POWDERS

Material	Particle Size (microns)	Density Range (gm/cm^3)	Radiative Term A ($watt/cm°K^4$)	Solid Conduction Term B ($watt/cm°C$)	Conductivity at 300°K ($watt/cm°C$)
Glass B[illegible]	8 0 [illegible] 8	1 [illegible]- 1 82	26 6 x [illegible]$^{-1}$	-6.6 x 10^{-7}	7.1 x 10^{-5}
Glass B[illegible]	3 [illegible]- 2 [illegible]	1 50 1 61	13 [illegible] x [illegible]$^{-1}$	9.5 x 10^{-7}	3.7 x 10^{-}[illegible]
G[illegible] s B[illegible] ds	125- 8[illegible]	1 [illegible]7 1 6[illegible]	8.5 x [illegible]$^{-1}$	32 2 x 10^{-7}	2 6 x 10^{-}[illegible]
Glass Be ds	74- [illegible]3	1 38 1 6[illegible]	3 [illegible] x 10^{-1}[illegible]	70 0 x 10^{-7}	1.6 x 10^{-}[illegible]
Glass B[illegible]	[illegible]	1 [illegible] 1.47	6 [illegible] x 10^{-13}	[illegible]5 [illegible] x 1 [illegible] ^{7}	2.[illegible] x 10^{-5}
[illegible] sh [illegible] Gla s B[illegible]	[illegible]- [illegible]	[illegible] 8- 0 86	[illegible].4 x 10^{-13}	17[illegible] [illegible] x 10^{-7}	2.7 x 1 [illegible]
Crushed Qu [illegible]	[illegible] - [illegible]	1 22 1 [illegible]6	[illegible] Z x 10^{-13}	3 5 [illegible] x 10^{-7}	4.5 x 1 [illegible]
Crush [illegible] Qua[illegible]	[illegible]	1 [illegible] 1 2[illegible]	[illegible] [illegible] x 10^{-13}	280.0 x 10^{-7}	4.2 x 1 0
[illegible] sh [illegible] Hornblende	[illegible]	1 11 1.50	[illegible] 7 x 10^{-13}	[illegible]2 [illegible] x 10^{-7}	3.5 x 1 0
Crushed Olivine	[illegible]	1 37	12 6 x 10^{-13}	1o9 [illegible] x 10^{-7}	4.5 x 1 0

Data from Watson (1[illegible]6)

contributions range from about 0 3 to 3 5 These values are in the range used by Linsky in his analyses of lunar temperatures, Our data will be compared to Watson's data in subsequent sections of this report

B. THEORETICAL CONSIDERATIONS

For particulate and porous materials in a simulated lunar environment, solid conduction and thermal radiation are the only important contributions to thermal conductivity. In our studies, the effects of gas conduction are eliminated by operation in high vacuum

1 Solid Conduction Contribution to Effective Thermal Conductivity

Solid conduction in powders can be examined in terms of two conduction paths: (1) conduction within the solid comprising the particles and (2) conduction across points of contact between the powder grains Theories of thermal conduction in solids have been described by several investigators (e g , Drabble and Goldsmid, 1961) A substantial amount of data is available in the literature on the thermal conductivity of non-metallic materials, particularly glasses, single crystals, and polycrystalline solids. Conduction in solids is generally attributed to several mechanisms: (1) phonon transport or lattice vibrations and (2) free electron conduction. Lattice vibrations are the important processes in dielectrics where the thermal conductivity is limited by phonon scattering (normal and umklapp processes) and boundary and impurity scattering In amorphous solids "boundary scattering" predominates; in a crystalline material phonon scattering by umklapp processes or impurities predominates Free electron conduction is the more important process in metals

The effect of temperature on the thermal conductivity of solids depends upon the type of material as well as the temperature range, According to classical theory, the lattice conductivity of a pure crystal will be proportional to $1/T$ at high temperatures (above the Debye temperature) As the temperature is lowered below the Debye temperature the lattice conductivity increases rapidly, reaches a maximum, and decreases with a dependence on T^3 near absolute zero The effects of impurities will modify these general rules

In many glasses, it is not possible to separate the radiative and conductive components of heat transfer when making thermal conductivity measurements, and effective conductivity data are used. Figure IV-1 shows the effects of temperature on the thermal conductivity of several glasses It can be seen that the crystalline materials show a decrease in thermal conductivity with temperature, whereas the conductivity of amorphous materials tends to increase in the temperature region between 100 and 400°K. The thermal conductivity of other glasses follows the trends shown in the figure. Given the type and composition of the glass and the state of crystallinity, it should be possible to evaluate or measure the conduction heat transfer within the solid

The phenomenon of conduction heat transfer across areas of contact between particles is more difficult to analyze The effective thermal conductance will depend upon the properties of the solid and the size and nature of the contact areas The size of the contact area is dependent upon the elastic properties of the material, the size, shape, and geometrical arrangement of the particles, and the forces between the particles, In addition, physically or chemically adsorbed gases on particle surfaces may change the contact resistance. In the lunar environment, for example, the lower gravitational force, absence of physically adsorbed gases, possible sintering and aggregation of dendritic structures caused by solar radiation or meteorite infall may have a strong influence on conduction across contact areas

Many empirical and semi-theoretical expressions have been described for evaluating the contribution of solid conduction to thermal conductivity. The independent parameters often used in characterizing the conduction are: true thermal conductivity of the solid, porosity of the media, particle radius, elastic modulus, particle shape factors, applied loading factors and others A review of many relationships used in relating the effective thermal conductivity of a heterogeneous material to these parameters was given in our previous studies (Wechsler, et al., 1963) None of these empirical relationships has been shown to be valid for a wide range of porosities, particle sizes, and material types, especially for fine particles

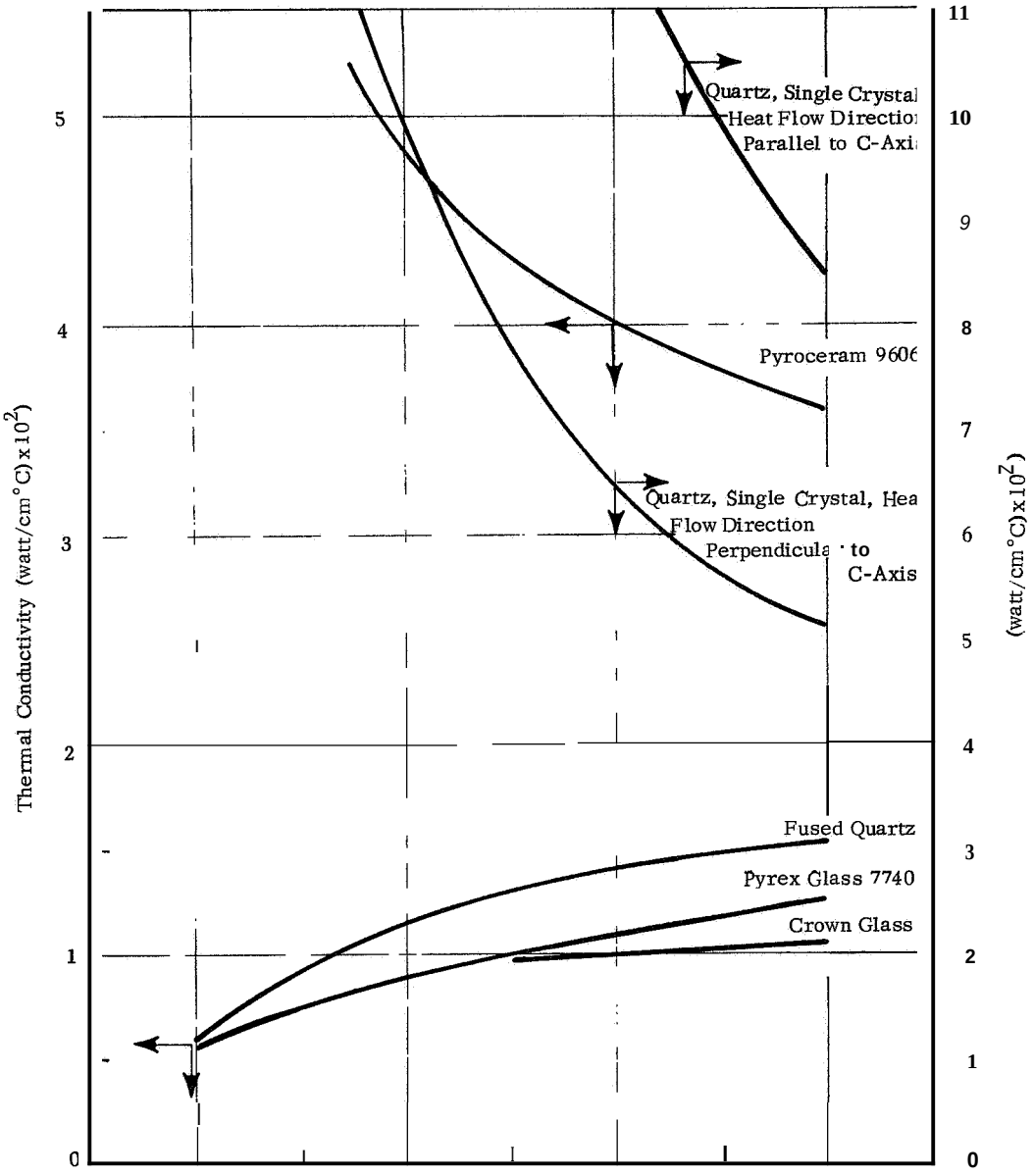
Thermal Conductivity (watt/cm °C) x 10²
(watt/cm °C) x 10²
Quartz, Single Crystal
Heat Flow Direction
Parallel to C-Axis
Pyroceram 9606
Quartz, Single Crystal, Heat
Flow Direction
Perpendicular to
C-Axis
Fused Quartz
Pyrex Glass 7740
Crown Glass
0
1
2
3
4
5
6
7
8
9
10
11

For foamed materials, where the solid conduction is large, agreement between experimental data and several empirical expressions is adequate (Loeb, 1954; Kunii and Smith, 1960)

The work of Watson (1964) in deriving an expression for solid conduction in a particle bed has been discussed (Section IV, A) Although the values obtained from theoretical calculations are of the same order of magnitude as those obtained by interpretation of experiments, the dependence of solid conduction on particle size was not as great as that observed. Because the same types of glass beads were used in Watson's investigations as in our work, his values of the solid conduction may be used to estimate the contribution of solid conduction to effective thermal conductivity These values for glass spheres, based upon a bulk solid conductivity of 10^{-2} watt/cm°C, were given in Section IV, A For other temperatures at which the bulk conductivity is not 10^{-2}, a simple ratio method can be used to estimate the solid conduction contribution.

For quartz at room temperature, Young's modulus varies from 7 86 x 10^{11} dynes/cm^2 to 10.3 x 10^{11} dynes/cm^2, depending upon crystal orientation, Also, there is an increase in modulus with decreasing temperature Because the dependence of contact conduction on the modulus is only the 1/3 power, the contact conduction for quartz should be quite similar to that of glass with a modulus of 7 x 10^{11} dynes/cm^2 If all the contacts were made in the high strength direction, the conduction contribution for quartz should be about 12% less than that of glass. However, the higher thermal conductivity of quartz significantly increases the contact conduction compared to glass

2. Radiation Contribution to Thermal Conductivity

Heat transfer in powders by thermal radiation can take place in several modes Radiation leaving a boundary surface may pass directly through voids to other boundary surfaces if the material is sufficiently porous In fine powders radiation is absorbed and scattered by individual particles and may encounter many reflections and direction changes on passing through the powder material

The calculation of radiative transfer from theoretical principles can be carried out in two stages: (1) calculation of the absorption and scattering characteristics of individual particles and (2) an analysis of the transfer process with allowance for multiple scatter and reradiation

a Single Particle Absorption and Scatter

The absorption and scatter of radiation by a single particle can be equated to the projected area of the particle and to an efficiency factor X_a or X_s which gives that fraction of the area which is effective in absorbing or scattering radiation. The efficiency factors are functions of the index of refraction n, the index of absorption κ, and a ratio of the particle characteristic dimension and the wavelength λ, as follows.

$$X_a = f_1 (n, \kappa, 2\pi r/\lambda) \qquad \text{(IV-11)}$$

$$X = f_2 (n, \kappa, 2\pi r/\lambda) \qquad \text{(IV-12)}$$

The ratio of the perimeter (for a spherical particle) to wavelength, $2\pi r/\lambda$, is usually defined as the size parameter and will be denoted by x.

The efficiency factors may in principle be obtained by the solution of Maxwell's equations A general solution, however, is available only for a sphere and, even then, the solution is in the form of a series of Bessel functions with complex arguments which are tedious to evaluate, Fortunately, when the particles are much larger or smaller than the wavelength of the radiation, solutions may be obtained without recourse to Maxwell's equations The fractions of the radiation incident on a large opaque particle which are absorbed and scattered are given by the absorptivity, α, and reflectivity, ρ, or, in terms of the nomenclature introduced above, when $r >> \lambda$,

$$X_a = \alpha_h = f_1 (n, \kappa) \qquad \text{(IV-13)}$$

$$X_s = \rho_h = f_2 (n, \kappa) \qquad \text{(IV-14)}$$

On the other hand, particles smaller than the wavelength or radiation absorb and scatter according to Rayleigh's equations, When $r < 0.1\lambda/n$,

$$X_a = \frac{24\, n\, \kappa\, x}{(n^2 - \kappa^2 + 2) + 4\, n^2\, \kappa^2} \qquad \text{(IV-15)}$$

$$X_s = \frac{8x^4}{3}\left[\frac{[(n^2 - \kappa^2 - 1)\,(n^2 - \kappa^2 + 2) + 4\, n^2\, \kappa^2]^2 + 36\, n^2\, \kappa^2}{[(n^2 - \kappa^2 + 2)^2 + 4\, n^2\, \kappa^2]^2}\right] \qquad \text{(IV-16)}$$

In the range of particle sizes, where the characteristic dimension is comparable to the wavelength of radiation, the solution to Maxwell's equations must be used Numerical values of X_a and X_s have been computed for spheres for a few values of n and κ and share-distributed programs are available for generating additional values for any n, κ combination.

The distribution of the scattered radiation is also of interest It is given by the phase function $p(\theta)$, which is defined as the ratio of the intensity, scattered in a direction θ to the direction of propagation of the incident beam, and the average intensity of all the scattered radiation. For large particles whose surface reflects specularly:

$$p(\theta) = \left(\frac{\pi - \theta}{2}\right)/\rho_h \qquad \text{(IV-17)}$$

where $\rho\left(\frac{\pi - \theta}{2}\right)$ is the reflectivity for a beam incident at an angle $\left(\frac{\pi - \theta}{2}\right)$ relative to the surface normal, and ρ_h is the hemispherical reflectivity

If the surface of the large sphere is a Lambert diffuse reflector,

$$p(\theta) = \frac{8}{3\pi}(\sin\theta - \theta\cos\theta) \qquad \text{(IV-18)}$$

For small particles,

$$p(\pi) = \frac{3}{4}(1 + \cos^2\theta) \qquad \text{(IV-19)}$$

For particles in the intermediate size range the directional distribution of the scattered intensity is a complex function of angle, in general with scatter predominantly in the direction of propagation (i.e., forward scatter).

b. Absorption and Scatter by Thin Powder Layers

Once the absorption and scatter cross sections and the phase function have been determined, the calculation of the absorptance, reflectance, and transmittance of a thin powder layer is straightforward. A thin layer here refers to a layer thin enough so that the radiation is scattered before it escapes from the layer The fractional absorption of the radiation incident on a layer of thickness dL is therefore given by:

$$\text{absorbed} = \left[\int_0^\infty N(r)\, \pi\, r^2\, X_a\, dr \;\; dL = K_a\, dL \right] \qquad \text{(IV-20)}$$

where N(r) is the number of particles per unit volume whose radius is between r + dr Similarly, the fraction of the incident radiation scattered is:

$$\text{ered} \left| \quad (r)\, \pi\, r^2\, X_s\, dr \;\; dL = K_s\, dL \right] \qquad \text{(IV-21)}$$

The terms in the brackets, representing the fractional attenuation per unit length due to absorption and scatter, are the conventional absorption and scatter coefficients K and K_s.

The reflectance equals the fraction of the radiation scattered backwards, and it may be calculated from the phase function for any directional distribution of incident radiation. The transmittance must, of course, equal the complement of the absorptance and reflectance

The above presentation has assumed that particles scatter independently *The* possibility of interaction has been the subject of a number of

investigations Van der Hulst (1957) gives as a criterion for independent scatter a center-to-center distance of separation between particles of at least 1.5 diameters (this corresponds to particle concentrations less than 20% of the total volume) Churchill, et al. (1960) have arrived at similar conclusions from a study of scatter by latex suspensions. We conclude that the assumption of independent scatter is good for powder systems except for materials which have been compacted under pressure

c Radiation through Deep Powder Layers

The mathematical formulation of the radiative transfer through deep powder layers with allowance for multiple scatter and reradiation by the particles gives rise to an integral equation identical in form to the equations studied extensively by the physicist and the astrophysicist The most general solution, due to Chandrasekhar (1950), gives the transmission and reflection of radiation through absorbing scattering media of thickness L in terms of the optical thickness of the medium $(K_a + K_s)L$, the ratio of the scatter to the total attenuation coefficient $K_s/(K_a + K_s)$, and the phase function $p(\theta)$ Numerical evaluation of Chandrasekhar's solutions have been given by Churchill, et al. (1961) for a number of different situations

A simplified approach to the calculation of radiative transfer through powdered insulation is possible when the powder layers are many mean free paths deep In this case the radiative transfer can be treated as a diffusion process with the flux density at any wavelength given by:

$$q_\lambda = \frac{4\ n^2}{3\ (K_a + K_s)} \frac{dE}{dL}\lambda \qquad \text{(IV-22)}$$

where E_λ is the monochromatic black emissive power The flux density, integrated over the entire spectrum, is then:

$$q = \int_0^\infty q_\lambda\ d_\lambda = \frac{4}{3} \int_0^\infty \frac{n^2}{(K_a + K_s)} \frac{dE}{dL}\lambda\ d_\lambda \qquad \text{(IV-23)}$$

A weighted mean absorption coefficient may be defined such that

$$q = \frac{4\,n^2}{3\,(K_a + K_s)_{ave}} \frac{dE}{dL} \qquad \text{(IV-24)}$$

where E is the total black emissive power given by the Stefan–Boltzman law. This average, known as the Rosseland mean, may be obtained from the following integral

$$\frac{1}{(K_a + K_s)_{ave}} = \int_0^1 \frac{n^2}{(K_a + K_s)_\lambda}\, dg \qquad \text{(IV-25)}$$

where values of g have been tabulated as functions of λT

The above derivations are valid provided $(K_a + K_s)L$ is greater than three throughout the spectrum and the scatter is isotropic Anisotropy of scatter can be included by defining an effective attenuation K related to the true value by the following equation:

$$K = K\,(1 - \overline{\cos\,\theta}) \qquad \text{(IV-26)}$$

where $\overline{\cos\,\theta}$ is a measure of the unbalance of the radiation scattered forward and backward It is given by

$$\overline{\cos\,\theta} = \phi\, p(\theta)\, \cos\,\theta\, d\Omega/4\pi \qquad \text{(IV-27)}$$

and it is zero for isotropic scatter, positive or negative for radiation scattered predominantly forwards or backwards, respectively

d. Application of Powder Systems

For particles which are large or small compared to the wavelength of radiation, absorption and scattering, parameters can be evaluated if the bulk optical properties and refractive indices are known For particles of intermediate size, more difficulty is encountered in evaluating the parameters, but adequate estimates can be made if the optical properties are known.

For most powder layers the diffusion approach to radiative heat transfer will be acceptable in view of the normally high values of absorption and scattering coefficients The effective thermal conductivity due to radiation can be estimated from equation IV-24 for a gray body, as follows:

$$k_r = q_r \frac{\Delta L}{\Delta T} \approx \frac{16\,\sigma\,n^2\,T^3_{ave}}{3\,(K_a + K_s)_{ave}} \qquad \text{(IV-28)}$$

The contribution of radiation to thermal conductivity would be proportional to the cube of the absolute temperature, provided that K_a and K_s were not functions of temperature For gray bodies, where the optical properties are independent of wavelength, the absorption and scattering parameters should be only slightly dependent upon temperature The equation above is the one normally used for radiative transport in porous and particulate materials, where the values of $(K_a + K_s)_{ave}$ are related to the emittance of the material and a function of the particle size or spacing. For real materials, Which in general are not gray, it is necessary to evaluate radiation conductivity from the following equation:

$$k_r = \frac{4}{3} \int \frac{n^2}{K_a + K_s} \frac{\partial E}{\partial T}\, d\lambda \qquad \text{(IV-29)}$$

It is thus necessary to have values for n, K_a, and K_s

e. Measurements of Absorption and Scatter Coefficients

We intended to make experimental measurements of the transmission of infrared radiation through powder samples in order to evaluate these parameters Such measurements proved impracticable for a number of reasons The first and greatest difficulty derives from the great opacity of silicate materials in the spectral range of importance (∿5-31μ for 400°K and ∿19-125μ for 100°K) In reasonable thicknesses most silicates are quite opaque throughout much of this region, although they become more transmissive toward the ends of the region The opacity due to absorption is only a lower limit, because for most particles sizes scattering will also increase the opacity. These conditions result in the requirements for exceedingly thin samples for experimental measurements. Such

powder samples would result in experimental problems involving uncertain areal coverage as well as introducing possible interference effects into the measurements

f Evaluation of Radiative Conductivity from Optical Constants

We decided, therefore, on an approach involving computer calculations, utilizing new theoretical results concerning the radiative properties of fine powders (Emslie, 1966b; Aronson, et al , 1966). By using a fine powder for the test model, we were able to neglect scattering, which falls off rapidly with particle size when the particle size is less than the wavelength Under these conditions the equation used in the calculations (Clark, 1957) was:

$$k_r = \frac{4}{3} \int_0^\infty \frac{n^2 (\lambda, T)}{\alpha (\lambda, T)} \frac{\partial E}{\partial T} d\lambda \qquad \text{(IV–30)}$$

where $\alpha = \frac{4 A K}{\lambda}$

It was shown (Aronson, Emslie, Allen and McLinden, 1966) that the optical constants, n and κ, of a composite medium where scattering is negligible can be represented by:

$$\frac{(n - i\kappa)^2 - 1}{(n - i\kappa)^2 + 2} = \sum_p f_p \frac{(n_p - i\kappa_p)^2 - 1}{(n_p - i\kappa_p)^2 + 2} \qquad \text{(IV–31)}$$

where p refers to the species present (and formally includes vacuum as one of the species) and f is the volume fractions of each of the various species

For several reasons, quartz was chosen as a material for use with equations IV–30 and IV–31 in order to test our calculations. First, the data in the relevant wavelength region (Spitzer and Kleinman, 1961) is of high quality and quartz is a well characterized, easily obtainable

material. Second, because anisotropic crystalline materials have different optical properties in different directions, we were able to test the mixing equation IV-31 by using data from crystals aligned both parallel and perpendicular to the incident radiation Since quartz has a chonchoidal fracture and, therefore, no significant preferred orientation of the crystallites, we were able to assume that twice as many crystallites would be oriented with their optic axis perpendicular (X-cut quartz) to the radiation beam than would be oriented parallel (Z-cut quartz) to it

Using the dispersion parameters obtained by Spitzer and Kleinman (19611, our computer program recomputed the optical constants of quartz in order to avoid errors in reading data points from their graphs The optical constants were then used with equation IV-31 to obtain the "averaged" optical constants. These in turn were used in equation IV-30 to calculate the radiative conductivity The results for a temperature of 400°K are shown in Table IV-4.

The integration was carried out from 5-37μ, excluding less than 7% of the black-body energy for a system at 400°K. It must be remembered that the value of k_r calculated here is an upper limit because scattering will decrease it further The validity of our approach is limited to small size particles and voids (less than a few microns) so that scattering will be small and our mixing rule for composites can be used

These results appear to be in reasonable agreement with the results of experimental measurements of the conductivity which are discussed later. This technique can be applied to other systems provided the optical constants are known. In many cases, it will be more direct to measure optical constants than to attempt to obtain the scatter and absorption coefficients. Furthermore, once the constants are measured, they can be used to predict the radiative conductivity over any temperature range for a variety of packing densities and factors.

3. The Thermal Parameter--$(k\rho c)^{-1/2}$

In many analyses of lunar temperatures the parameter $(k\rho c)^{-1/2}$ has been used. As explained in our last report (Wechsler, 1964) this forms

TABLE IV-4

CALCULATED RADIATIVE CONDUCTIVITY OF QUARTZ AT 400°K

Material	Fraction	k_r watts/cm°K
Z-cut Quartz	1	3.48×10^{-5}
X-cut Quartz	1	2.83×10^{-5}
"Random" Quartz	0.33 Z-cut	2.86×10^{-5}
	0 67 X-cut	
Diluted Random Quartz	0 5 random	$4\ 82 \times 10^{-5}$
	0.5 vacuum	
Diluted Random Quartz	0.1 random	1.91×10^{-4}
	0 9 vacuum	

part of the parameter which controls the surface temperature during lunations and eclipses When the conductivity or specific heat is a function of temperature, the thermal parameter has less significance because it is not constant but varies during the course of the lunation To provide a common point of comparison for use with the data of other investigators we will calculate values of $(k\rho c)^{-1/2}$ taken at temperatures from 200 to 400°K. This temperature range was chosen because it is near the middle of the lunar temperature range and is commonly used for reporting thermal conductivity data.

C THERMAL CONDUCTIVITY MEASUREMENTS

1 Approach

To provide a better understanding of the mechanisms and rates of heat transfer in powdered and vesicular materials, we have carried out a series of measurements of thermal conductivity and analyzed the results in order to ascertain the relative magnitudes of the conduction and radiation mechanisms. The following steps were carried out:

a, Selection and preparation of powdered and porous samples for the test program;

b Measurement of the effective thermal conductivity of the powdered and porous materials in the temperature range from 100°K to 400°K;

c. Determination from the literature or experimental measurements of the dependence of the bulk phase thermal conductivity on temperature;

d. Analysis and correlation of the data on the basis of theoretical models to obtain the radiation and solid conduction contributions to thermal conductivity;

e. Evaluation of the radiation contribution to thermal conductivity by an independent analytical or experimental method and comparison of the results with those obtained from analysis of the experimental thermal conductivity data; and

f Examination and comparison of the experimental data and the ratio of conduction to radiative heat transfer with the results of other experimental measurements

The details of the measurements and the program results are discussed below.

2 Sample Materials

In our initial considerations, we proposed to examine two glasses and two crystalline materials; a natural and an artificial material of each type was to be used Original choices were enstatite, olivine, and silica particles, It became evident that the preparation of these materials in the required size ranges and volumes for the experimental program would not be possible within our present scope of work Also, it was desirable to use materials which had been examined by other investigators and materials for which radiation calculations could be made For these reasons we chose glass beads, pumice, basalt, and quartz powders; pumice and basalt in the natural vesicular form; solid glass and quartz for the program. The principal characteristics of the materials used are summarized in Table IV-5 Experimental measurements were carried out on all samples except vesicular basalt and solid quartz, sufficient literature data were already available on these two materials.

Glass beads were purchased from Microbeads, Inc , Jackson, Mississippi The beads are a soda lime glass and are prepared in a variety of size ranges. Two sizes were ordered. 44-62μ and 22-28μ Also, a sample of the bulk glass used for making the microbeads was obtained The beads with a size of 22-28μ were a special order After eight months' delay, the material could not be provided by Microbeads, Inc , and the order was cancelled.

Approximately 98-100% of the larger size beads pass a No 230 sieve (62μ); 92–100% are retained on a No 325 sieve (44μ). The manufacturer indicates that the thermal conductivity of the bulk material is 2 5 x 10^{-3} cal/cm sec°C (1 05 x 10^{-2} watt/cm°C), that its density is 2 5 gm/cm^3, and that the modulus of elasticity is 11 x 10^6 lb/in^2 (7.6 x 10^{11} dynes/cm^2)

TABLE IV-5

SAMPLES USED IN CONDUCTIVITY MEASUREMENTS

Material	Particle Size (microns)	Density (gm/cm^3)	Porosity (%)	Remarks
Microbeads	44-62	1.42	[illegible]	From Microbeads, Inc ; baked for 14 hours at 600°K in high vacuum.
Pumice powder	[illegible]	0 [illegible]4	[illegible]	Air ground from pumice block, baked at 420°K for six hours in air and at 600°K for 16 hours in high vacuum.
Pumice powder	[illegible]0 [illegible]7	0.82	69	Air ground from pumice block; baked at 430°K for 48 hours in air and at 560°K for 240 hours in high vacuum.
Basalt powder	4[illegible] 7[illegible]	1.4[illegible]	[illegible]	Air ground; baked at 670°K for 48 hours in high vacuum.
Basalt powder	10 3	1 [illegible]6	[illegible]	Air ground; baked at 420°K f r [illegible]Z hours in high vacuum.
Quartz powder	1[illegible]	1.00	62	--
Pumice block	--	0 ≤2	[illegible]	Same as in previous w rk
Solid microbead glass	--	2 5	-	Prepared by melting glass an[illegible] pouring into mold (see text)

Prior to use, the sample was baked out for 14 hours at 600°K under vacuum.

Pumice powder samples were prepared from the pumice sample used in our previous work (Wechsler, et al , 1963) The pumice has an average composition of SiO_2-70.4%, Al_2O_3-15.8%, FeO-1 4%, TiO_2-0.3%, and H_2O-3 2% The powder was prepared by grinding the pumice in air and separating the material by standard sieving methods Two size samples were used 44-74μ and < 37μ. Examination of the sample with smaller particle size showed that 95% of the particles were within the range of 10-37μ. The samples were baked under atmospheric pressure and under vacuum prior to use,

Basalt powder samples were prepared from the vesicular basalt sample (Arizona basalt) used in our previous work (Wechsler, et al., 1963) The nominal composition is: SiO_2-49 1%, Al_2O_3-15.7%, FeO-6.7%, Fe_2O_3-5 4%, MgO-6.2%, CuO-9.0%, Na_2O-3 1%, K_2O-1 5%, TiO_2-0.4%, P_2O_5-0 2%, and H_2O-1 3%. The material was ground in a ball mill in air and sieved to the desired size fraction. Samples with particle sizes of 44-74μ and 10-37μ were obtained. Samples were dried before use in the conductivity measurements

Quartz powder was prepared by crushing and grinding a crystalline quartz sample The particle size range, obtained from microscopic counts of several samples, is estimated as follows:

Size	Volume %
<1μ	1
1- 5μ	95
5-10μ	3
10-30μ	<0.5
'3Q	Negligible

The pumice sample was obtained from the same material used in our previous work No special preparation techniques were used The line heat source (probe) apparatus was drawn through the center of a large sample (See discussion of apparatus) The sample was not baked out prior to use but was evacuated for several days prior to measurements

A solid microbead glass sample was prepared by melting a portion of the glass supplied by the manufacturer in a clay crucible and pouring the

molten glass into a ceramic sample holder containing the wires for the thermal conductivity apparatus The techniques used for making the apparatus are discussed below.

3 Experimental Methods and Apparatus

a Powder Samples

(1) Method. The line heat source method was used for all measurements of thermal conductivity of powders The method was chosen because of its simplicity, the small volume of sample required, and the suitability for use in a high vacuum system.

The constant heat production by a line source of heat enclosed in an infinite volume of material produces a cylindrical temperature field. The temperature rise at any point above the initial ambient (assumed to be uniform) temperature is:

$$T = -\frac{q}{4\pi k} \text{Ei}\left(-\frac{r^2}{4\alpha t}\right) \qquad \text{(IV-32)}$$

where q is the power per unit length, k and α are the effective conductivity and diffusivity of the material, t is the time from the initiation of heating, and Ei represents the exponential integral and is given by:

$$-\text{Ei}(-x) = \int_x^\infty \frac{e^{-x}}{x}\, dx \qquad \text{(IV-33)}$$

The boundary conditions are: $t = 0,\ r \neq 0,\ T = 0$; $t > 0,\ r = \infty,\ T = 0$; and $t > 0,\ r \to 0,\ q = \text{const} = -2\pi r k \frac{dT}{dr}$.

From measurements of the rate of rise of temperature, the conductivity of the sample may be ascertained. In most applications of the line heat source apparatus, it is customary to carry out the experiment for sufficiently long durations so that the exponential integral may be approximated as: $-0.577 - \ln \frac{r^2}{4\alpha t}$. Then, the temperature rise at any distance from the source becomes proportional to time, and the conductivity may be computed from a plot of temperature rise versus logarithm of time In this case, it is not necessary to know the thermal diffusivity or the distance from the source.

Because of the low thermal diffusivity of the powders, it is not desirable to wait the long times required for the logarithmic formula to be valid The conductivity can still be evaluated in the following manner, The temperature rise at any point in the sample is proportional to the heater power, inversely proportional to the thermal conductivity, and proportional to a generalized function of the form Ei $(-\frac{1}{Z})$, where Z represents $4\alpha t/r^2$ Therefore, a plot of logarithm temperature rise versus logarithm time should have the same shape as a generalized plot of logarithm Ei $(-\frac{1}{Z})$ versus logarithm Z

To find the conductivity, the experimental data plot (ln T versus ln t) is fitted to the generalized plot of ln Ei $(-\frac{1}{Z})$ versus ln Z, and the temperature, T*, corresponding to an ordinate (Ei $(-\frac{1}{Z})$) of unity is obtained (In matching the curves it is necessary to maintain the axes parallel) The conductivity is then given as:

$$k = \frac{q}{4\pi T^*} \qquad \text{(IV–34)}$$

Because of the characteristic shape of the curves, they are easy to match and matching errors are usually small.

Several sources of error must be considered in the use of the line heat source, namely: (1) in an actual system, the heat source is neither infinitely long nor thin; (2) the sample has been assumed to be infinite in extent and homogeneous; (3) heater power may vary during a measurement; and (4) temperature measurements may be in error The last two errors may be controlled by careful experimental technique Heater power was constant in our experiments to within $\pm$ 1% and was measured to an accuracy of $\pm$ 2%.

The finite length and diameter of the heat source (and temperature sensor) affect the measurement in two ways. (1) heat is lost by axial conduction along the wire and temperature sensor, and (2) some of the material is displaced by the heater and sensor wires Methods for analyzing these effects are described by Salisbury and Glaser (1964). The error introduced by the finite wire diameter is less than 0 5%for the

wire spacing 0 11 inch and diameter 0 001 inch used The relative error caused by axial heat loss in the heater and thermocouples is given by the equation:

$$\text{error} = \frac{k_w}{2\,k_s}\left(\frac{\pi a}{L}\right)^2 \ln\left(\frac{\pi a}{L}\right) \qquad \text{(IV-35)}$$

where k_w is the conductivity of the heater (or thermocouple) wire; k_s is the sample conductivity; and a and L are the radius and length of the wires We have chosen constantan for the heater wire and an iron-constantan thermocouple because of the low conductivities of these materials For the system we used:

$k_{constantan}$ = 0.225 watt/cm°C

k_{iron} = 0.55 watt/cm°C

a = 0.0005" = 0,0013cm

L = 15 2 cm

k_{sample} = 10^{-5} watt/cm°C

For the worst case of the iron wires in a typical powder sample, the relative error is less than 2%; for the actual case where there is a combination of constantan and iron wires, the relative error should be less than 1% Thus, a line heat source of 15 cm length should be adequate for our measurements We have also examined the effects of sample size and concluded that for most powders a sample 2 cm thick and 2 cm deep should be satisfactory for experiment durations up to four hours It is difficult to assess the effects of sample homogeneity and initial temperature distribution However, care was taken in placing the sample on the apparatus and assuring that a homogeneous sample of relatively uniform density was used. Although the initial temperature distribution in the sample is not known, the change in temperature with time at the sensor was monitored prior to tests. Tests were not initiated unless the temperature drift was less than 0.2°C per hour

In summary, the errors in the applicability of the theory of the line heat source method should be less than ± 2%; errors in evaluating the conductivity from matching the experimental curves with the standard curve are about ± *4%;* errors in measurement of the heater power and length are less than ± 2% Thus the overall error in the measurements should be less than ± 8%

(2) Apparatus and Procedure. A small chamber suitable for use with an ion pumped vacuum system was designed and constructed, Figure *IV-2* shows a schematic diagram of the chamber It is constructed of stainless steel and contains several Conflat flanges which are connected to (1) pumping ports, *(2)* an ionization guage, (3) the sample holder, and *(4)* heater and thermocouple wire feedthroughs The entire system may be baked out by surrounding the chamber with an oven Two Varian 8-liter VacIon pumps are normally used, one during system bakeout and the second during the measurements A copper sample holder was fabricated from sheet copper and copper coils were brazed to the holder The sample holder has dimensions of 16 *5* cm long x 2 *4* cm square The copper coils are attached to stainless steel "pant legs", so that a fluid can be introduced to the interior of the chamber and circulated in the coil around the sample holder. The sample holder and thermocouple–heater wire feedthrough are attached to the vacuum chamber by means of a Conflat flange, so that the holder can be removed from the chamber without disconnecting the cooling fluid or electrical connections Figure IV-3 is a photograph of the sample holder showing the high vacuum flange, electrical lead wires and sample (Basalt powder), Figure *IV-4* shows the line heat source apparatus The base is a copper plate 0 16 cm thick which fits snugly into the sample holder, Pyrex glass supports were originally used to support the heater and thermocouple wires, but these were changes to stainless steel hypodermic tubing (0.020 in. diameter) to reduce breakage during sample preparation A small piece of ceramic tubing was cemented to the stainless steel post to insulate the electrical leads. The heater wire was 0 001 in, (0 *0025* cm) constantan, *8* in (20.4 cm) long. The length of unsupported wire (between the stainless steel or glass posts) was 6 in (15 2 cm) An iron–constantan thermocouple (silver brazed), 0.001 in. (0.0025 cm) diameter

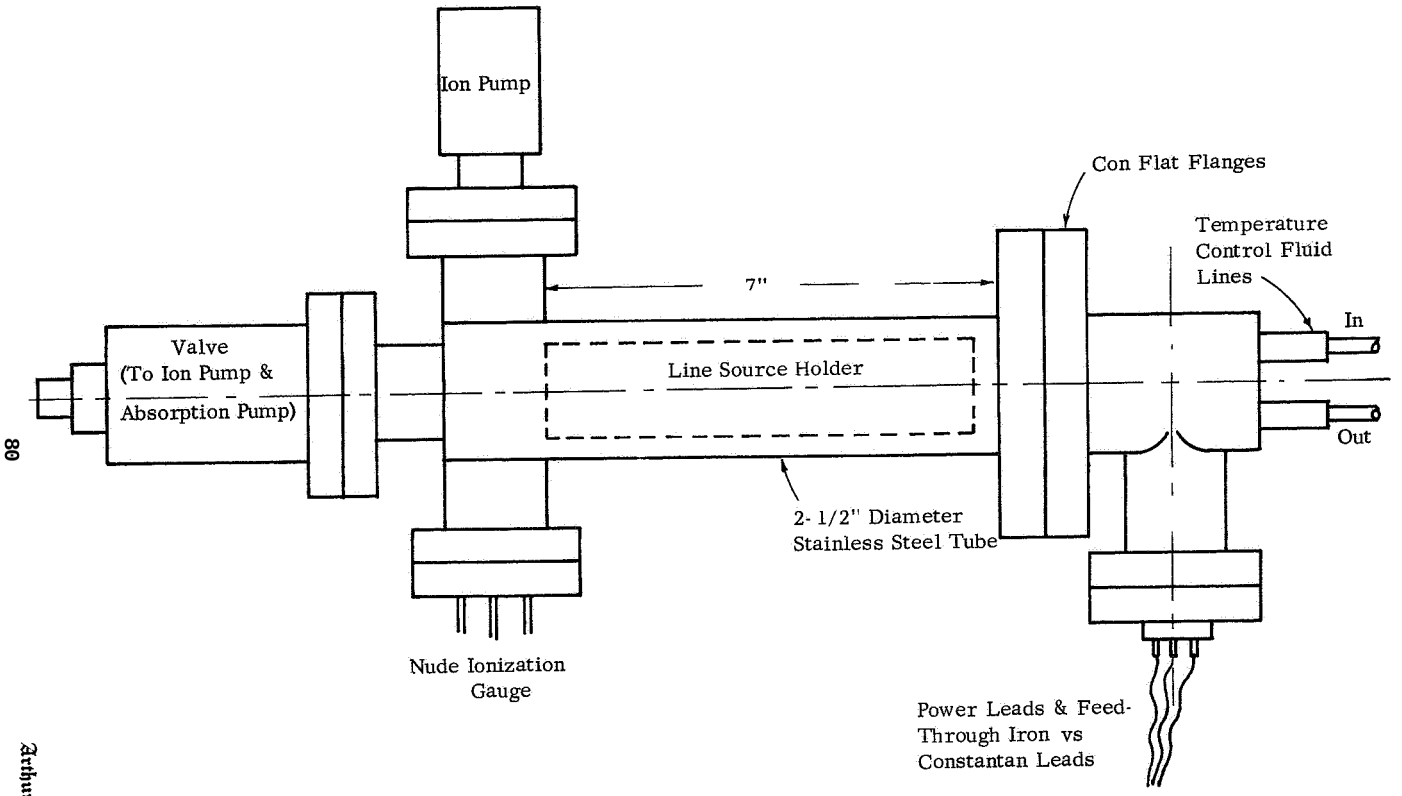

FIGURE IV-2 SCHEMATIC DIAGRAM OF LINE HEAT SOURCE VACUUM CHAMBER

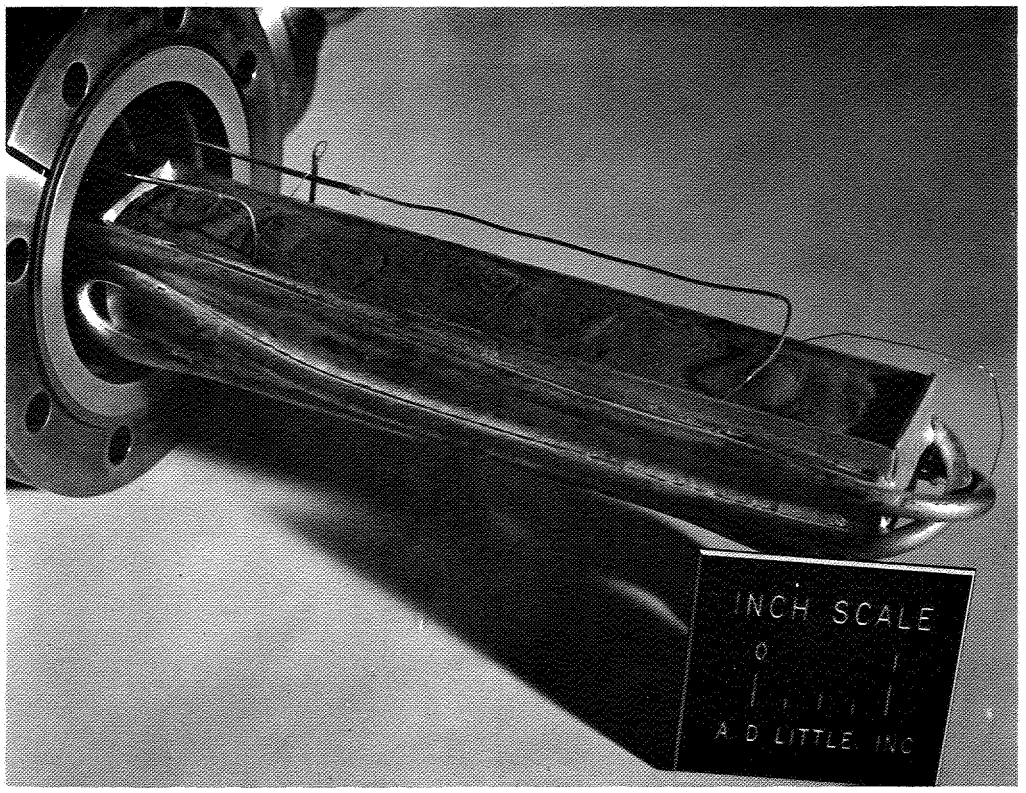

FIGURE IV-3 SAMPLE HOLDER FOR LINE HEAT SOURCE APPARATUS

FIGURE IV-4 LINE HEAT SOURCE APPARATUS

was placed total thermocouple wire length was also 8 in. (20 4 cm) Heavier copper, iron and constantan leads were used for connecting the heater and thermocouple to the feedthrough The feedthroughs, which were silver brazed at one end, were hollow tubes through which the continuous heater or thermocouples were led The resistance of the heater leads was less than 1% of the resistance of the 8 in, length of the one mil constantan heater wire

The remainder of the apparatus consisted of a 12-volt battery as a power supply, a K-3 potentiometer for temperature measurements, a Honeywell Electronik recorder with a full scale deflection of 100 μvolts, and Weston ammeters and voltmeters A recirculating fluid bath with a dry ice-Freon mixture was used to obtain temperatures near -40°C For other temperatures, cold or hot water, hot oil, or liquid or gaseous nitrogen was used as the circulating fluid Pressure measurements were made with a Varian gauge control and a "nude" gauge

The following test procedure was used for all powder tests:

(1) The sample was baked in an oven in air for at least 24 hours and cooled in a dessicator.

(2) The sample was carefully placed on the line heat source apparatus and slightly vibrated to obtain a uniform distribution, the sample was weighed and its dimensions obtained,

(3) The sample holder was carefully placed into the sample chamber and sealed, and the system was baked again under high vacuum after the chamber was slowly evacuated with absorption pumps

(4) After bakeout, the sample and chamber were allowed to cool The high vacuum valve between one of the pumps and the sample was closed, and the other pump (i e , the one which had been baked out) was started

(5) When the sample was at the desired temperature, controlled by the temperature of the circulating fluid, and the temperature change was less than 0 2°C per hour, the initial temperature was measured and a test was started.

(6) Power was applied to the heater, and the response of the thermocouple was recorded, Measurements of the system pressure and heater power were recorded several times during the two hour test period

(7) At the conclusion of the test, the system was allowed to return to thermal equilibrium and another test was carried out at a different heater power or initial temperature,

During the tests with quartz powder and basalt 10-37μ powder, only one VacIon pump was in operation; nevertheless, low sample pressures were obtained.

b Solid Glass Samples

The guarded cold plate, thermal conductivity probe, and line heat source methods were considered for use with solid samples The cold plate has several disadvantages: (1) a large sample size is required; (2) the sample should be flat and have parallel sides; and (3) large gradients are normally used which, in the case of glasses, may introduce boundary effects The use of the probe also requires a fairly large sample in which a hole has been carefully drilled; also, the contact resistance between the probe and the sample may introduce errors.

We chose the line heat source method for the program because it requires the smallest sample, avoids contact resistance problems, and permits measurements to be made as a function of temperature However, it is necessary to embed heater wires and temperature sensors within the glass. Several methods for forming a line heat source in the glass were considered feasible: (1) use of resistance wires embedded in a sample by casting the molten sample into a frame containing and supporting the wires, (2) use of a heater and thermocouple wires casted as above, (3) vapor deposition of thin resistance elements onto carefully prepared glass samples, and (4) preparing two plates of the solid and "sandwiching" the heater and temperature sensors between them. The fourth technique was eliminated after an experimental trial because of the difficulties in preparing the sample in flat plates and eliminating gaps between the plates. The third technique was eliminated because of the high cost and

requirements for plating one sample and then fusing it to another sample On the basis of our past use of thermocouples, we chose to cast a heater and thermocouple wire into a glass sample

In a first attempt to prepare such a sample, glass beads similar to those to be used were melted in a clay crucible and poured into a mold made from magnesia firebrick Although the wires suspended in the mold were distorted because of their thermal expansion and inadequate tension devices, the glass formed a clear mass surrounding the platinum/platinum-rhodium thermocouple and Nichrome heater wires In other tests, we placed platinum wires on a flat slab of glass and covered the glass with an identical slab The slabs were fused in a vacuum oven at 620°C and annealed A distinct interface between the two slabs remained even though they were fused Because this interface could invalidate the experiments, we again tried the casting method After several unsuccessful attempts we prepared a glass sample from the bulk Microbead material by pouring the molten glass onto a heated cast iron "casting plate" containing tensioned wires By slowly cooling the plate, an adequate sample about 4 in. long and 1 in square was obtained A platinum heater wire and a platinum–rhodium thermocouple were used because of their stability in the high temperature molten glass However, the emf of this couple decreases at low temperatures so that it was not satisfactory for use below about -20°C We attempted to prepare another glass sample using a chromel-alumel thermocouple, but a reaction with the hot glass sample prevented us from obtaining a suitable sample

Because of the high melting point of the pumice and basalt samples, we were unable to prepare adequate solid samples of these materials Literature data will be used to estimate the solid conduction contribution for these materials and for quartz

Using the techniques described earlier, we analyzed the effects of axial heat losses and sample size for the line heat source method with solid glasses The results indicated that the effects of sample boundaries would be negligible for experimental times of 4–5 minutes for the 4 x 4 x 10 cm sample Axial heat flow in the sample would not seriously affect the results until after 5 or 6 minutes

Experiments were carried out using a 24 volt battery power supply, and the instrumentation and technique described above for powder samples All measurements were made at atmospheric pressure. The sample was immersed in a Dewar flask containing a stirred fluid for temperature control during measurements

Data were reduced from plots of temperature rise versus logarithm time, Because of the high diffusivity of the glass, the logarithmic method is applicable.

c Vesicular Samples

The principal vesicular material examined in this study was pumice Several attempts were made to prepare a vesicular glass by sintering the glass bead powder, but this approach was not useful until large particle sizes were used The thermal conductivity probe method was chosen to study the vesicular material Analysis of the initial time lag errors and axial heat flow errors was carried out prior to the design of the probe The results indicated that a probe 6 in long and 1/16 in, diameter would be suitable for the measurements. This type of probe was used satisfactorily in our earlier work (Wechsler and Glaser, 1964) Because of the extremes of temperature and vacuum to be used in the program, we investigated the possibility of using a swaged and sheathed probe construction similar to that used in commercially available protected thermocouple assemblies After discussion with manufacturers, a design for a stainless steel sheath, MgO insulated probe 1/16 in diameter, 6-1/2 in. length was evolved The probe would contain a "U" shaped heater running the length of the probe and either a chromel-alumel or copper-constantan thermocouple at the center. With this construction the probes could be baked out at 400°C if desired

Several probes were ordered from Conax Corporation, and a four month delivery was required for this special order. When the probes were received, several difficulties were encountered. The thermocouple locations were only 2 in from the upper end of the probe and several of the internal wires were shorted to the sheath Two probes were returned for repair.

In order not to delay the program, a modified probe was constructed and used for room temperature measurements at pressures of 10^{-4} to 10^{-5} torr The probe consisted of a 0 *023* in *(0,058* cm) diameter stainless steel hypodermic tube, 10 in. (25 *4* cm) long A butt welded copper–constantan thermocouple (#40 wire) was pulled through the stainless steel tube after the tube had been drawn through a block of pumice with dimensions of approximately *25 4* x *14* x *24* cm Current leads and voltage leads were attached to the ends of the stainless steel tube, Thus, the tube itself formed the heater and contained the temperature sensor The sample was placed on a vacuum table, covered with a bell jar, and evacuated to pressures in the 10^{-5} torr range Probe tests were carried out at several power levels, using the instrumentation described earlier

The results of these initial tests were disappointing The time-temperature rise data could not be correlated easily by the logarithmic or the curve matching method The linear relation between temperature rise and logarithm of time existed for only a few minutes rather than the long times expected Furthermore, when the data were reduced as well as possible using either of these methods, the conductivity values were not reproducible, and they were at least an order of magnitude lower then expected Two sources of error may have been poor contact of the probe and the sample or the thermocouple and the sample and resultant axial heat losses. The results obtained in the first five tests carried out at pressures of 1.6 to *3* 8 x 10^{-5} torr, with the data reduced by both methods are shown in Table IV-6

Two tests were then carried out at atmospheric pressure with dry nitrogen Test results at widely different power levels gave conductivity values of 1 29 x 10^{-3} and 1.31 x 10^{-3} watt/cm°C The data were well represented by a linear temperature rise–logarithm time relationship and the results were in agreement with our previous pumice measurements In an attempt to improve the contact between the stainless steel heater and the sample, a larger *0.035* in. diameter tube was inserted in the same hole in the sample, a new copper–constantan couple was used, and two additional tests were carried out. The conductivity values obtained were 5 7 x 10^{-5} and 2.0 x 10^{-4} watt/cm°C. Because these values were also

TABLE IV-6

RESULTS OF THERMAL CONDUCTIVITY MEASUREMENTS OF PUMICE USING 0.023" DIAMETER PROBE

Test	Heater Power (mw)	Thermal Conductivity (watt/cm°C) Curve Matching	Logarithmic Method
F-1	18.9	2.6×10^{-5}	3.0×10^{-5}
F-2	19.9	1.9×10^{-5}	2.1×10^{-5}
F-3	14.2	1.9×10^{-5}	2.3×10^{-5}
F-4	8.3	2.1×10^{-5}	2.4×10^{-5}
F-5	12.0	2.0×10^{-5}	2.2×10^{-5}

lower than expected and not reproducible, we replaced the probe with a 0 032 in diameter stainless steel sheath which contained a #40 heater wire folded 8 times within the tube A copper–constantan thermocouple was used again. As shown in Table IV–7, poor test results were again obtained.

The results could not be explained other than on the basis that there was poor contact between the probe and sample or that the pumice has a very low conductivity in vacuum. Previous test measurements discount the latter possibility Extensive pumice measurements were carried out in our previous work and those results will be used later in the discussion.

4. Experimental Results

The results of the thermal conductivity measurements of powders and solid glass are shown in Table IV–8 and in Figures IV–5 through IV–8 Data are plotted as effective thermal conductivity versus absolute temperature. The curves drawn through the data points are least square lines based upon appropriate theoretical models (See discussion in next section) Also shown in the figures are literature data for each material The density and particle size have been indicated

Examination of the figures shows that the scatter of the data is generally within the reproducibility of the line heat source method As mentioned previously, we have estimated the accuracy of the method to be better thank 8% The reproducibility of the data points should be better than ± 5% (± 4% for error in curve matching and ± 1% in power measurement) "Error bars" corresponding to ± 8% are shown on the curves Several data points which differ significantly from the others are usually the results of tests made at the completion of the thermal cycle

5 Discussion and Interpretation of Results

a. Comparison with Literature Data

In general, good correlation with literature data is shown in the figures The values obtained for the Microbeads are within about 20% of the values reported for similar size and density beads by Watson (1964)

TABLE IV-7

RESULTS OF THERMAL CONDUCTIVITY MEASUREMENTS OF PUMICE USING *0.032"* DIAMETER PROBE

Test	Pressure (torr)	Heater Power (mwatt)	Thermal Conductivity (watt/cm°C) Curve Matching	Logarithmic Method
J-1	1×10^{-5}	*52.0*	3.4×10^{-5}	4.30×10^{-5}
J-2	1×10^{-5}	*12.2*	3.5×10^{-5}	3.80×10^{-5}
5-3	1×10^{-5}	**25.1**	3.6×10^{-5}	3.90×10^{-5}
5-4	5×10^{-2}	*48.3*	4.3×10^{-5}	5.00×10^{-5}
J-5	760	**58.3**	-	1.39×10^{-3}
J-6	760	*112.0*		1.47×10^{-3}

TABLE IV-8

SUMMARY OF THERMAL CONDUCTIVITY DATA

Test No.	System Pressure (torr)	Time at High Vacuum Since Last Test (hrs.)	Heater Power (millivolts)	Initial Temperature (°K)	Thermal Conductivity (watt/cm°C)
Glass Beads 44-62μ					
A-1	2.8×10^{-8}	--	35.9	347	1.70×10^{-5}
A-2	2.3×10^{-8}	24	50.1	345	1.57×10^{-5}
A-3	3.0×10^{-8}	24	27.1	339	1.56×10^{-5}
A-4	4.0×10^{-8}	72	23.6	280	1.34×10^{-5}
A-5	2.0×10^{-8}	24	92.8	283	1.29×10^{-5}
A-6	1.0×10^{-8}	168	50.0	246	1.12×10^{-5}
A-7	1.0×10^{-8}	24	52.1	245	1.07×10^{-5}
A-8	1.0×10^{-8}	168	35.7	223	0.71×10^{-5}
A-9	1.0×10^{-8}	24	51.1	191	0.62×10^{-5}
A-10	1.0×10^{-8}	432	35.5	296	1.10×10^{-5}
Pumice Powder 44-74μ					
B-1	3.0×10^{-8}	--		SYSTEM NOT STABLE	
B-2	2.0×10^{-8}	24	37.1	297	1.21×10^{-5}
B-3	1.5×10^{-8}	24	21.3	297	1.24×10^{-5}
B-4	6.0×10^{-7}	72	35.2	344	1.68×10^{-5}
B-5	7.0×10^{-7}	24	21.9	342	1.80×10^{-5}
B-6	6.0×10^{-7}	24	36.0	340	1.88×10^{-5}

TABLE IV-8 cont'd

Test No.	System Pressure (torr)	Time at High Vacuum Since Last Test (hrs.)	Heater Power (millivolts)	Initial Temperature (^{o}K)	Thermal Conductivity (watt/cm^{o}C)
B-7	2.0×10^{-8}	480	38.2	300	1.22×10^{-5}
B-8	1.8×10^{-8}	48	37.6	238	$.61 \times 10^{-5}$
B-9	2.0×10^{-8}	48	21.3	237	$.79 \times 10^{-5}$
B-10	2.0×10^{-8}	48	21.1	238	$.76 \times 10^{-5}$
B-11	2.0×10^{-8}	72	21.0	207	$.64 \times 10^{-5}$
B-12	2.0×10^{-8}	24	13.2	213	$.72 \times 10^{-5}$
B-13	2.0×10^{-8}	10	14.9	201	$.54 \times 10^{-5}$
B-14	2.0×10^{-8}	72	21.0	300	1.26×10^{-5}
B-15	2.0×10^{-8}	192	23.9	298	1.26×10^{-5}
Basalt Powder 44-74 μ					
C-1	2.0×10^{-6}	--	36.3	298	1.26×10^{-5}
C-2	2.0×10^{-6}	24	45.0	299	1.02×10^{-5}
C-3	1.5×10^{-6}	96	52.8	326	1.65×10^{-5}
C-4	1.0×10^{-6}	72	21.6	351	1.44×10^{-5}
C-5	7.0×10^{-8}	144	48.1	231	0.79×10^{-5}
C-6	6.0×10^{-8}	24	36.3	231	0.92×10^{-5}
C-7	6.0×10^{-8}	24	45.9	229	0.86×10^{-5}
C-8	6.0×10^{-8}	96	50.0	189	0.84×10^{-5}

TABLE IV-8 cont'd

Test No.	System Pressure (torr)	Time at High Vacuum Since Last Test (hrs.)	Heater Power (millivolts)	Initial Temperature (^{o}K)	Thermal Conductivity (watt/cm^{o}C)
C-9	6.0×10^{-8}	24	36 5	184	$0\ 75 \times 10^{-5}$
C-10	6.0×10^{-8}	96	48 1	295	$1\ 12 \times 10^{-5}$
C-11	1.5×10^{-6}	48	50 5	298	1.22×10^{-5}
Solid Glass					
D-1	ATM	--	1270	299	9.76×10^{-3}
D-2	ATM	4	6350	301	$1\ 08 \times 10^{-2}$
D-3	ATM	3	2750	302	$1\ 02 \times 10^{-2}$
D-4	ATM	18	1560	401	$1\ 21 \times 10^{-2}$
D-5	ATM	24	7180	397	$1\ 13 \times 10^{-2}$
D-6	ATM	24	6890	354	0.95×10^{-2}
D-7	ATM	6	3690	354	1.02×10^{-2}
D-8	ATM	72	5650	280	1.05×10^{-2}
D-9	ATM	24	8500	281	0.95×10^{-2}
Pumice Powder 10--37μ					
E-1	3.0×10^{-7}	--	43.3	343	$1\ 73 \times 10^{-5}$
E-2	6.0×10^{-6}	24	33.8	379	$2\ 13 \times 10^{-5}$
E-3	8.0×10^{-6}	24	23.1	381	$2\ 10 \times 10^{-5}$
E-4	6.0×10^{-8}	24	23 0	298	1.45×10^{-5}

TABLE IV-8 cont'd

Test No.	System Pressure (torr)	Time at High Vacuum Since Last Test (hrs.)	Heater Power (millivolts)	Initial Temperature (°K)	Thermal Conductivity (watt/cm°C)
E-5	6.0×10^{-8}	48	22.7	298	1.37×10^{-5}
E-6	3.0×10^{-8}	72	24.6	218	0.99×10^{-5}
E-7	2.0×10^{-8}	24	18.5	218	0.97×10^{-5}
E-8	1.0×10^{-8}	144	19.0	167	0.64×10^{-5}
E-9	1.0×10^{-8}	7	15.0	166	0.60×10^{-5}
E-10	1.0×10^{-8}	24	21.8	164	0.62×10^{-5}
E-11	2.0×10^{-8}	72	21.0	297	1.19×10^{-5}
Quartz Powder < 10μ					
H-1	5.0×10^{-6}	--	20.8	396	4.08×10^{-5}
H-2	5.0×10^{-6}	24	50.3	400	4.19×10^{-5}
H-3	1.0×10^{-6}	24	51.6	387	4.25×10^{-5}
H-4	8.0×10^{-8}	72	51.0	311	3.56×10^{-5}
H-5	5.0×10^{-8}	24	70.5	295	3.46×10^{-5}
H-6	4.0×10^{-8}	24	78.6	296	3.38×10^{-5}
H-7	4.5×10^{-8}	24	50.7	229	3.01×10^{-5}
H-8	6.0×10^{-8}	8	70.5	228	2.97×10^{-5}
H-9	3.0×10^{-8}	24	51.1	200	2.78×10^{-5}
H-10	2.3×10^{-8}	72	50.6	217	3.10×10^{-5}
H-11	1.8×10^{-8}	24	51.2	157	2.42×10^{-5}

TABLE IV-8 cont'd

Test No.	System Pressure (torr)	Time at High Vacuum Since Last Test (hrs.)	Heater Power (millivolts)	Initial Temperature (^{o}K)	Thermal Conductivity (watt/cm^{o}C)
H-12	1.6×10^{-8}	24	66.6	158	2.44×10^{-5}
H-13	4.0×10^{-8}	24	50 3	294	3.28×10^{-5}
H-14	$3\ 7 \times 10^{-8}$	24	67.0	297	$3\ 36 \times 10^{-5}$
Basalt Powder 10-37μ					
I-1	3.0×10^{-6}	-	21.8	356	$1\ 97 \times 10^{-5}$
I-2	3.0×10^{-6}	24	51 9	356	2.08×10^{-5}
I-3	6.0×10^{-8}	24	51.6	297	1.80×10^{-5}
I-4	6.0×10^{-8}	24	34.4	297	1.86×10^{-5}
I-5	3.0×10^{-8}	72	33.3	296	1.81×10^{-5}
I-6	2.0×10^{-8}	24	43.0	229	1.46×10^{-5}
I-7	2.0×10^{-8}	24	34.0	227	1.42×10^{-5}
I-8	$1\ 5 \times 10^{-8}$	24	38 3	177	1.28×10^{-5}
I-9	$1\ 5 \times 10^{-8}$	24	28 7	175	1.22×10^{-5}
I-10	$1\ 7 \times 10^{-8}$	72	33 1	173	$1\ 17 \times 10^{-5}$
I-11	$1\ 8 \times 10^{-8}$	24	31 7	296	$1\ 72 \times 10^{-5}$
I-12	$1\ 0 \times 10^{-5}$	360	30 8	300	$1\ 79 \times 10^{-5}$
I-13	1.0×10^{-8}	196	33 6	297	$1\ 75 \times 10^{-5}$

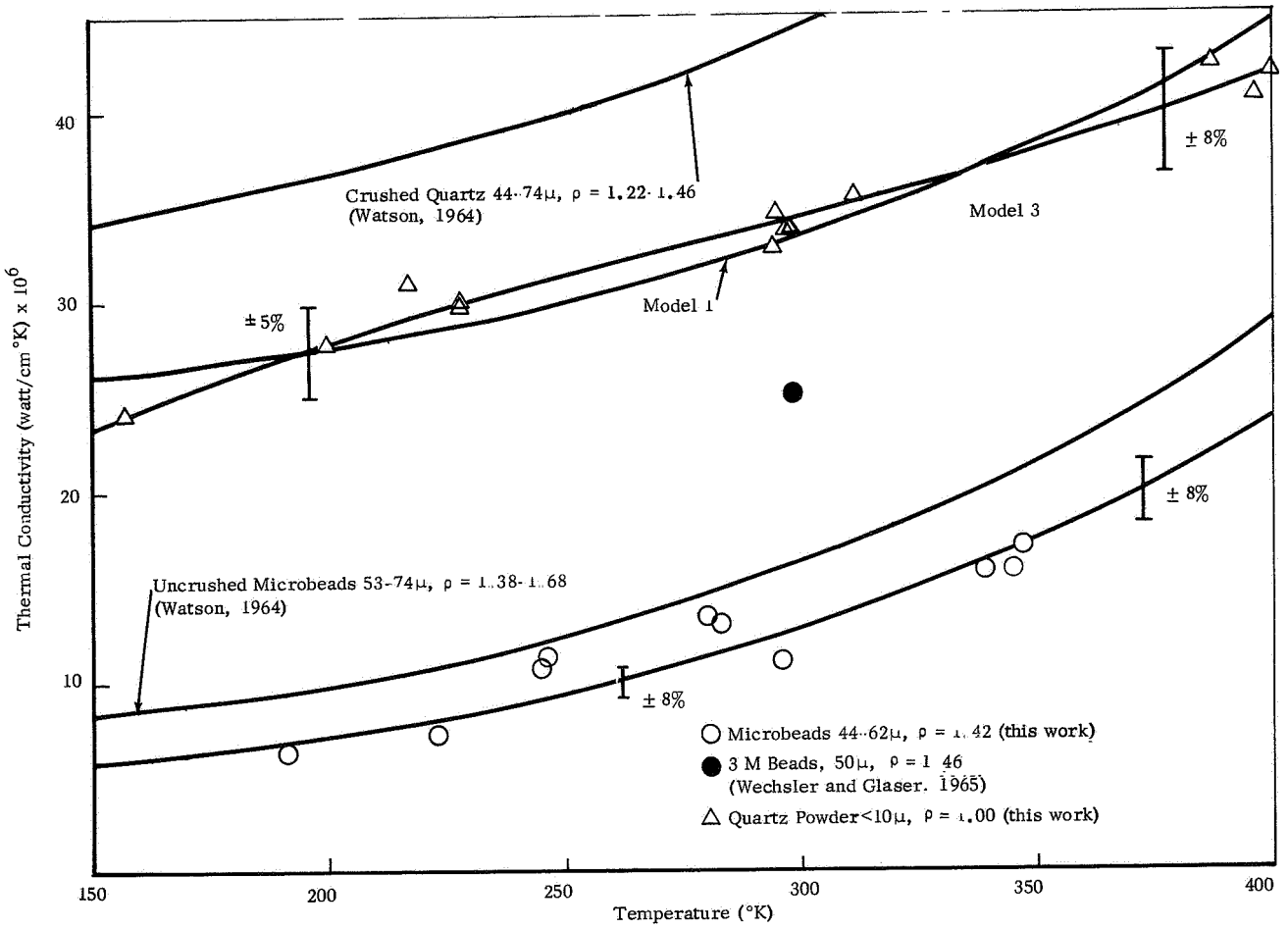

FIGURE IV-5 EFFECTIVE THERMAL CONDUCTIVITY OF GLASS BEADS AND QUARTZ POWDER

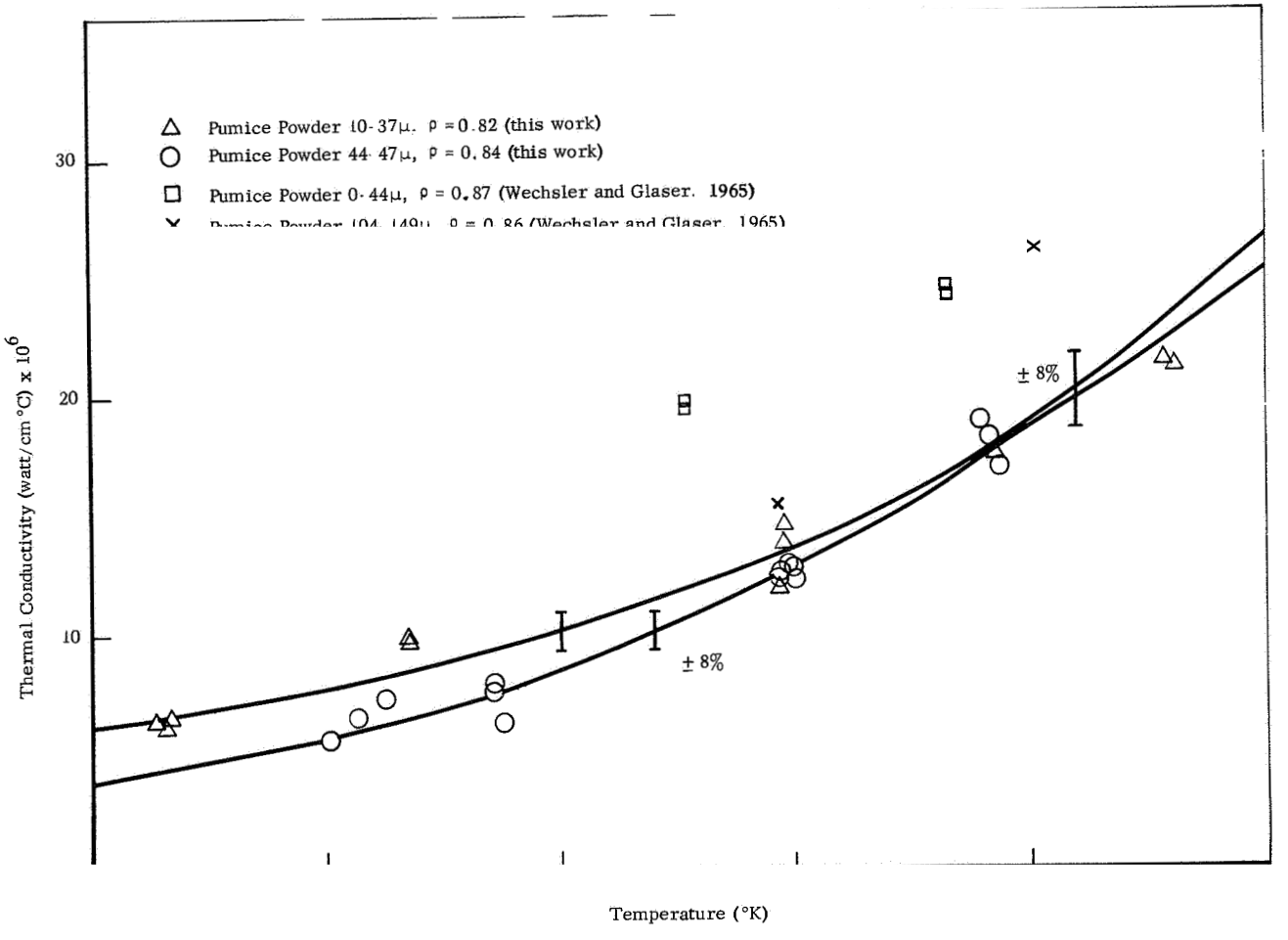

FIGURE IV-6 EFFECTIVE THERMAL CONDUCTIVITY OF PUMICE POWDER

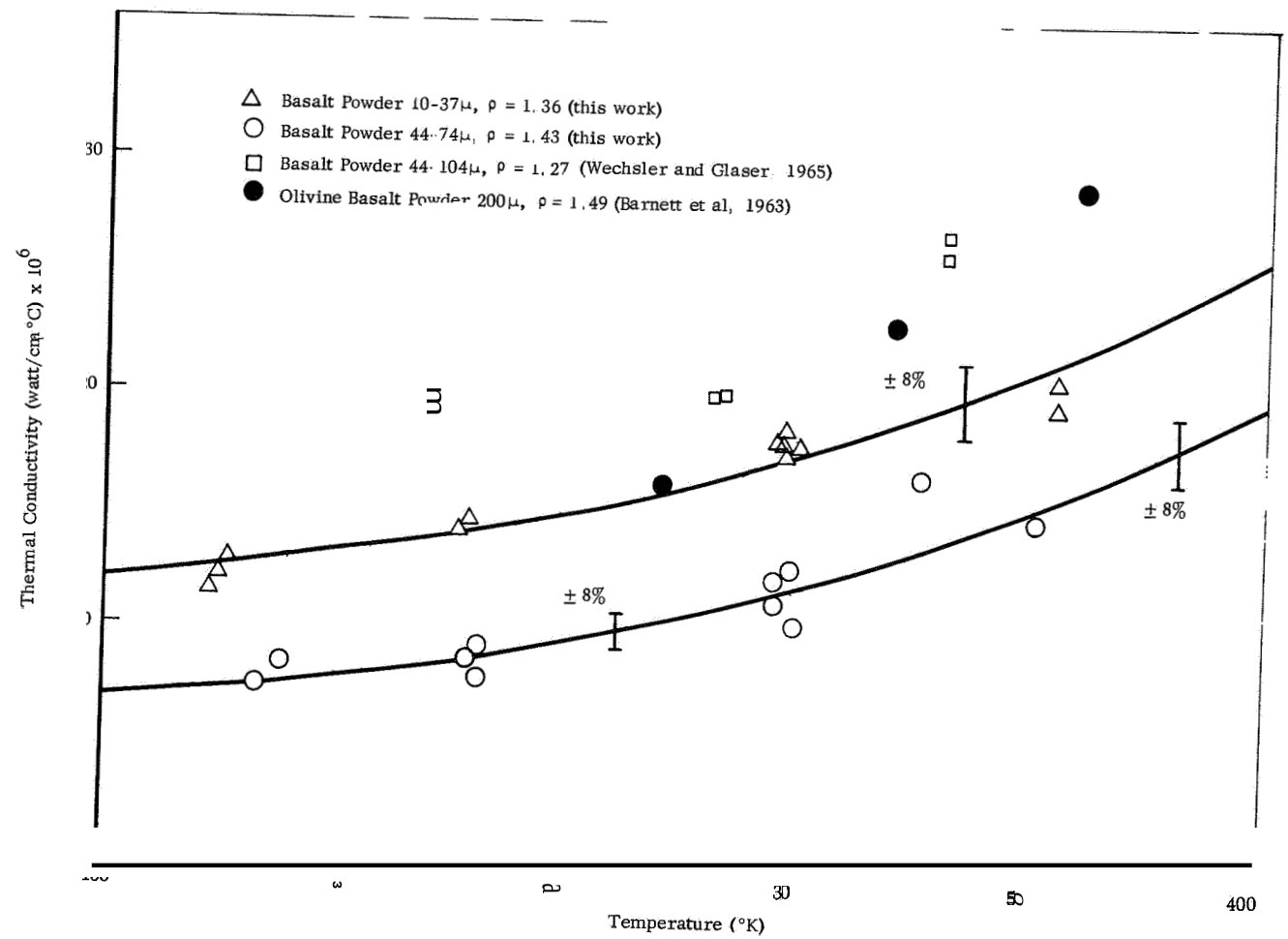

FIGURE IV-7 EFFECTIVE THERMAL CONDUCTIVITY OF BASALT POWDERS

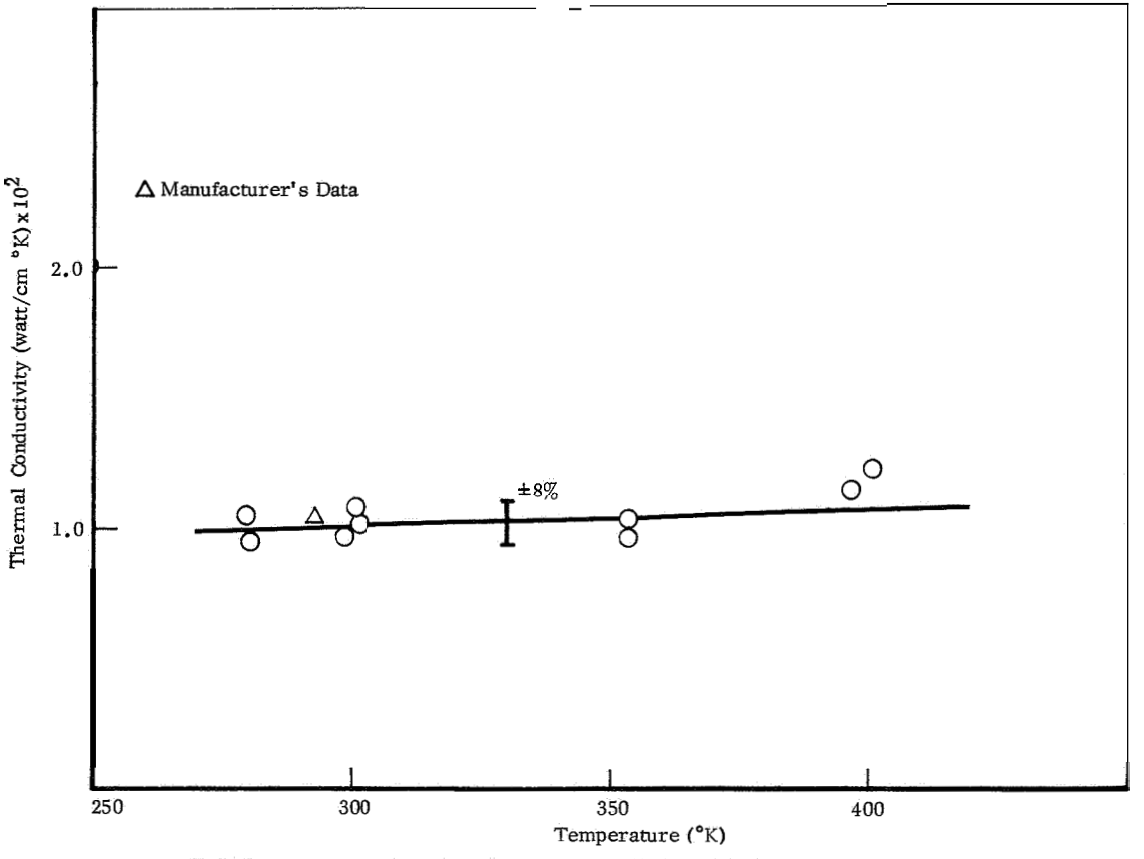

FIGURE IV-8 EFFECTIVE THERMAL CONDUCTIVITY OF SOLID CROWN GLASS

Also the shapes of the curves are very similar Data reported in our previous work on "3M" glass beads of similar size are about twice the values obtained in this work This may be a result of the greater cleanliness of the material used in the present work or a difference in composition.

Data on crushed quartz are within 25% of that reported by Watson (1964) We note that the particle size and densities are considerably different The smaller size powder used in the present experiment could result in a larger solid conduction and smaller radiation contribution which could account for the displacement of our curve from Watson's curve. The shapes of the curves are similar up to 300°K but diverge above this range

Data on pumice powder are only in fair agreement with that given in our previous work. Difference in particle shape, size distribution, and composition (the powders were ground from two similar samples but not necessarily of the same composition) could account for the differences We note that the effect of temperature for both types of samples is nearly the same.

Data on basalt powder are in reasonable agreement with that reported earlier although the trend in decreasing conductivity with increasing particle size does not seem to hold when the present data are compared to the previous work. Discrepancies may be due to the type of basalt, grinding method, and the lower pressure in the present work. All materials show the trend of increasing conductivity with temperature. The data of Barnett, et al (1963) are in fair agreement with the present work but show a slightly greater temperature effect

Data for the solid glass are in excellent agreement with the manufacturer's value. There is essentially no effect of temperature on thermal conductivity The data have also been plotted in Figure IV-1 to show the comparison with Pyrex and fused quartz The values are close to those of Pyrex

b Evaluation of Heat Transfer Mechanisms

(1) Experimental Evaluation. Evaluation of the contributions of solid conduction and thermal radiation to effective thermal conductivity may be carried out by analysis of the effects of temperature on thermal conductivity. As discussed previously, the solid conduction contribution in a powder is a function of the particle size, packing, loading, and other factors, as well as the thermal conductivity of the solid The solid conduction contribution at any temperature can be represented as:

$$k_c = F_1 (\rho, d, \text{load, etc.}) \times k_s \qquad \text{(IV-36)}$$

where F_1 (ρ, d, load, etc.) represents the unknown function of particle parameters, and k is the bulk solid conductivity We have assumed a direct proportionality on the conductivity of the material from which the powder is prepared As shown in Figure IV-1, the bulk solid conductivity varies with temperature in a manner which depends upon the type of solid For glasses, the solid conductivity generally has one of the following forms:

$$\text{glass:} \quad k = \text{constant} = B' \qquad \text{(IV-37)}$$

$$\text{or} \quad k = B' + C' T \qquad \text{(IV-38)}$$

In crystalline materials, the conductivity (over the temperature range we are considering) may often be represented by:

$$k = B' + \frac{D'}{T} \qquad \text{(IV-39)}$$

Thus, the solid conduction contribution to effective conductivity may have any of the following forms:

$$k_c = F_1 B' = B \qquad \text{(IV-40)}$$

$$k_c = F_1 (B' + C' T) = B + C T \qquad \text{(IV-41)}$$

$$k = F_1 (B' + \frac{D'}{T}) = B + \frac{D}{T} \qquad \text{(IV-42)}$$

The radiation contribution to thermal conductivity, as discussed earlier in this section, often has the form:

$$k = AT^3 \qquad \text{(IV-43)}$$

Thus, the effective conductivity of a powder may be represented by any of the following equations:

$$\text{Model 1} \quad k_e = k_c + k_r = B + AT^3 \qquad \text{(IV-44)}$$

$$\text{Model 2} \quad = B + CT + AT^3 \qquad \text{(IV-45)}$$

$$\text{Model 3} \quad = B + \frac{D}{T} + AT^3 \qquad \text{(IV-46)}$$

Models 1 and 2 should be representative of a powder prepared from a glassy material with little or no temperature coefficient of conductivity Model 3 is more representative of a powder prepared from a crystalline material with a strong temperature coefficient The terms B and A should be positive (i.e , the radiation term and the solid conduction should both be positive at low temperatures) The terms C and D may be positive or negative, depending on the type of glass; positive values of C indicate a conductivity increase with temperature, positive values of D indicate a conductivity decrease with temperature.

The experimental data were fitted by least squares techniques to the equations for each model given above The values of the coefficients and the root mean square deviations were examined to establish which model best represented the data

Glass beads. On the basis of experimental data for solid glass (see Figure IV-8), it was clear that Model 1 or Model 2 would be more appropriate

than Model 3 The least squares fit using Model 2 resulted in negative coefficients for C and A, thereby indicating that Model 1 was more appropriate. Values of the coefficients using Model 1 were: B = 4.66 x 10^{-6} watt/cm°C and A = 2.99 x 10^{-13} watt/cm°K^4. The standard deviation of the data from this least squares line was 12%. Using these values, the solid conduction contribution is 4 66 x 10^{-6} watt/cm°C, and the radiative contribution is 2.99 x 10^{-13} T^3 watt/cm°C Values obtained by Watson (1964) for similar size powder were B = 7 0 x 10^{-6} watt/cm°C and A = 3 4 x 10^{-13} watt/cm°K^4 (see Table IV-3) The agreement between our results and Watson's is very good, We also note that there is good agreement between the value of the solid conduction contribution and that calculated from the model described earlier in this section The ratios of the radiation to solid conduction contribution at several temperatures are shown in Table IV-9

Quartz powder. From examination of the data on solid quartz, it was apparent that Model 3 should best correspond to this powder The least squares analysis showed that the root mean square deviations of the data were 5%, 3%, and 2% for Models 1, 2, and 3, respectively. However, the coefficients obtained for Model 2 were unreasonable Values for the coefficients using Model 3 were: B = 37.5 x 10^{-6} watt/cm°C, D = -2 165 x 10^{-3} watt/cm, and A = 1 53 x 10^{-13} watt/cm°K^4 These values indicate that the solid conduction contribution increases with increasing temperature; this tendency is not expected of crystal quartz but is representative of fused quartz For crushed quartz of a larger size, Watson obtained a value of 33.5 x 10^{-6} watt/cm°C for the solid conduction contribution This compares with values of 26.8 x 10^{-6}, 30 3 x 10^{-6}, and 32 1 x 10^{-6} watt/cm°C at temperatures of 200, 300, and 400°K, respectively, using Model 3 If Model 1 is accepted, the value of B is 25 2 x 10^{-6} watt/cm°C. The high value of the solid conduction contribution may be caused by the high conductivity of crystalline quartz Watson's value of the radiative term A was 4.2 x 10^{-13} watt/cm°K^4, compared with the value of 1 53 x 10^{-13} watt/cm°K^4 we obtained using Model 3 and the value of 3.03 x 10^{-13} watt/cm°K^4 obtained using Model 1.

TABLE IV-9

SUMMARY OF SOLID CONDUCTION AND RADIATION CONTRIBUTIONS TO THERMAL CONDUCTIVITY

Material	Solid Conduction Contribution (watt/cm°C)	Radiation Contribution (watt/cm°C)	Ratio of Radiation/Conduction 200°K	300°K	400°K
Glass beads	4.66×10^{-6}	2.99×10^{-13}	0.01	1.73	5.1
Quartz powder	25.2×10^{-6}	3.03×10^{-13}	0.096	0.33	0.77
Pumice powder					
10-37μ	5.09×10^{-6}	3.12×10^{-13}	0.43	1.67	3.9
44-74μ	2.51×10^{-6}	3.57×10^{-13}	1.1	3.83	9.1
Basalt powder					
10-37μ	$6.6 \times 10^{-6} - 1.57 \times 10^{-3} T$	0.83×10^{-13}	0.05	0.154	0.3
44-74μ	6.14×10^{-6}	2.15×10^{-13}	0.28	0.94	2.2

T in °K

On the basis of this comparison, it appears that Model 1 is a better representation of the quartz powder In Figure IV-5, least squares lines for both Model 1 and Model 3 are drawn The radiative contributions may be compared to those calculated earlier. For the quartz powder at 400°K we calculated a maximum k_r of about 60 x 10^{-6} watt/cm°C (extrapolated to the appropriate porosity) The experimental value at 400°K was 19 3 x 10^{-6} watt/cm°C Although the agreement is not excellent, the calculated value is the upper limit which would be further reduced by scattering The fact that some of the particles were comparable to the wavelength would also tend to reduce the calculated value Relative values of the radiative and solid conduction contributions to thermal conductivity at several temperatures are shown in Table IV-9

Pumice powders. Data for pumice powders were best fitted by using Model 1 When Models 2 and 3 were used, no appreciable reduction of the room mean square deviation was observed, and the coefficients C and D were not consistent with the temperature coefficient of vesicular pumice or solid glass For the 10-37μ pumice powder, B and A were 5 09 x 10^{-6} watt/cm°C and 3 12 x 10^{-13} watt/cm°K^4, respectively For the 44-74μ pumice, B and A were 2 51 x 10^{-6} watt/cm°C and 3.57 x 10^{-13} watt/cm°K^4, respectively. The root mean square deviations were 8%for both sets of data Thus the solid conduction contribution decreased for the larger particle size (in agreement with Watson's data), but the radiative term increased only slightly. We note that the conduction term is much smaller than it is €or quartz and is comparable to that for glass beads

Basalt powder. Data for the 10-37μ basalt powder were best fitted by Model 3. Values of the coefficients were: B = 20.6 x 10^{-6} watt/cm°C, D = -1.57 x 10^{-3} watt/cm, and A = 0.88 x 10^{-13} watt/cm°K^4 The rms deviation was 2 7% (compared to 13%for Model 1) Thus the solid conduction contribution increases with temperature Data for 44-74μ basalt powder were best fit by Model 1 with coefficients B = 6.14 x 10^{-6} watt/cm°C and A = 2 14 x 10^{-13} watt/cm°K^4; and an rms deviation of 9% Thus the solid conduction contribution decreases with increasing particle size, and the radiation contribution increases with increasing particle size

Solid glass. The data for the solid glass were well represented by the equation:

$$k_e = B + CT \qquad \text{(IV–47)}$$

where B = 0 845 x 10^{-2} watt/cm°C and C = 0 537 x 10^{-5} watt/cm°C^2, with an rms deviation of 6.6%

The contributions of solid conduction and radiation for the materials studied are also summarized in Table IV–9. The important trends to be observed are: (1) an increase in radiative contribution with increased particle size, (2) a decreased conduction contribution with increased particle size, (3) the relatively high values for solid conduction for quartz and basalt powders, (4) the low radiative contribution for the small diameter basalt powders, and (5) the ratio of radiative to conduction contribution for the powders studied increases with temperature and has values from 0 05 to 9 1 over the temperature range of 200 to 400°K

(2) Analytical Evaluation, Theoretical models for the radiation contribution to thermal conductivity in a particulate or fibrous material prepared by various investigators have the form given by equation IV–43. The values of the constants are given below

$A = 4 \sigma \varepsilon D_p$ 6	Damkohler (1937)
$A = 4 \sigma \varepsilon D_p (\delta^{-1} - \delta^{-1/3} + \delta^{1/3})$	Russell (1935)
$A = 4/3 \sigma D_p$	Rosseland (1936)
$A = 4/3 \sigma D_p \frac{(1 - \delta)}{\varepsilon}$ (for fibers)	Strong, et al (1960)
$A = 4 n_r^2 \sigma D_p \varepsilon \frac{\delta}{1 - \delta}$	Godbee and Ziegler (1966)
$A \approx 4 \sigma \varepsilon D_p$	Schotte (1960)

where

σ = Stefan–Boltzman constant

ε = particle emittance

D_p = particle diameter

δ = porosity

n = refractive index

Values of the radiation constant term for the powders investigated shown in Table IV 10 are generally lower than those obtained by experimental fit of the data, One reason for the difference in values is that the optical mean free path in the expressions given above is assumed to be equal to the product of the particle diameter and a porosity factor For materials which are partially transparent, as quartz and glass are in the wavelength region of 0 5–5μ, the mean free path may be significantly greater than a particle diameter. Furthermore, only the equation of Godbee and Ziegler correctly includes the index of refraction, Closest agreement of the experimental data is obtained with the predicted values of Godbee and Ziegler Variations in the index of refraction and the incorrect use of an average value can account for the discrepancy between the predictions and experiment.

We have calculated the radiative conductivity for quartz at 400°K, according to the method outlined in Section IV, E, 2, f The value obtained for powder of 62%porosity is 6.0 x 10^{-5} watt/cm°C at 400°K This value compares with that of 3.33 x 10^{-6} watt/cm°C, evaluated from the Godbee and Ziegler correlation, and that of 1 94 x 10^{-5} watt/cm°C obtained experimentally. The significant difference between the results of the simplified correlation and the more complex calculation procedure indicates the effects of taking into account the variation of optical constants with wavelength and the distribution of the solid phase material, The experimental value is lower than the value we calculated because the method used in Section IV, B, 2, f does not include scattering which will further reduce the radiation heat trasnfer contribution,

TABLE IV-10

CALCULATED VALUES OF RADIATION CONSTANT A, w/cm°K^4*

Method	Material					
	Quartz <10μ	Glass Beads 44-62μ	Pumice 10-37μ	Pumice 44-74μ	Basalt 10-37μ	Basalt 44-74μ
Damkohler (1937)	3.4 x 10^{-1C}	4.0 x 10^{-14}	3 7 x 10^{-14}	8.9 x 10^{-14}	2.9 x 10^{-14}	6.6 x 10^{-14}
Russell (1935)	1.76 x 10^{1C}	2 7 x 10^{-13}	6.5 x 10^{-14}	1 5 x 10^{-13}	8.0 x 10^{-14}	1.9 x 10^{-13}
Rosseland (1936)	c 5 x 10^{-15}	4.0 x 10^{-14}	1.8 x 10^{-14}	4.5 x 10^{-14}	1.8 x 10^{-14}	4.5 x 10^{-14}
Strong, et al. (1960)	1 7 x 10^{-15}	2.7 x 10^{-14}	5.8 x 10^{-15}	1.4 x 10^{-14}	8.5 x 10^{-15}	2.2 x 10^{-14}
Godbee and Ziegler** (1966)	5 2 x 10^{-1C}	1.3 x 10^{-13}	2.6 x 10^{-13}	6.2 x 10^{-13}	1.4 x 10^{-13}	3.0 x 10^{-13}
Schotte (1960)	1.4 x 10^{-1C}	1.2 x 10^{-13}	5.4 x 10^{-14}	1 3 x 10^{-13}	5.4 x 10^{-14}	1.3 x 10^{-13}
Experimental	3 03 x 10^{-13}	2.99 x 10^{-13}	3 12 x 10^{-13}	3 57 x 10^{13}	0.88 x 10^{-13}	2.14 x 10^{-13}
Watson (1964)	c z x 10^{-13}	3.4 x 10^{-13}	-	-	-	-

* Calculated using an emi[illegible]ance of 1 [illegible]dpor s:[illegible] = [illegible] f [illegible] i e given in Tab[illegible] IV-3
**Calculated using an ind[illegible] of ef a [illegible]onof 1 '

The solid conduction contributions to effective thermal conductivity have been evaluated by the method proposed by Watson (1964) and described in **111,** B, 2 For a material with elastic modulus E (dynes/cm^2), and Poisson's ratio v, the ratio of solid conduction in the powder to solid conduction in the bulk may be written as:

$$\frac{k_c}{k_b} = \frac{b^{-2/3} L \left\{\frac{\pi \rho g (1 - \nu^2)}{E}\right\}^{1/3}}{2 \sum_{i=1}^{L/2b} i^{-1/3}} \qquad \text{(IV-48)}$$

where L is the particle depth, b is the particle radius, ρ is the bulk density; and g is the acceleration due to gravity Using available data for the moduli and solid thermal conductivity (Birch, 1942), the values of solid conduction contribution of the powder shown in Table **IV-11** were evaluated for a temperature of 300°K

As noted on Table IV-11, and in the work of Watson, particle size has little effect on the solid conduction contribution calculated from the equation given above The high value for quartz is caused by the high thermal conductivity at 300°K. Except for the agreement between the measured and calculated values for the smaller size basalt powder, the experimentally obtained values of the contact conduction are lower by a factor of 2 to 5 than those calculated These results indicate that a detailed understanding of contact resistance between particles has not yet been established. To increase **our** understanding, additional analyses of the solid conduction contribution must be performed In addition, experimental measurements should be carried out under conditions where solid conduction can be examined independently of other system variables

D. CORRELATION OF THERMAL CONDUCTIVITY AND DIELECTRIC CONSTANT MEASUREMENTS

In order to evaluate the correlations between dielectric and thermal parameters using the results obtained on the various materials studied, we calculated the values of the parameter C_1 which, according to equation III-31 should be a constant and independent of density and possibly other

TABLE IV – 11

CALCULATED VALUES OF SOLID CONDUCTION CONTRIBUTION OF VARIOUS POWDERS

Material	Size μ	k_c (experimental)	k_c (calculated)	
Glass beads	44-62	0.47 x 10^{-5}	116 x 10^{-5}	watt/cm°C
Pumice	44-74	0 51 x 10^{-5}	1.37 x 10^{-5}	"
Pumice	10-37	0.25 x 10^{-5}	1 35 x 10^{-5}	"
Basalt	44-74	0 61 x 10^{-5}	1.58 x 10^{-5}	"
Basalt	10-37	1.54 x 10^{-5}	1 56 x 10^{-5}	"
Quartz	10	2.50 x 10^{-5}	9.49 x 10^{-5}	"

variables. The results are shown in Table IV-12 Even though the experimental evidence presented here concerns only three materials it is evident that the presumed "constant" C_1 varies greatly with density This cases some doubts on the assumptions made in the derivation of equation III-31.

One of these assumptions was that of the proportionality of δ to the wavelength (equation III-30). δ_n is the ratio of the electromagnetic to the thermal penetration depth as defined by equations III-3 and III-24 While the ratio of δ_n/λ_o should be independent of wavelength, we find that it varies considerably; in pumice powder it has values of 13 and 9.8 at 3 28 and 1.18 cm wavelengths, respectively, and in basalt powder it has values 10 and 5.8 at the same wavelengths, respectively

We also attempted to obtain an empirical correlation between dielectric constant (or loss tangent) and thermal conductivity The results were not satisfactory. The correlation between dielectric constant and thermal conductivity can easily be evaluated by examining the effect of density on each of these parameters. Figure IV-9 shows the variation dielectric constant (3.28 cm) and the loss tangent at the same wavelength with density. As expected from the discussion presented earlier, there is a strong correlation between ε' and density; namely, that the logarithm of the dielectric constant is proportional to density A similar relation holds for the loss tangent, if the data for pumice (the lowest of the loss tangent data points) are assumed to be on a separate curve. The dependence of thermal conductivity on density for the materials we studied is shown in Table IV-13

Although there is a general trend toward increasing thermal conductivity with density, there are several exceptions; namely, (1) the vesicular pumice's having a very low density with a moderately high conductivity, (2) the insensitivity of thermal conductivity with density of the powders, and (3) the increase of thermal conductivity of over 1000 with a 3-fold increase in density. (The dielectric constant varies only by a factor of 3 or 4 for the same density variation.)

TABLE IV–12

VALUES OF "CONSTANT" C OF EQUATION 111–31

Material	T (°K)	$\sqrt{k/\rho C}$ (cm sec^{-2})	$C_1 = \sqrt{\epsilon'} \tan \delta \sqrt{k/\rho C}$ at A = 3.28 cm	at A = 1.18 cm
Glass, beads (ρ = 1.6 gm/cm^3)	300	3.2×10^{-3}	4.2×10^{-5}	4.2×10^{-5}
	400	4.4×10^{-3}	6.2×10^{-5}	7.3×10^{-5}
Glass, solid (ρ = 2.8 gm/cm^3)	300	7.5×10^{-2}	2.5×10^{-3}	not determined
Basalt, powder (ρ = 1.2–1.4 gm/cm^3)	300	4.1×10^{-3}	4.5×10^{-5}	8.2×10^{-5}
	400	5.7×10^{-3}	1.3×10^{-4}	2.8×10^{-4}
Basalt, solid (ρ = 2.6–2.8 gm/cm^3)	300	6.9×10^{-2}	2.8×10^{-3}	not determined
Pumice, powder (ρ = 0.80–0.90 gm/cm^3)	300	4.2×10^{-3}	2.75×10^{-5}	4.0×10^{-5}
	400	6.1×10^{-3}	4.4×10^{-5}	9.3×10^{-5}
Pumice, vesicular* (ρ = 0.4–0.5 gm/cm^3)	300	4.5×10^{-2}	1.1×10^{-4}	4.5×10^{-4}
Pumice, glass** (ρ = 2.5 gm/cm^3)	300	6.5×10^{-2}	1.0×10^{-3}	not determined

* Thermal conductivity data from previous work (Wechsler, 1964).
** Thermal conductivity of solid pumice assumed equal to solid crown glass

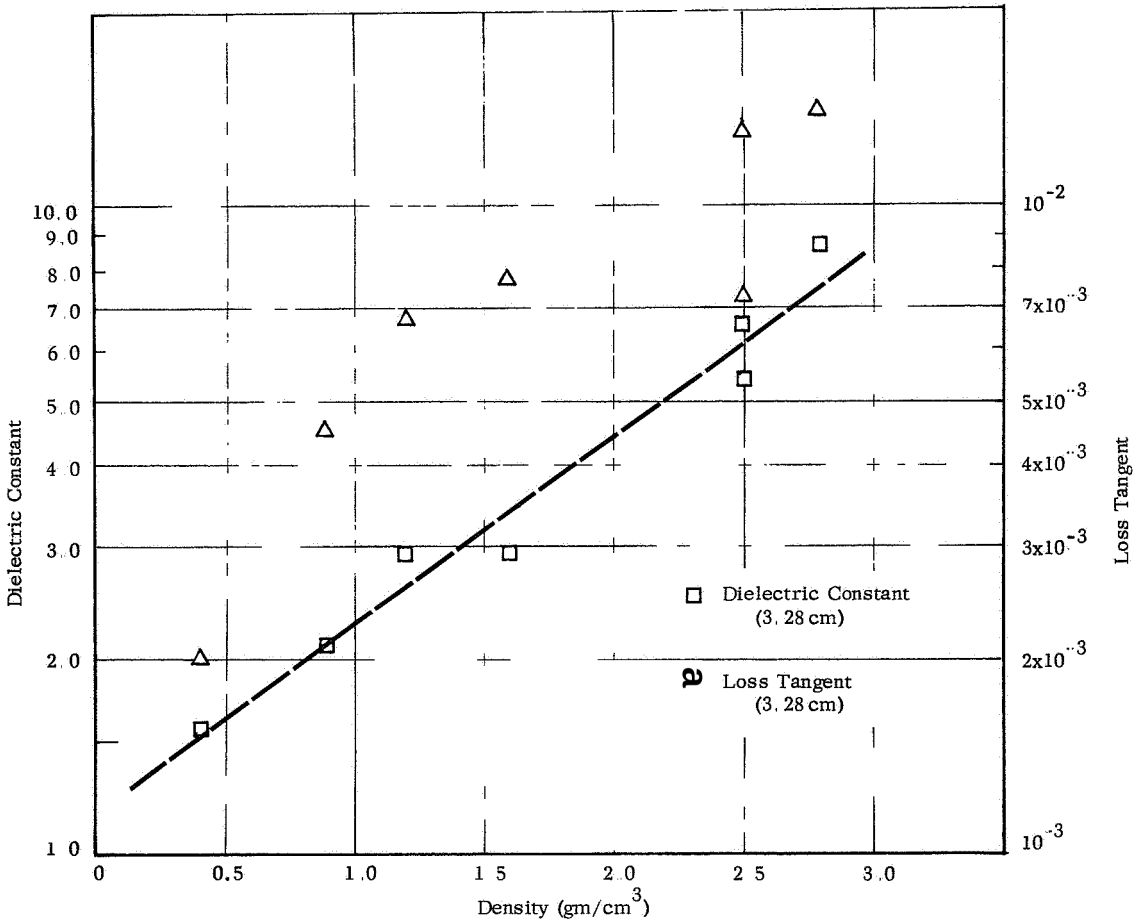

FIGURE IV-9 VARIATION OF DIELECTRIC CONSTANT AND LOSS TANGENT WITH DENSITY

TABLE IV–13

DEPENDENCE OF **THERMAL** CONDUCTIVITY ON DENSITY

Material	Density (gm/cm^3)	Measured Thermal Conductivity at 300°K (watt/cm°C)	Thermal Conductivity Calculated from Troitskii Equation (watt/cm°C)
Pumice	0.4 –0.5	1×10^{-3}	4×10^{-4}
Pumice powder	**0.8**	$1.2–1.4 \times 10^{-5}$	$1\ 7 \times 10^{-4}$
Quartz powder	1.0	$3.2–3.5 \times 10^{-5}$	$2\ 1 \times 10^{-4}$
Basalt powder	***136–1.43***	$\mathbf{1.0\text{-}1.8} \times 10^{-5}$	2.9×10^{-4}
Glass beads	1.42	$1\ 2 \times 10^{-5}$	3.0×10^{-4}
Solid glass	2.5	$\mathbf{1} \times 10^{-2}$	$\boldsymbol{2.8} \times 10^{-2}$
Solid basalt	2.8	$2–3 \times 10^{-2}$	3.1×10^{-2}

Also given in the table are the thermal conductivity values calculated from the correlations used by Troitskii (see Section IV, A). The values obtained for the vesicular and solid materials are in good agreement with experimental data however, calculated values for the particulate materials are much higher than those measured This difference between calculated and measured values has considerable bearing on the conclusions reached by Troitskii concerning the properties of lunar surface materials

Whereas the dielectric constant is directly related to density, the thermal conductivity is apparently more a function of mechanical strength, cohesion, or state of aggregation of the material. For this reason we would expect a more adequate correlation of thermal conductivity with bearing strength, sonic velocity, or other indications of the structural properties of the samples

E APPLICATION OF THE RESULTS OF POSTULATED LUNAR MATERIALS

The objective of this program has been to provide data on the thermal conductivity and dielectric constant of silicate powders and solids It was not our primary aim to attempt to assess possible lunar surface materials on the basis of the observational data and measurements made in this study; however, some of the results and conclusions we have reached have direct application to the evaluation of lunar materials and possibly materials on other planetary surfaces

1 The Thermal Parameter $(k\rho C)^{-1/2}$

As discussed in Section IV, the thermal parameter $(k\rho C)^{-1/2}$ is often used in evaluating lunar surface materials because, for constant thermal properties and density and assumed constant emittance and absorptance, the thermal parameter completely specifies the surface temperature of a semi-infinite material exposed by periodic radiation flux The experimental measurements carried out in this program have shown that the assumption of constant thermal properties is not justified in analyzing lunar temperature data, particularly when powdered materials are considered. As an illustration Table IV-14 gives values of the thermal parameter ($sec^{1/2}$ cm^2 °C/cal) at various temperatures. In calculating

TABLE IV-14

EFFECT OF TEMPERATURE ON **THERMAL** PARAMETER

Material	Thermal Parameter ($sec^{1/2}$ cm^2 °C/cal) 200°K	300°K	400°K
Glass beads	1480	1070	790
Quartz powder	820	790	700
Pumice powder (14-74μ)	2140	1380	970
Pumice powder (10-37μ)	1820	1380	1010
Basalt powder (44-74μ)	1380	1120	820
Basalt powder (10-37μ)	1080	930	770
Pumice (vesicular)	200	180	160
Solid glass	31	29	27

these values, we have assumed the specific heat to have the constant value of 0 2 cal/gm°C

Although the value of $(k\rho C)^{-1/2}$ for evacuated powders is near 1000 and in agreement with most data, there is a variation of over a factor of 2 in the thermal parameter of some powders over the lunar temperature range. (Because the specific heat of most silicates also increases with temperature, the actual variation of the thermal parameter would be greater than that shown in the table.) We recommend that in all subsequent analyses of lunar infrared data the thermal conductivity be represented by a constant term plus a term with a cubic temperature dependence, as was done by Linsky (1966) and Chiang (1965) Also, the effect of temperature on specific heat should not be overlooked in these analyses For simplified calculations, values of $(k\rho C)^{-1/2}$ of *700-1500* ($sec^{1/2}$ cm^2 °C/cal) represent most of the powdered materials we studied over the range of 200 to *400°K.*

2. Ratio of Radiation to Conduction Heat Transfer

As discussed in Section IV, Linsky (1966) uses values of 1 to 3 for the ratio of the radiative to conductive heat transfer at 350°K The ratios we obtained experimentally at *350°K* were: glass beads, 2 *75;* quartz powder, 0.51; pumice powder (10-37μ), 2 63; pumice powder (44-74μ), 6 1; basalt powder (10-37μ), 0 23; basalt powder (44-74μ), 1 50 Our results indicate that the range of values used by Linsky should be expanded However, the thermal parameter values which we obtained differ by less than *40%* from those used in Linsky's analysis. We recommend that in subsequent calculations values of radiative/conductive flux of about 0 3 to 6 be used, depending upon the powder size and composition

3 Lunar Surface and Subsurface Temperatures

The surface and subsurface temperatures of the moon may be calculated using the thermal conductivity data presented in this report and estimates of the emittance and absorptance of the lunar surface As an example, we have calculated the surface temperatuare for a homogeneous particulate surface and a homogeneous vesicular surface (see Figure IV-10) The thermal properties used in the calculations were:

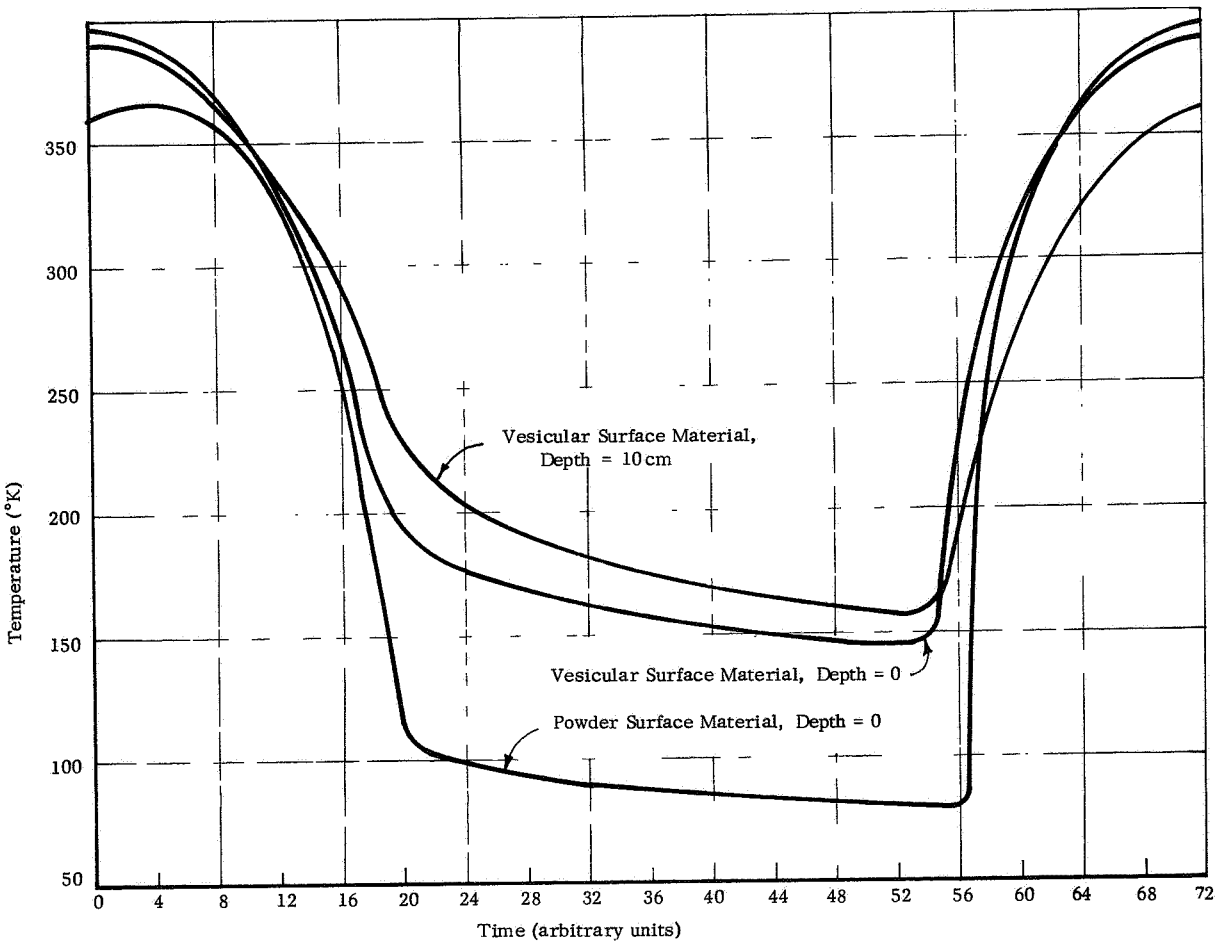

FIGURE IV-10 CALCULATED SURFACE AND SUBSURFACE TEMPERATURES DURING A LUNATION

	k (watt/cm°K)	ρ (gm/cm^3)	C (joules/gm°K)
Powder	$4.62 \times 10^{-6} + 3.05 \times 10^{-13} T^3$	1.1	$0.502 + 7.4 \times 10^{-4} T$
Vesicular	$1.5 \times 10^{-3} + 0.2 \times 10^{-5} T$	0.9	$0.502 + 7.4 \times 10^{-4} T$

where T is in °K

Values of infrared emittance and solar absorptance were chosen as 0.93 (These calculations were performed in another program carried out at Arthur D. Little, Inc Details of the computation program may be obtained in the report, "A Study of Thermal Response of the Lunar Surface at the Landing Site during the Descent of the Lunar Excursion Module (LEM)", Technical Report prepared by J T Holland and H. C Ingrao, Harvard College Observatory, Cambridge, Massachusetts, April 1, 1966)

Although the surface temperatures obtained from calculations with the powder properties are not exact duplications of observational data, the maximum and minimum temperatures and the slope of the temperature-time curve during lunar night are in relatively good agreement with published data. The curves presented here would differ considerably from those obtained with materials having constant thermal properties

4. Dielectric Constant Values

The values of the dielectric constant obtained in this program may be considered typical for silicate powders We suggest that in the analysis and evaluation of radio emission data from silicate particulate surfaces, values of 2.0 to 2 9 be used for the real part of the dielectric constant and values of 0.004 to 0.015 be used for the loss tangent The variation of the dielectric constant and loss tangent with density shown in Figure IV–9 and the trend of increasing loss tangent with temperature as shown in Table III-2 and III-3 should be considered when examining radio emission data in detail.

V. CONCLUSIONS

On the basis of the results presented in the preceding sections, we have made the conclusions which are detailed below

A DIELECTRIC CONSTANT

1. The dielectric constants of the silicate powders we studied at 3 28 cm and 1.18 cm wavelengths have values ranging from 1.9 to 2 9 The loss tangents of these materials vary from about 0.004 to 0 030. The dielectric constants of the solid silicates from which the powders were prepared are in the range 5.4–8.6.

2. There is no significant difference in the dielectric constant of the powders at the two wavelengths studied. The loss tangents of the powders are larger at the shorter wavelength

3 The effect of temperature on the real part of the dielectric constant of the powders is negligible over the range 77°K to 400°K The imaginary part of the dielectric constant and the loss tangent tend to increase at the upper temperature limit of this range, particularly for basalt powders.

4. The dependence of the dielectric constant of the powders on density is adequately represented by theoretical formulas which relate the dielectric constant to the fraction of the solid and the dielectric constant of the solid.

5. There is no well defined correlation between thermal conductivity and dielectric constant of the silicate powders The correlation proposed by Troitskii does not hold for the powders and solids we studied

6. If the dielectric properties of the lunar surface are similar to those of the minerals and powders studied in this work, the penetration depth of microwaves is much greater than the thermal penetration depth (approximately 40 times greater for 3 28 cm waves and 10 times greater for 1.18 cm waves)

7 Small amounts of metallic (iron) particles present in the dielectric silicates tend to decrease the penetration depth significantly

B. **THERMAL** CONDUCTIVITY

1 **The** effective thermal conductivities of typical evacuated quartz, pumice, basalt, and glass powders of particle size 5-75μ vary from about 4×10^{-6} w/cm°C to near 40×10^{-6} w/cm°C over the temperature range 150 to 400°K.

2. **The** effective conductivity of the evacuated powders studied is well represented by the sum of the constant term and a term which has a cubic temperature dependence

3. In the temperature range of 150 to 400°K, the ratio of the radiation to solid conduction contributions to effective thermal conductivity varies from **less** than 0.1 to more than 5, depending upon the particular powder size and composition

4. In the powders we examined, the solid conduction contribution to effective thermal conductivity decreases with increasing particle size, and the radiation contribution increases with increasing particle size,

5 The radiation contribution to effective thermal conductivity can be predicted adequately on the basis of available correlations which take into account the refractive index and its variation with wavelength.

6 **The** solid conduction contribution to thermal conductivity cannot be predicted adequately using correlations which consider only Hertzian contact areas and the thermal conductivity of the solid.

7. **There** is no direct correlation between thermal conductivity of particulate, vesicular, and solid silicates and density. The structure of the material seems to influence thermal conductivity more than density

8. In analyzing lunar infrared temperature data, the thermal parameter should not **be** treated as independent of temperature. A more desirable procedure is to include the variation of both specific heat and density with temperature.

VI. RECOMMENDATIONS

To gain more insight into the mechanism of heat transfer in particulate and porous materials under conditions such as exist in the lunar and other planetary environments, we recommend that studies be continued to establish the following in more detail: (1) the conduction and radiation contributions to effective thermal conductivity as a function of particle or cell size and temperature, (2) the absorption and scattering mechanisms for radiation attenuation as a function of particle or cell size, (3) the effects of adsorbed gases on the conduction contribution to heat transfer

The results of the first two studies will be of fundamental importance in determining the thermal behavior of powders and vesicular materials that may be present in the lunar environment *The* third study is also of importance in determining the behavior of powders or vesicular materials in the terrestrial and Martian environments.

To carry out these studies four types of experimental measurements or calculations must be made: (1) measurement, using the modified line heat source method, of the thermal conductivity of a specific material in the solid form as a function of temperature over an extended range; (2) measurement of the effective thermal conductivity of the particulate and vesicular form of this material as a function of temperature (70 to 450°K), particle size (1-100μ), and adsorbed gases (e.g , water, nitrogen, and carbon dioxide); (3) calculation of the effective radiation conductivity of these forms of the same material, making allowance for both absorption and scattering; and *(4)* acoustic measurements, such as compression wave velocity, attenuation, and bulk modulus To obtain the most complete information and to establish most accurately the relative importance of the heat transfer mechanisms, we recommend restricting attention to various physical forms of a single material that has a well-characterized composition.

Because of the importance of dielectric parameters for the interpretation of radio-astronomical and radar observations of lunar and planetary surface properties, we recommend that the measurements be extended both to

shorter and longer wavelengths than those used in this work. We recommend using those materials considered for thermal property measurements Also, the effects of adsorbed gases, primarily water and carbon dioxide, on the dielectric constant and loss tangent should be evaluated.

VII REFERENCES

Aronson, J R , Emslie, A. G., Allen, R. V , and McLinden, H G.(1966), "Far Infrared Spectra of Silicate Minerals for Use in Remote Sensing of Lunar and Planetary Surfaces", Final Report, Contract NAS8–20122 to George C. Marshall Space Flight Center, NASA.

Barnett, E. C , et al (1963), AIAA Journal, 1, 6, p 1402

Birch, F edit (1942) "Handbook of Physical Constants", Geological Soc of America, Special Paper No 36

Butt, J B. (1965), AIChE Journal, 11, 1, p 106.

Chandrasekhar, S (19501, "Radiative Transfer", Oxford, Clarendon Press, 1950

Chiang, C. W. (1965), Unpublished work conducted by University of Denver for Air Force Research Laboratories under Contract No AF 19(628)-4797

Churchill, S W , Clark, G C., and Sliepcevich, C. M (1960), Disc Faraday Soc., 30, 192

Churchill, S W., et al (1961), "Exact Solutions for Anisotropic, Multiple Scattering by Parallel Plane Dispersions", University of Mich , College of Engineering, DASA–1257

Clark, Jr , S. P (1957), Trans Amer Geophys. Union, ***38,*** p 931

Damkohler, G. (1937), Der Chemi–Ingenieur, Eucken–Jacob Vol III, Part I, 445, Akrademische Verlagegesellschaft MBH, Leipsig

Daniels, F B (1961), J Geophys Res , ***66,*** p 1781

Drabble, J R., and Goldmid, H J (1961), "Thermal Conduction in Semi–conductors", Pergamon Press, New York.

Emslie, A G (1966), Monthly Progress Report No 9, this program, Contract No NAS8-20076), 10 January 1966,

Emslie, A, G (1966b), "Theory of the Diffuse Spectral Reflectance of a Thick Layer of Absorbing and Scattering Particles", AIAA Paper, No 65–667, to be published in Progress in Astronautics and Aeronautics.

Evans, J V , and Pettengill, G H (1963), J Geophys Res , 68, P 423.

Everest, A., Glaser, P E , and Wechsler, A, E. (19621, "Thermal Conductivity of Non–Metallic Materials", Summary Report, Contract No, NAS8–1567, Arthur D. Little, Inc , 27 April 1962

Fensler, W. E., Knott, E. F , Olte, A., and Siegel, K M. (1962), "The Electromagnetic Parameters of Selected Terrestrial Rocks and Extraterrestrial Rocks and Glasses", in "The Moon", Ed., by Z. Kopal and Z Mikhailov, Academic Press, London, p 545–565

Fremlin, J H. (1959), Nature, 183, p 1316

Gardon, R (1950), J. Amer Ceram. Soc., 39, 278, 1950.

Gary, B , Stacey, J , and Drake, F D. (1965), Astrophys J , Suppl. No, 108, 12, p 239.

Gibson, J E. (1958), Proc, Inst Radio Eng , 46, p 280

Godbee, H. W., and Ziegler, W T (1966), J Appl, Phys , 37, 1, p 40

Grieg, D. D., Metzger, S , and Waer, R (1948), Proc I.R.E , 36, p 652

Hagfors, T (1964), J. Geophys Res , 69, p 34–41.

Hagfors, T , Brockelman, R. A., Danforth, H. H , Hanson, L. B , and Hyde, G. M (1966), "Evidence of a Tenuous Surface Layer on the Moon as Derived from Radar Observations", to be published

Halajian, J D., and Richman, J (1965), "Correlation of Mechanical and Thermal Properties of Extraterrestrial Materials", 1st Progress Report prepared for NASA/Marshall Space Flight Center by Grumman Aircraft Eng. Corp. under Contract NAS8-20084, September 28, 1965

Jaeger, J C. (1953), Aust, J Phys , 6, p 10

Johnson, C L., and Hollweger, D. J (1965), "Some Heat Transfer Considerations in Non–Evacuated Cryogenic Power Insulation", AF 33(657)–11200, August 1965.

Krotikov, V. D., and Troitskii, V S (1963a), Soviet Phys, Usp, English Trans., 6, p 841

Krotikov, V. D., and Troitskii, V S. (1963b), Soviet Astronomy, AJ, 7, p 119,

Krotikov, V D., and Shchuko, O. B (1963), Soviet Astronomy, AJ, 7, p 228.

Kunii, D., and Smith, J. M. (1960), AIChE Journal, 6, 71.

Linsky, J L. (1966). "Models of the Lunar Surface including Temperature Dependent Thermal Properties", Scientific Report No. 8, Havard College Obs., January 15.

Loeb, A. L. (1954), J Amer. Ceram. Soc., 37, 96

Markov, M. I. V , and Khokhlova, V L (1964). Soviet Physics - Doklady, 9, 8, p 621

Masamune, S., and Smith, J M. (1963a), J Chem. & Eng Data, 8, 1, p 54

Masamune, S., and Smith, J M. (1963b), Ind & Eng. Chem Fundamentals, 2, 2, p 136

Mischke, R. A., and Smith, J M (1962), Ind & Eng. Chem. Fundamentals, 4, 1, p 288.

Muncey, R W (1963), Aust J Phys , 16, 1, p *24*

Murray, B C., and Wildey, R. L (1964), Astrophysics J , 139, p 734.

Pettengill, G H., and Evans, J V (1965), "Radar Studies of the Moon", Chapter 7 in the proposed book on "Radar Astronomy", by John V Evans and Tor Hagfors.

Pettit, E,, and Nicholson, S B. (1930), Astrophys J , 71, p 102

Pettit, E, (1940), Astrophys J , 91, p 408.

Piddington, J H , and Minnett, H C. (1949), Aust J Sci Res , 2A, p 63.

Piddington, J H., and Minnett, H C (1951), Aust J Sci Res., 4A, p 459.

Rea, D. G., Hetherington, N , and Mifflin, R. (1964), J Geophys Res , 69, p 5217

Redheffer, R.M. The Measurement of Dielectric Constants, p 669; in Technique of Microwave Measurements, C G Montgomery, Editor, Vol II of The MIT Radiation Laboratory Series, McGraw-Hill Book Co , New York, 1947

Roberts, S., and von Hippel, A J Appl Phys 17, 610, 1946; see also A von Hippel, Dielectric Materials and Applications, p 67, MIT Press, 1954

Rosseland, S (1936), Theoretical Astrophysics, Oxford Univ Press, Clarendon

Russell, H W (1935), J. Amer. Ceramic Soc., 18, 1

Saari, J , and Shorthill, R. W (1963), Icarus, 2, p 115–136.

Salisbury, J W., and Glaser, P E, (1964), AFCRL 64–970, "Studies of the Characteristics of Probable Lunar Surface Materials,"

Schotte, W. (1960), AIChE Journal, 6, 63

Scott, R. B. (1957), J Res. Nat, Bur Stand , 58, p 317

Senior, T B A., Siegel, K. M , and Giraud, A. (1962), "Some Physical Constants of the Lunar Surface as Indicated by Its Radar Scattering and Thermal Emission Properties", in "The Moon", Ed by Z. Kopal and Z. Mikhailov, Acad. Press, London, p 533-543

Spitzer, W.G., and Kleinman, D.A (1961), Physical Review, 121, p 1324

Straiton, A. W., and Tolbert, C W (1947), "Measurement of Dielectric Properties of Soils and Water at 3.2 cm Wavelength", El. Eng. Res Lab Report No. 4, U of Texas.

Strong, H M , Bundy, F P , and Bovenkirk, H P (1960), J. Appl. Phys., 31, No 1, p 39

Troitskii, V. S (1962), "Radio Emission of the Moon, Its Physical State and the Nature of its Surface", in "The Moon", Ed by Z. Kopal and Z Mikhailov, Acad Press, London, p 475-489

Troitskii, V S. (1962a), Radiophysics, 5, 5, p 885

Troitskii, V S. (1962b), Soviet Astronomy, AJ, English Trans , 6, p 51

Van de Hulst, H. C. (1957), "Light Scattering by Small Particles", J Wiley & Sons, New York

von Hippel, A. R. (1954), Editor, M.I T Press, Cambridge, Mass , p 314.

Watson, K. (1964), "I Thermal Conductivity Measurements of Selected Silicate Powders in Vacuum from 150-350°K, II. An Interpretation of the Moon's Eclipse and Lunation Cooling as Observed through the Earth's Atmosphere from 8-14 Microns", Thesis, Calif Inst. of Tech

Wechsler, A. E., Glaser, P. E., , and Allen, R. V (1963), "Thermal Conductivity of Non-Metallic Materials", Summary Report, Contract NAS8-1567, Arthur D. Little, Inc.

Wechsler, A. E., and Glaser, P E. (1964), "Thermal Conductivity of Non-Metallic Materials", Summary Report, Contract NAS8-1567, Arthur D. Little, Inc.

Wechsler, A E., and Glaser, P E. (1965), Icarus, 4, No 4, p 335-352,

Wilhelm, R. H. , et al (1948), Chem. Eng Prog., *44*, p 105.

Winter, D. F (1965), "Transient Radiative Cooling of a Semi-Infinite Solid with Parallel-Walled Cavities", Boeing Scientific Res Lab. Report D1-82-0449

Woodside, W., and Messmer, J (1961), J Applied. Phys , *32*, p 1688.

ACKNOWLEDGMENTS

This program was sponsored by the Research Projects Laboratory of the G C Marshall Space Flight Center under Contract NAS8-20076.

The assistance and guidance of Dr Klaus Schocken, Mr J Fountain, and Mr. C. D. Cochran of the Research Projects Laboratory and Dr P E Glaser of Arthur D. Little, Inc , throughout the program is acknowledged

The authors wish to thank Drs John V Evans and Tor Hagfors of the Lincoln Laboratory for helpful discussions and for the opportunity of reading some of their papers prior to publication.

The experimental work on the dielectric properties of powders was performed by F. Margosian under the guidance of I Simon They were aided in the theoretical parts of the work by P Strong

Thermal conductivity measurements were carried out by Mr E Boudreau Mr R Read and Mr. S Perry assisted the authors by reducing the experimental data Dr J. Aronson and Dr R McConnell assisted in analytical evaluation of the radiation contribution to heat transfer